A STUDY OF MODIFICATIONS OF FILLER DIMENSIONS AND THE EFFECT OF PHYSICAL AND MECHANICAL PROPERTIES OF PINEAPPLE LEAF FIBRE REINFORCED POLYPROPYLENE COMPOSITES

BY
SAMUEL GADZAMA WADZANI

DEPARTMENT OF POLYMER & TEXTILE ENGINEERING

FACULTY OF ENGINEERING

AHMADU BELLO UNIVERSITY, ZARIA

MAY, 2021

A STUDY OF MODIFICATIONS OF FILLER DIMENSIONS AND THE EFFECT OF PHYSICAL AND MECHANICAL PROPERTIES OF PINEAPPLE LEAF FIBRE REINFORCED POLYPROPYLENE COMPOSITES

BY

SAMUEL GADZAMA WADZANI, B.Eng (UniMaid), 2005, M.Eng (UnZik), 2013

(P13SCTX9002)

A THESIS SUBMITTED TO THE SCHOOL OF POSTGRADUATE STUDIES,

AHMADU BELLO UNIVERSITY, ZARIA

IN PARTIAL FULFILMENT OF THE REQUIREMENTS FOR THE AWARD OF DOCTOR OF PHILOSOPHY IN POLYMER AND FIBRE TECHNOLOGY

DEPARTMENT OF POLYMER & TEXTILE ENGINEERING

FACULTY OF ENGINEERING

AHMADU BELLO UNIVERSITY, ZARIA

MAY, 2019

DECLARATION

I declare that the work in this thesis entitled "A Study of Modifications of Filler Dimensions and the Effect of Physical and Mechanical Properties of Pineapple Leaf Fibre Reinforced Polypropylene Composites" has been performed by me in the Department of Polymer and Textile Engineering. The information derived from the literature has been duly acknowledged in the text and a list of references provided. No part of this thesis was previously presented for another degree or diploma at this or any other Institution.

WADZANI Samuel Gadzama	_____	_____
Name of Student	Signature	Date

CERTIFICATION

This thesis entitled A STUDY OF MODIFICATIONS OF FILLER DIMENSIONS AND THE EFFECT OF PHYSICAL AND MECHANICAL PROPERTIES OF PINEAPPLE LEAF FIBRE REINFORCED POLYPROPYLENE COMPOSITES by Samuel Gadzama WADZANI meets the regulations governing the award of the degree of Doctor of Philosophy in Fibre and Polymer Technology of Ahmadu Bello University, and is approved for its' contribution to knowledge and literary presentation.

Prof. O.K. Sunmonu Chairman, Supervisory Committee	_____ (Signature)	_____ (Date)
Prof U.S. Ishiaku Member, Supervisory Committee	_____ (Signature)	_____ (Date)
Prof. Abdullahi Danladi Member, Supervisory Committee	_____ (Signature)	_____ (Date)
Prof. M.M. Bukkari Head of Department	_____ (Signature)	_____ (Date)
Prof. Sani A. Abdullahi Dean, School of Postgraduate Studies	_____ (Signature)	_____ (Date)

ACKNOWLEDGMENT

Firstly, I will start by appreciating the tireless and inspiring mentorship and tutorship I received from my supervisors. Indeed, this study would not have been possible without the academic support base they gave me. To Prof. O.K Sunmonu, Prof. U.S. Ishiaku and Prof. Abdullahi Danladi, words cannot express how indebted I am to be graced and privileged to be under your supervision.

I deeply acknowledge the support I received from the management and staff of the Scientific Equipment Development Institute, under the wings of the Managing Director/Chief Executive, Prof. (Engr). S.N. Ndubisi. I am thankful for the technical support I received when I was designing the metal molds which Engr. Mbanu Kingsley was always available to render and other technical staff of Advanced Manufacturing Unit, to the Technical Staff of Plastic Production and Plastic Recycling, units, for their support during the period of test running the molds on the injection molding machine and during production of test samples. To the staff of Material testing laboratory, I want to appreciate you for working with me when I conducted some bench work in the laboratory. To Engr. E.C. Ufomba, my Head of Section, I want to put on record your moral support in making my programme seem easy despite the distance, you were opened to permitting me to attend to issues of my studies at the shortest notice.

To my friends and colleagues, Engr (Mrs) Zita Ujuchukwu Okoh, your tireless efforts, down to going to the Pineapple plantation to collect the pineapple leaves with me and assisting me to interface with the local community in Awgu to get the right direction to the Pineapple plantation signify how priceless your contribution towards the success of this research has been. To Engr (Mrs) Christina Agu-Bruno, Engr (Mrs) Ogochukwu Ugwueze and Engr, Imoh Uchechi, I want appreciate your assistance during the sorting out of the extracted pineapple

leaf fibre, washing them and during the surface modification experiments, I want to say a very big thank you for staying with me all thru most of the experiments I carried out at the Scientific Equipment Development Institute. To Dr. Godwin Ugwu, of the Department of Pharm Tech, University of Nigeria, Nsukka. I owe the breakthrough of achieving nanofibrils of the pineapple leaf with your guidance, technical support and wealth of academic and practical expertise in the area of micro cellulose production.

Lastly, to the technical staff of the Council for Scientific and Industrial Research (CSIR), Pretoria, South Africa, you guys were a wonderful host, to each and every question I asked in respect to the characterization of the micro and nanofibrils of the pineapple leaf, you guys were ever ready to give me attention and grant answers to my questions, you allowed me access into your research facility and even gave me access to other sections of your facility that were not related to my purpose of visit, but relevant to my research work, notable of mention are Popoti Maake, Rhandzu Rikhotso and Solly Motaung.

To my wife Abosede and my daughters Janada and Japari, words cannot express how you girls supported me all thru the period of my study, your sacrifices made this dream a reality.

ABSTRACT

This research studied the effect of filler dimensions on some major properties of pineapple leaf fibre-reinforced polypropylene composites. In this study, composites of PALF/PP were produced, the PALF were extracted from pineapple leaves. This was achieved by adopting the mechanical scrapping method. The surface of the extracted PALF were modified with 6% NaOH, 14% $C_3H_6O_3$, 6% HNO_3 and 3% ZnCl. The surface modified PALF as well as the control (untreated/unmodified) gave FTIR spectrum indicated that the modified PALF chemical structures were not significantly altered. Microbial load analysis were carried out to ascertain and determine the shelf life for the PALF, aspergillus was identified as the microorganism that predominantly affected the PALF after a 12 months observation period. Molds were fabricated using mild steel plates by adopted the modern methods of producing molds, with the aid of a computer numerically controlled machine (CNCm) called the vertical milling center (VMC). TAPPI methods were used to ascertain the composition of the PALF, specifically the percentage composition of lignin, hemicellulose and cellulose in the PALF. Elemental composition of the PALF were equally analyzed, the data were subsequently compared and analyzed with the data collected from analyzing same samples using a more accurate and state of the art equipment called the SEM-EDX. The PALF went through particle size reduction stages, broadly classified into the macro (2-6 mm), micro (70 - 300 µm) and nano (20 - 500 nm). The method adopted in the conversion of the PALF into micro and nano fibrils is termed chemo-mechanical method. The PALF micro fibrils were characterized using JOEL JSM 750F SEM, the micographs of the modified PALF showed morphologies of PALF that could easily produce composites with enhanced properties. Similarly, the PALF nanofibrils were characterized using JEOL JEM 2100 High resolution (HR-TEM), the micrographs of the modified nanofibrils displayed a spider web-like structure with nano scale diameter cellulose fibrils or branches of similar fibril bundle hooked up to produced larger aggregates of nano cellulose. The PALF/PP composites exhibits improved mechanical, physical and thermal and properties at the macro cellulose, micro and nano fibrils dimensions of PALF respectively. These enhanced behaviours are seen even in the unmodified PALF/PP composites, where the TS at the optimal performance with ratio of 30/70 of PALF/PP, there is an increase by 27.88 % of TS for the micro PALF/PP composite and an amazing 70.65 % increase at the nano fibrils PALF/PP composites level. However, the behaviour of the modified PALF are higher than the unmodified PALF/PP composites when compared. The results show that the reinforced HNO_3 modified PALF/PP composites have higher performance index than the reinforced $C_3H_6O_3$ modified PALF/PP composites which gives better performance index that the reinforced NaOH modified PALF/PP composites which performs higher than the reinforced ZnCl modified PALF/PP composites, which gave higher performance index than the unmodified reinforce PALF/PP composites.

TABLE OF CONTENTS

Cover Page i
Fly Page ii
Declaration iv
Acknowledgment vi
Abstract viii
Table of Contents ix
List of Figures xiii
List of Table xvi
List of Plates xvii
List of Abbreviations, Definitions, Glossary and Symbols xix
CHAPTER ONE 1
INTRODUCTION 1
1.1 Background 1
1.2 Statement of Problem 6
1.3 Justification / Significance of the Study 7
1.4 Scope and Limitations 7
1.5 Aim and Objectives of the Study 8
CHAPTER TWO 9
LITERATURE REVIEW 9
2.1 Pineapple Leave Fibre 9
2.1.1 Extraction of Pineapple Leaf Fibre (PALF) 9
2.1.2 Chemical Composition of Pineapple Leaf Fibre (PALF) 11
2.1.3 Physical and Mechanical Properties of Reinforced PALF 12
2.2 Some Surface Modifications Techniques of PALF 13
2.2.1 Alkali Treatment 15
2.2.2 Acetylation Treatment 16
2.3 Polypropylene as a Thermoplastic 16
2.3.1 Polypropylene Properties and Types 18
2.4.1 Short Fibre PALF Reinforced Composites 22
2.4.2 Long Fibre PALF Reinforced Composite 26
2.4.3 Epoxy Based PALF Reinforced Composites 28
2.4.4 Polyethylene based PALF Reinforced Composites 28
2.4.5 Polypropylene based PALF Reinforced Composites 29
2.4.6 Vinyl ester based PALF Reinforced Composites 29
2.4.7 Polyester Based PALF Reinforced Composites 30

2.4.8 Low Density Polyethylene based PALF Composites 30
2.4.9 PALF based Hybrid Composites 31
2.5 Some PALF/PP Composites Characterization Equipment 31
2.5.1 Fourier Transmission Infrared Spectroscopy (FTIR) 31
2.5.2 Scanning Electron Microscopy (SEM) 32
2.5.3 Energy Dispersive X-ray (EDX) 32
2.5.4 Transmission Electron Microscopy 33
2.6 PALF Applications and Future Prospects 34
2.6 Nano PALF Fibrils 35
2.6.3 Morphology and Dimensions of Cellulose Nanocrystals 36
2.6.4 Applications of Nano Cellulose Reinforced Composites 37
CHAPTER THREE 39
MATERIALS AND METHODS 39
3.1 Background 39
3.2 Materials 39
3.2.1 Reagents Used 39
3.2.2 Equipment Used 39
3.2.3 Raw Material 39
3.3.1 PALF Extraction 40
3.3.2 Yield of PALF and Classification in Different Particle Sizes 41
3.4 Pineapple Leave Fibre (PALF) Surface Modification 41
3.4.1 Treatment with Sodium Hydroxide 42
3.4.2 Treatment with Acetic Anhydride 42
3.4.3 Treatment with Nitric Acid 42
3.4.4 Treatment with Zinc Chloride 43
3.5 Pineapple Leaf Fibre Characterization 43
3.5.1 Preparations of Test Samples 43
3.5.2 Compositional Analysis of the Pineapple Leaf Fibre (PALF) 43
3.6 Proximate Composition of the PALF 46
3.7.2 Fungi Characterization and Possible Identification 49
3.8 Fourier Transform Infrared Spectroscopy of the Pineapple Leaf Fibre (PALF) 49
3.9 Fabrication of Mold for the Mechanical and Thermal Property Tests of the Composites 50
3.10 Production /Isolation of Micro and Nano Particles from the PALF 50
3.10.1 Determination of Percentage Yield of micro and nano PALF fibrils 51
3.11 Characterization of the PALF Micro Fibrils 52
3.12 Characterization of the Nano Cellulose PALF 52

3.13 EDX -SEM on PALF at the Micro and Nano Fibrils Dimensions 53
3.14 Compounding of the PALF/PP Composites 54
3.14.1 PALF/PP Composite Preparation at the Macro PALF Level 55
3.14.2 PALF/PP Composite Preparation at the Micro and Nano Cellulose Dimension 55
3.15 Physical Property Test on the PALF/PP Composites 55
3.15.1 Water Absorption 55
3.16 Mechanical Properties Tests of the PALF/PP Composites 56
3.16.1 Tensile Properties Test 56
3.16.2 Flexural Properties Test 57
3.16.3 Impact Strength Test 58
3.17 Thermal Property Test on the PALF/PP Composites 59
3.17.1 Thermal Conductivity Test 59
CHAPTER FOUR 60
RESULTS AND DISCUSSION 60
4.1 Background 60
4.2 Extraction of the Pineapple Leave Fibre (PALF) 60
4.3 Chemical Compositions of the Pineapple Leave Fibre (PALF) 60
4.3.1 Cellulose 61
4.3.2 Lignin 61
4.3.3 Hemicellulose 62
4.4 Proximate Analysis of the Pineapple Leave Fibre (PALF) 64
4.5 Identification of Bacterium and Fungi on the PALF 68
4.6 Fourier Transform Infrared Spectroscopy of the Pineapple Leaf Fibre (PALF) 71
4.7 Production of Molds for the production of PALF/PP Composites 77
4.8 Production / Isolation of PALF Micro and Nano fibrils 77
4.9.3 Characterization of the PALF Nano Fibrils 82
4.11 Physical Property Analysis of the PALF/PP Composites 91
4.11.1 Water Absorption Data of the PALF/PP Composites 91
4.12 Mechanical Properties Analysis Data of the PALF/PP Composites 96
4.12.1 Tensile Strength Results of the PALF/PP Reinforced Composites 97
4.12.2 Young's Modulus Data of the PALF/PP Reinforced Composites 100
4.12.3 Flexural Strength Data of the PALF/PP Composites 104
4.12.4 Flexural Modulus Data of the PALF/PP Composites 107
4.12.4 Impact Strength Data of the PALF/PP Composites 110
4.13 Thermal conductivity Analysis of the PALF/PP Composites 116
CHAPTER FIVE 122

SUMMARY, CONCLUSION AND RECOMMENDATION 122
5.1 Summary 122
5.2 Conclusion 124
5.3 Recommendations 125
5.4 Contribution to Knowledge 126
REFERENCES 127
APPENDICES 139

LIST OF FIGURES

Figure 1.1 Chemical Structure of Cellulose……..2
Figure 1.2 Chemical Structure of Hemicellulose……..3
Figure 1.3 Chemical Structure of Lignin…….….4
Figure 2.1 Scheme of Acetylation Reaction……16
Figure 2.2 Polypropylene Structure…….17
Figure 3.1 Schematics of the Compositional Analysis of the Palf……...44
Figure 4.1 An Experimental set-up Showing Aspergillum as the Fungus Identified on the Palf…….71
Figure 4.2 Water Absorption Property of the Reinforced Unmodified PALF/PP Composites……...……91
Figure 4.3 water Absorption Property of the Reinforced PALF/PP Composite Modified With NaOH……...……92
Figure 4.4 Water absorption property of the reinforced PALF/PP Composite modified with ZnCl……..……93
Figure 4.5Water absorption property of the reinforced PALF/PP Composite modified with $C_3H_6O_3$ …….……93
Figure 4.6 Tensile strength (MPa) of the unmodified reinforced PALF/PP composites against weight ratio…….……97
Figure 4.7 Tensile strength (MPa) of the NaOH modified reinforced PALF/PP composites against weight ratio……..……..……98
Figure 4.8 Tensile strength (MPa) of the ZnCl modified reinforced PALF/PP composites against weight ratio……...…98
Figure 4.9 Tensile strength (MPa) of the $C_3H_6O_3$ modified reinforced PALF/PP composites against weight ratio……99
Figure 4.10 Tensile strength (MPa) of the HNO_3 modified reinforced PALF/PP composites against weight ratio……99
Figure 4.11 Young's modulus against % weight ratio of PALF/PP composites…….100
Figure 4.12 Young's modulus against % weight ratio of the NaOH modified PALF/PP composites……..101
Figure 4.13 Young's modulus against % weight ratio of the ZnCl modified PALF/PP composites……...…102

Figure 4.14 Young's modulus against % weight ratio of the $C_3H_6O_3$ modified PALF/PP composites……102
Figure 4.15 Young's modulus against % weight ratio of the HNO_3 modified PALF/PP composites……..103
Figure 4.16 Flexural strength against % weight ratio of the unmodified reinforced PALF/PP composites…….....104
Figure 4.17 Flexural strength against % weight ratio of the NaOH modified reinforced PALF/PP composites……104
Figure 4.18 Flexural strength against % weight ratio of the ZnCl modified reinforced PALF/PP composites…….....105
Figure 4.19 Flexural strength against % weight ratio of the $C_3H_6O_3$ modified reinforced PALF/PP composites…….105
Figure 4.20 Flexural strength against % weight ratio of the HNO_3 modified reinforced PALF/PP composites……106
Figure 4.21 Flexural modulus against % weight ratio of PALF/PP composites……...107
Figure 4.22. Flexural modulus of the NaOH modified PALF/PP composites against % weight ratio…….....108
Figure 4.23 Flexural modulus of the ZnCl modified PALF/PP composites against % weight ratio……108
Figure 4.24 Flexural modulus of the $C_3H_6O_3$ modified PALF/PP composite against % weight ratio…….109
Figure 4.25 Flexural modulus of the HNO_3 modified PALF/PP composites against % weight ratio…….109
Figure 4.26 Impact strength against % weight ratio of unmodified /PP composites……..…110
Figure 4.27 Impact strength against % weight ratio of NaOH modified PALF/PP composites…….111
Figure 4.28 Impact strength against % weight ratio of ZnCl modified PALF/PP composites…….112
Figure 4.29 Impact strength against % weight ratio of $C_3H_6O_3$ modified PALF/PP composites…….……112
Figure 4.30 Impact strength against % weight ratio of HNO_3 modified PALF/PP Composites……113
Figure 4.31 Thermal conductivity against % weight ratio of unmodified PALF/PP Composites……117

Figure 4.32 Thermal conductivity against % weight ratio of NaOH modified PALF/PP composites……..…117
Figure 4.33 Thermal conductivity against % weight ratio of ZnCl modified PALF/PP composites…….118
Figure 4.34 Thermal conductivity against % weight ratio of $C_3H_6O_3$ modified PALF/PP composites…….119
Figure 4.35 Thermal conductivity against % weight ratio of HNO_3 modified PALF/PP composites…….119

LIST OF TABLES

Table 2.1. Chemical compositions of pineapple leaf fibre……12

Table 2.2 Physical and Mechanical Properties of PALF……...13

Table 2.3 Advantages and Disadvantages of polypropylene……..…20

Table 2.4 Mechanical and Thermal Properties of polypropylene……..….21

Table 2.5 Thermal Conductivity……....21

Table 3.1 Characteristics of the Polypropylene used in this research work……..40

Table 3.2 PALF/PP Composites weight load Ratio……..55

Table 3.3 Dumb bell-shaped specimen dimension for Type I in ASTM D638……57

Table 4.1 Chemical Composition of the PALF at the macro particle sizes……..60

Table 4.2 Chemical Composition of the Micro Cellulose PALF……..63

Table 4.3 Chemical Composition of the Nano Cellulose PALF……...63

Table 4.4 Proximate Analysis of the PALF using AFM……...64

Table 4.5 Proximate Analysis of the Micro/Nano PALF using EDX-SEM……..…65

Table 4.6 Result of the fungal load on the PALF after 24 hours Observation……..…68

Table 4.7 Result of the Bacterial Load on the PALF after three Months Observation……69

Table 4.8 Result of the Fungal Load on the PALF after three Months Observation……....69

Table 4.9 Results on Fungal Load on PALF after Six Months…….69

Table 4.10 Result of the Fungal Load on the PALF after Three Months Observation…….70

Table 4.11 Result of the Fungal Load on the PALF after Twelve months Observation…...70

LIST OF PLATES

Plate I. EDX of the unmodified PALF……..65

Plate II. The EDX of the PALF modified with NaOH……..…65

Plate III. The EDX of PALF modified with ZnCl……..…..…..66

Plate IV. The EDX of the PALF samples modified with $C_3H_6O_3$…….....66

Plate V. The EDX of the PALF modified with HNO_3 ……..67

Plate VI. The FTIR spectrum of the unmodified PALF……71

Plate VII. The FTIR spectrum of the PALF modified with sodium hydroxide…...……..73

Plate VIII. The FTIR spectrum of the PALF modified with zinc chloride……..….74

Plate IX. The FTIR spectrum of the PALF modified with nitric acid……..75

Plate X. The FTIR spectrum of the PALF modified with acetic anhydride…….….76

Plate XI. SEM of the unmodified PALF micro cellulose at different magnifications…….….77

Plate XII. SEM of the PALF micro samples modified with NaOH at different magnifications…….....78

Plate XIII. SEM of the PALF micro samples modified with NaOH at X50, 000 and X 100, 000 magnifications……....79

Plate XIV. SEM of the PALF samples modified with acetic anhydride……...79

Plate XV. SEM of the PALF micro samples modified with Zinc Chloride at different magnifications……...80

Plate XVI. SEM of the PALF micro samples modified with Zinc Chloride at X50,000 and X100,000 magnifications……....80

Plate XVII. SEM of the PALF micro samples modified with Nitric acid at X10,000 and X25,000 magnification……....81

Plate XVIII. TEM of the unmodified (control) PALF nanocellulose agglomerate at different magnifications……..……..82

Plate XIX. TEM of the unmodified (control) PALF nanocellulose agglomerate at higher magnification of 500 nm……....83

Plate XX. TEM of the PALF nanocellulose agglomerate modified with NaOH……....84

Plate XXI. TEM of the PALF nanocellulose agglomerate modified with NaOH at higher resolution of 500 nm……...…84

Plate XXII. TEM of the PALF nanocellulose agglomerate modified with acetic anhydride (depicting a more readily dispersed agglomerate)……85

Plate XXIII. TEM of the PALF nanocellulose agglomerate modified with acetic anhydride (depicting a more readily dispersed agglomerate) at a magnification of 200 nm……85
Plate XXIV. TEM of the PALF nanocellulose agglomerate modified with acetic anhydride (depicting a more readily dispersed agglomerate) at a magnification of 500 nm……86
Plate XXV. TEM of the PALF nanocellulose agglomerate modified with ZnCl (depicting a more readily dispersed agglomerate) at a magnification of 2 µm……...86
Plate XXVI. TEM of the PALF nanocellulose agglomerate modified with ZnCl (depicting a more readily dispersed agglomerate) at a magnification of 200 nm……87
Plate XXVII. TEM of the PALF nanocellulose agglomerate modified with ZnCl (depicting more readily dispersed agglomerate) at a magnification of 1µm and 500 nm……87
Plate XXIII. TEM of the PALF nanocellulose agglomerate modified with nitric acid (depicting a more readily dispersed agglomerate) at a magnification of 1µm……88
Plate XXIX. TEM of the PALF nanocellulose agglomerate modified with nitric acid (depicting a more readily dispersed agglomerate) at a magnification of 200 nm……88
Plate XXX. TEM of the PALF nanocellulose agglomerate modified with nitric acid (Depicting a more readily dispersed agglomerate) at a magnification of 500 nm……...89

LIST OF ABBREVIATIONS, DEFINITIONS, GLOSSARY AND SYMBOLS

µm	Micrometers
AFM	Atomic Force Microscopy
ASTM	American Society for Standards and Materials
BNC	Bacterial Nanocellulose
cfu	Colony Forming Unit
CNC	Carbon Nano Crystals
CNC	Computer Numerically Controlled Machine
CP/MAS NMR	Cross-Polarization Magic Angle Spinning Nuclear
CSIR	Council for Scientific and Industrial Research
DAP	Diammonium Phosphate
DLS	Dynamic Light Scattering
EDS	Energy Dispersive Spectroscopy
EDX	Energy Dispersive X-ray
EHMA	Ethyl-a- (hydroxyl methyl) acrylate
FAO	Food and Agricultural Organization for the United Nations
FESEM	Field Emission Scanning Electron Microscopy
FM	Flexural Modulus (MPa)
FRP	Fibre Reinforced Plastics
FS	Flexural Strength (MPa)
FTIR	Fourier Transmission Infrared
g	Grams
GPa	Giga Pascal
HDPE	High Density Polyethylene
HRTEM	High Resolution Transmission Electron Microscopy
IFSS	Interfacial Shear Stress
IR	Infrared Radiation
IS	Impact Strength (J/m)
Kev	Kilo Electron Volts
Kg	Kilograms
KV	Kilovolts
LDPE	Low Density Polyethylene
LOI	Lateral Orientation Index
	Magnetic Resonance
MFR	Melt Flow Ratio
mm	Millimeters
MPa	Mega Pascal
NA	Nutrient Agar
NCC	Nanocrystalline Cellulose
NCNSM	National Centre for Nanostructured Materials
NFC	Nano Fibrillated Cellulose
nm	Nanometers
NMR	Nuclear Magnetic Resonance
PALF	Pineapple Leaf Fibre
PAPF	Pineapple Peal Fibre
PE	Polyethylene
PP	Polypropylene
PS	Polystyrene
PVC	Polyvinylchloride

RIBE	Reactive Ion Beam Etching
RIM	Reaction Injection Molding
RS	Raman Spectroscopy
SA	Sabouraud Agar
SAXRD	Small Incidence Angle X-ray
SDA	Sabouraud Dextrose Agar
SDD	Si Drift Detectors
SEM	Scanning Electron Microscopy
SON	Standards Organization of Nigeria
TAPPI	Technical Association of Pulp and Paper Industry
TC	Thermal Conductivity (W/mK)
TCI	Total Crystalline Index
TEM	Transmission Electron Microscopy
TGA	Thermogravimetric Analysis
TS	Tensile Strength (MPa)
UV	Ultravalent
VMC	Vertical Milling Machine
WAXS	Width Angle X-ray Scattering
YM	Young's Modulus

CHAPTER ONE

INTRODUCTION

1.1 Background

Fibres are materials that are hair-like in nature that have discrete elongated pieces, similar to pieces of thread. They can be spun into filaments, threads or ropes. They can also be used as a component of composite materials. Fibres are classified into two main groups, namely; man-made fibre and natural fibre. In general, natural fibres can be subdivided as to their origin of source such as plants, animals, or minerals; while man-made fibres can be subdivided to synthetic and natural polymers (Mohammed *et al.,* 2015).

Fibres can also be classified based on their length, broadly as long and short fibres. Short fibres, sometimes referred to as chopped fibre may be converted into a lightly bonded preform or mat that can be later impregnated with resin to fabricate single-layer composites. Chopped fibres may also be blended with resins to make are in forced molding compound. These fibres tend to become oriented parallel to the direction of material flow during a compression or injection molding operation and thus get a preferential orientation (Abasiwie, 2015).

According to Sain and Panthapulakkal (2004), the age of the plant, climatic conditions and fibre processing techniques influence the structure of fibres as well as their chemical composition. Bledzki and Gassan (1999) summarized that component or chemical composition constituents of plant fibre as cellulose, hemicellulose, lignin, pectin, waxes and water-soluble substances, of which, cellulose, hemicellulose and lignin are the major components with regard to the physical properties of the fibres. The percentages and properties of the components contribute to the overall properties of the fibres. (Sain and Panthapulakkal 2004).

In higher plants, cellulose is the main component of fibre cell walls for the main functions of protection and formation of structures during plant life. The other components in natural cellulose fibres are hemicellulose, lignin, and a comparably small amount of extractives, that

is, pectin and waxes. In fibre cell walls, the spirally oriented cellulose plays the role of reinforcements in soft hemicellulose and lignin matrix. Cellulose is a linear carbohydrate polymer chain consisting of *D*-glucopyranose units joined together by *β*-1,4-glycosidic linkages (Bledzki *et al.*, 1999; Eichhorn and Young, 2001; Klemm *et al.*, 2005; Li *et al.*, 2000)). Figure 1.1 shows the chemical structure of cellulose.

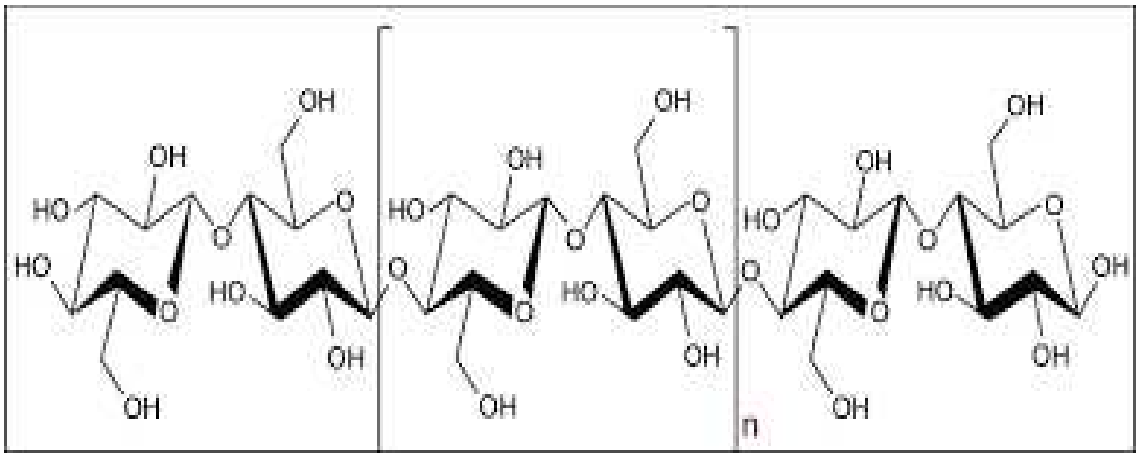


Figure 1.1 Chemical structure of cellulose (Source: Johnsy and Sabapathi, 2015)

Hemicellulose is a highly branched polymer compared to the strictly linear nature of cellulose (Figure 1.2). Its structure contains many different sugar units whereas cellulose contains only 1,4-*β*-*D*-glucopyranose units and its degree of polymerization is ten to one hundred times lower than that of cellulose. Moreover, the constituents of hemicellulose differ from plant to plant unlike cellulose. (Bledzki *et al.*, 1998; Eichhorn and Young, 2001).

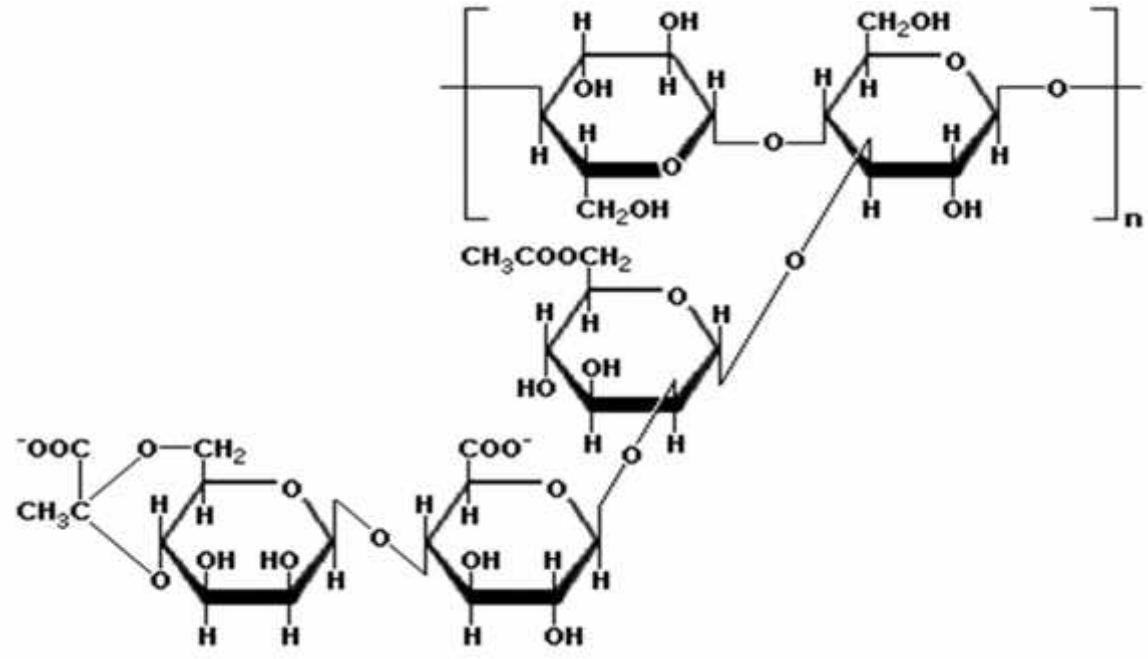


Figure 1.2 Chemical Structure of Hemicellulose (Source: Kulkarni *et al.*, 2017)

Lignin is a hydrocarbon polymer with a highly complex structure consisting of aliphatic and aromatic constituents, as shown in Figure 1.3. Their major monomer units are various ring substituted phenyl-propane linked together in ways which are still not fully understood. It forms the matrix sheath around the fibres that holds the natural structure together. Lignin structural details differ from one source to another. (Bledzki *et al.,* 1999; Eichhorn and Young, 2001).

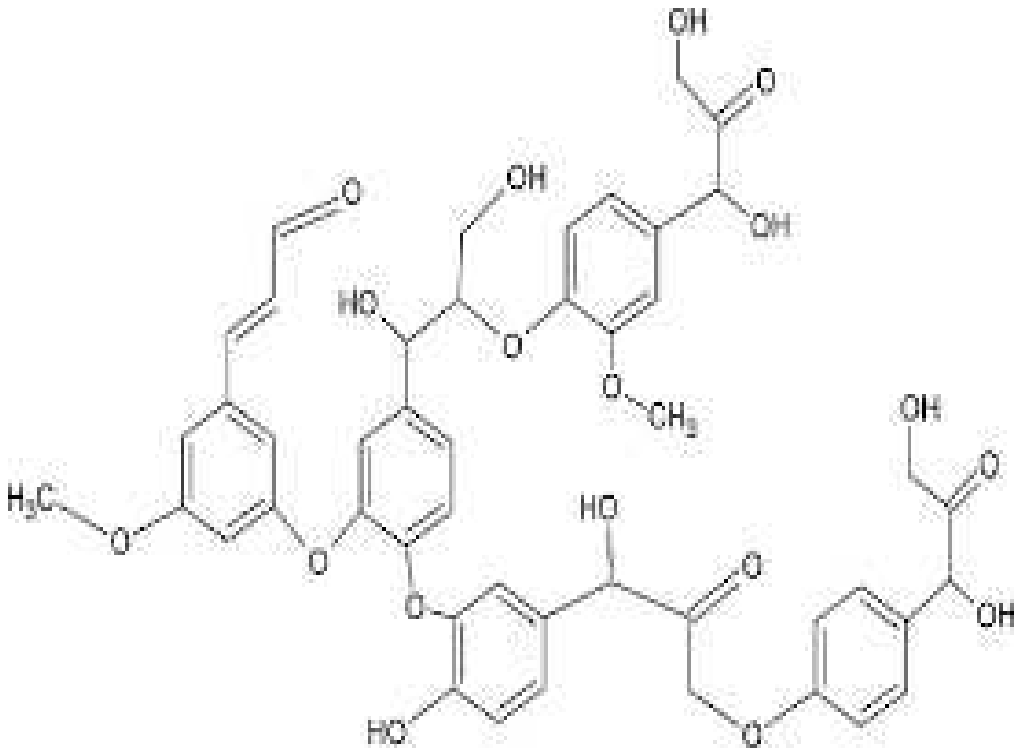


Figure 1.3 Chemical structure of lignin (Source: Mahmood *et al.*, 2018).

Pectins are a collective name for heteropolysaccharides, which consist of α-1, 4-linked galacturonic acid units, sugar units of various composition and their respective methyl esters. Pectins are soluble in water only after a partial neutralization with alkali or ammonium hydroxide. Finally, the waxes consist of various alcohols which are insoluble in water as well as in several acids (palmitic acid, oleaginous acid, stearic acid). Waxes form a small percentage of the structure and can be extracted with organic solutions. (Bledzki *et al.*, 1999; Eichhorn and Young, 2001).

Natural fibres exhibit considerable variation in diameter along with the length of individual filaments. Quality and other properties of fibres depend on factors such assize, maturity and processing methods adopted for the extraction of fibre. Properties such as density, electrical resistivity, ultimate tensile strength and initial modulus are related to the internal structure and chemical composition of fibres. Desirable properties for fibres include excellent tensile strength and modulus, high durability, low bulk density, good moldability and recyclability.

Natural fibres have an advantage over glass fibres in that they are less expensive, abundantly available from renewable resources and have a high specific strength (Mohanty *et al.,* 2001). Natural fibres are incompatible with the hydrophobic polymer matrix and have a tendency to form aggregates. These are hydrophilic fibres and thus exhibit poor resistance to moisture. To eliminate the problems related to high water absorption, treatment of fibres with hydrophobic aliphatic and cyclic structures has been attempted. These structures contain reactive functional groups that are capable of bonding to the reactive groups in the matrix polymer. Thus, modification of natural fibres is attempted to make the fibres hydrophobic and to improve interfacial adhesion between the fibre and the matrix polymer. Chemical treatments such as dewaxing (defatting), delignification, bleaching, acetylation, and chemical grafting are used for modifying the surface properties of the fibres and for enhancing its performance (Zhan *et al.,* 2009).

Mechanical properties are determined by the cellulose content and microfibril angle. A high cellulose content and low microfibril angle are desirable properties of a fibre to be used as reinforcement in polymer composites (Han *et al.,* 2013). The tensile strength is more sensitive to the matrix properties, whereas the modulus is dependent on the fibre properties. To improve the tensile strength, a strong interface, low stress concentration, fibre orientation is required whereas fibre concentration, fibre wetting in the matrix phase, and high fibre aspect ratio determine tensile modulus (Han *et al.,* 2013).

The aspect ratio is very important for determining the fracture properties. In short-fibre-reinforced composites, there exists a critical fibre length that is required to develop its full stressed condition in the polymer matrix. Fibre lengths shorter than this critical length lead to failure due to debonding at the interface at lower load. On the other hand, for fibre lengths greater than the critical length, the fibre is stressed under applied load and thus results in a higher strength of the composite. For good impact strength, an optimum bonding level is

necessary. The degree of adhesion, fibre pullout, and a mechanism to absorb energy are some of the parameters that can influence the impact strength of a short-fibre-filled composite. The properties mostly vary with composition as per the rule of mixtures and increase linearly with composition. However, it has been observed that this linear dependence on percentage of fibre content does not hold at high percentage (80 %) of the fibre, probably due to lack of wetting of the fibre surface by the polymer (Cui *et al.*, 2011).

A composite is a material that contains two or more distinct constituents or phases, and the amount of the minor phase must be greater than a reasonable proportion (~5 %) so that the composite properties are much different from those of the constituents. (Boluk *et al*. 2012). The continuous and often major phase is termed matrix, which can be ceramic, metallic or polymeric. The second phase is referred to as the reinforcement, either fibrous or particulate.

The food and agricultural organization (FAO) in her report on Pineapple cultivation, indicated that Nigeria is the 7th largest world cultivator of pineapple plants, with about 0.9 million tons of fruit harvested annually (FAOSTAT, 2016). Old leaves must be removed regularly. The weight of these leaves is about 7 % that of the fruit. Hence, in Nigeria, around 63,000 tons of fibre-rich pineapple leaves are removed from the plants each year. One possible way to increase the profitability of pineapple by-products, such as the pineapple leave fibre (PALF) is to convert these discarded leaves by compounding them with thermoplastics such as Polypropylene (PP) material to form reinforced biocomposites (Gadzama *et al.*, 2020).

1.2 Statement of Problem

Pineapple leaf is predominantly considered as an agricultural waste, most especially in Nigeria. Research has proven that it is a very good source of natural fibre. The aforementioned fact gave birth to the desire to convert this enormous quantity of agricultural waste to useful industrial, commercial or domestic use. Based on research conducted, there is no known research carried

in the area of interest of this research work, most especially at the micro and nano dimensions of the PALF. This study does not only seek to bring some solutions to the issue of environmental pollution associated with the pineapple leave waste in Nigeria, but seeks to study the effect the PALF dimensions would have on the physical, mechanical and thermal behaviour of the PALF / PP composites to be produced.

1.3 Justification / Significance of the Study

The significance of this research work stems from the need to study the effect of texture of PALF reinforced PP composites on its physical, mechanical and thermal properties. The research is also, focused on the effect the surface modifications of PALF at different dimensions specifically, macro (2 to 6 mm,), micro (70 - 300 µm) and nano (20 - 500 nm) would have on the aforementioned properties of the PALF reinforced PP Composites. Using NaOH, ZnCl, HNO_3 and $C_3H_60_3$ as surface modification agents. Again, the research work aside contributing to the bank of knowledge, seeks to not only introduce a new class of reinforced composite, but to seek industrial areas of utilization of the composites fabricated. To date a number of research has been done on PALF reinforced PP composites at micro level, no available data indicates that work has been carried out on the effect of surface modifications of the PALF on the physical, mechanical and thermal properties of PALF reinforced PP composites at the micro and nano fibrils dimensions of the filler. It is believed that the behaviour of same material at the nano dimensions improves tremendously when compare with same materia at the nano dimensions. It is this very gap this research work is set to study.

1.4 Scope and Limitations

This research is limited to the study of modifications of filler dimensions and the effect of the modification on thephysical and mechanical properties of pineapple leaf fibre reinforced polypropylene composites. It is limited to the study of the effects of NaOH, ZnCl, HNO_3 and $C_3H_60_3$ as surface modification agents. It is also, limited to the study of the effect of dimensions

of the PALF within the ranges of 2 to 6 mm, 70 - 300 µm and nano 20 - 500 nm at the macro, micro and nano dimensional scales respectively.

1.5 Aim and Objectives of the Study

The Aim of the Research is to study the effect of Filler Dimensions on some major Properties of Pineapple leaf fibre-Reinforced Polypropylene Composites.

The Objectives of the Research are to:

1. Extract fibre from pineapple leaves.
2. Treat the fibres with surface modification agents namely; NaOH, ZnCl, HNO_3 and $C_3H_60_3$
3. Characterize the extracted pineapple leaf fibres; to determine the cellulose, hemicellulose and lignin contents.
4. Convert the PALF into micro- and nano- particles (70 - 300 µm and nano 20 - 500 nm) respectively.
5. Produce composites using polypropylene as matrix and pineapple leaf fibre as the reinforcing agent.
6. Study the effect of filler dimensions/sizes (macro, micro and nano) respectively on the:
    i. Physical Property of the composites.
    ii. Mechanical Properties of the composites.
    iii. Thermal Property of the composites.
7. Study effect of surface area changes as filler reduces from macro to micro and from micro to nano.
8. Fabricate molds that will be used for the mechanical property tests, using ASTM D638-11 for tensile tests, ASTM D256-11 for flexural tests and ASTM D790-17 for Izod impact test and thermal properties test using ASTM E1530-II standard.

CHAPTER TWO

LITERATURE REVIEW

2.1 Pineapple Leave Fibre

Every year tonnes of pineapple leaf fibres are being produced, though very small portions are being used in the field of feedstock and energy production. The expansion of bio composites has amplified industrial usage that would release the possibilities to minimize the wastage of renewable materials. PALF promotes a non-food-based market for agricultural industry as reported by Cherian *et al.,* (2010) It is white in colour, smooth, and glossy as silk, medium length fibre with high tensile strength, it has a softer surface than other natural fibres and it absorbs and maintains a good colour (Bengtsson *et al.,* 2005).

PALF constitute cellulose (70–82 %) and arrangement of fibres is the same as in cotton (82.7 %). In all the collection, pineapple leaf fibre is more compatible natural fibre resource and constitutes a good chemical composition. PALF has better mechanical strength than the jute when it is used in making of fine yarn as reported by Debasis and Sanjoy (2007).

The cellulosic molecules model of PALF is a three-dimensional structure and parallel to crystalline region of the fibre. Remaining parts of molecular structure are supposed to associate within amorphous regions. Pineapple leaf fibre (PALF) is vital natural fibre, which have high specific strength, rigidity, and flexural and torsional rigidity as much as jute fibres. Considering these exclusive properties of PALF, industries can use it as an outstanding alternative raw material in the prospect of reinforcing composite matrixes. (Lopattananon *et al.,* 2006).

2.1.1 Extraction of Pineapple Leaf Fibre (PALF)

It is essentially important to understand the extraction of pineapple leaf fibres before discussing further into the fabrication processes involved in producing the reinforced composites.

Traditional extracting techniques of the PALF are by using hand scraping, decortications and retting (Danladi and Shu'aib, 2014).

It is more common to find that the PALF leaves are extracted from the plant by hand, which involve stripping off of the fibre from the retted leaves, hence leading to several constraints; labor intensive and costly process in addition to affecting the properties of the fibre. Due to these problems, extraction by machine have been developed and used, although such processes is relatively much slower than hand scrapping but aid in production processes (Mwaikambo, 2006).

Asim *et al.,* (2015) described the extraction process of the pineapple leaves as a process that involves the scrapping, retting, followed by mechanical separation of the fibres prior to drying in air. During the scrapping process, the pineapple leaves are fed through a feed roller, passing through the second roller called scratching roller in which the upper leaf is scratched and the wax layer is removed. Lastly, the leaves will enter the area where the serrated roller is position for the leaves to be crushed and makes several breaks for the entry passage for the retting microbes. They further described that following the scarping process, the scratched pineapple leaves are immersed in a water tank containing substrate: liquor in 1:20 ratio and 5 % of urea or diammonium phosphate (DAP) for fast reaction during the retting process. Consequently, the fibres are segregated mechanically during rinsing process in pond water prior to drying in the air. In addition, there are two ways in which PALF can be extracted; these being ball mill and disc mall, with the wet ball milling offering greater number of elementary fibre although the speed of process is much slower. Such extraction methodology is claimed to be simpler and able to produce high fibre yield and smaller fibre relative to conventional methods (Asim *et al.*, 2015).

A mechanical extraction process was reported by Munirah *et al.,* (2007) in which the pineapple leaves were pressed using a two-roll milling machine to remove circa that is about 90 % of the

water content. The fibres were then extracted manually from the semi-dried pineapple leaves using knife or sharp tool. Following these, the short fibres undergone cleaning process where they were washed thoroughly in 2 % detergent solution at temperatures of approximately 70 °C followed by rinsing in tap water. The purpose of this cleaning process is to remove foreign objects and impurities present in the fibres. This is followed by drying process in the oven at 70 °C for 24 hours before undergoing further processing and characterization (Munirah *et al.*, 2007).

Yusof *et al.*, (2015) did not only came up with a novel and sustainable technology in extracting the pineapple leaf fibres in fabricating the reinforced composites. They developed a customize decortication machine called Pineapple Leaf fibre Machine 1 (PALF M1) in Universiti Tun Hussein Onn (UTHM), Batu Pahat, Johore, Malaysia to extract the pineapple leaf fibre in a more efficient and sustainable way (Yusof *et al.*, 2015) .

2.1.2 Chemical Composition of Pineapple Leaf Fibre (PALF)

The chemical composition of PALF is depicted in Table 2.1. Pineapple leaf fibres have many chemical constituents like cellulose, pentosans, lignin, fat and wax, pectin, nitrogenous matter, ash content, degree of polymerization, crystallinity of cellulose, and antioxidants, PALF has a large quantity of cellulose (81.27 %), low quantities of hemicelluloses (12.31 %), and lignin content (3.46 %) as reported by Rahman *et al.*, (2011). PALF has higher cellulosic content as compared to other natural fibres like oil palm frond, coir, and banana stem fibres (Khalil *et al.*, 2006). The higher quantity of cellulose in PALF supports the higher weight of the fruit (Reddy and Yang 2005). The chemicals composition fibre directly affects performance of fibres as reported by Wirawan *et al.*, (2009).

Table 2.1. Chemical compositions of pineapple leaf fibre

Chemical Composition (%)	Source		
	Yu (2015)	Mishra *et.al* (2004)	Munirah *et al.*,2007
Cellulose	56 - 62	70-82	-
Hemicellulose	16 -19	5-12	9.45
Hollocellulose	-	-	87.56
Alpha cellulose	-	-	78.11
Lignin	9 - 13.0	5-12	4.78
Pectin	2.0 - 2.5	-	-
Fat and wax	4.7	-	-
Ash	2.0 - 3.0	-	-

(Source: Mishra *et al.,* 2004, Munirah *et al.,* 2007 and Yu 2015)

2.1.3 Physical and Mechanical Properties of Reinforced PALF

Fibre composite plays a huge share in biocomposite and material science. PALF has been proved as a good substitute of synthetic fibres, because of its economical and renewable nature. Specific strength of natural fibre supports in enhancing the physical and mechanical strength of polymer matrix without using any additional processing. The superiority of PALF mechanical properties is related with the high content of alpha cellulose content and low microfibrillar angle (14°)**.** Due to extraordinary qualities of PALF, it can be used as reinforcing composite matrix. (Lopattananon *et al.,* 2006). The physical and mechanical properties of any natural fibres depend on fibre-matrix adhesion, volume fraction of fibre, aspect ratio, orientation, and stress transfer efficiency at interface (Arib *et al.,* 2006).

Table 2.2 shows the physical and mechanical strength of PALF. The PALF exhibits a modulus range from 34.5 to 82.51 MPa, tensile strength ranges from 413 to 1627 MPa, and an elongation at break-point ranges from 0.8 to 1.6 %. PALF can sustain abrasiveness as reported by Chad *et al.,* (1988).

Table 2.2 Physical and Mechanical Properties of PALF

Properties	Source		
	George *et al.*,1998	George *et al.*, 2001	Leão *et al.*, 2015
Cell length (mm)	-	-	-
Diameter (µm)			5.0-30.0
Moisture content (%)	-	-	-
Vicat softening point (°C)	104.0	-	-
Density (gcm-3)	1.526		1.44
Tensile strength (MPa)	170.0	-	170
Ultimate tensile strength (MPa)	-	413-1627	-
Young's Modulus (MPa)	6.25	-	6.26
Elongation at break (%)	3.0	0.8-1	1.6
Flexural Modulus	-	0.24 - 0.40	-

(Source: George *et al.*, 1998, George *et al.*, 2001, Leão *et al.*, 2015)

2.2 Some Surface Modifications Techniques of PALF

The development of natural fibres reinforced composites or biocomposites has not progress as rapidly as its competing synthetic glass fibre due to two main major challenges, which are poor moisture resistance and low impact strength. Also, fabricating natural fibre reinforced composites normally involves bringing together two or more materials that are incompatible. Since natural fibres are hydrophilic while the matrix systems are normally hydrophobic, to overcome this compatibility issue, it is common practice to introduce surface treatment of the fibres with the intent of changing the interfacial chemistry or physical properties of the fibres. In order to enhance the composite system performance, surface treatments of the raw natural fibres may include acetylation, biological treatments, bleaching, grafting, mercerization, oxidation, plasma treatment and scouring, etc (Siregar *et al.* 2012)

Often more combination of two types of treatment was employed to improve the adhesion of the fibre / matrix. Siregar *et al.*, (2012) reported that by combining the alkaline treatment and poly (styrene-co-maleic anhydride) compatibilising agent in 50 % PALF reinforced high

impact polystyrene (HIPS) gave a tremendous improvement on their tensile strength. Alkaline treatment removed the natural and artificial impurities which in turn increased wettability of the alkali treated fibres with the matrix. Mwaikambo and Ansell (2003) concluded that by removing of the impurities created a rougher surface and help to form a better mechanical in-terlocking and increased the interfacial adhesion. They also noted that by adding 2 weight % poly(styrene-co-maleic anhydride) coupling agents, the composite strength increased by about 34 MPa, approximately by 48 % in comparison to the untreated fibres. During fabrication, the chemical composition from the compatibilising agent interacts with the fibres and forming a bridge of chemical bonds between the fibre and matrix resulting in increased in their mechanical properties (Siregar *et al.,* 2012).

Huda *et al.* (2008) studied the effect of modifying surfaces of the PALF using both alkaline treatment and silane treatment on the overall mechanical properties of the PALF reinforced PLA biocomposites. For the alkaline treatment, sodium hydroxide (5 weight % w/v) was used in which the PALF were immersed in the solution for 2 hours at room temperature. Following this, the PALF fibres were washed with distilled water which contained a few drops of acetic acid and distilled water until the sodium hydroxide was removed. Consequently, the fibre underwent air drying for 2 days and lastly, the fibres were oven dried at 80 °C for six hours before vacuum oven dried at the same temperature and duration of time. They claimed that this treatment will roughened topography of the fibre surface hence improve the adhesion between the fibre and the polymer matrix (Huda *et al.* 2008).

The second surface treatment considered in the study by Huda *et al.,* (2008) is using silane treatment. Here, 5 weight % silane (3-aminopropylsilane (APS)) was hydrolyzed in a mixture of water and ethanol with the ratio of 40: 60 w/w. Such chemical treatment is expected to initiate bonding between the silanol groups with the PALF fibre surface, which in simple words function as connector molecules between the matrix and the fibre. In addition, they also

investigated the effect of using both alkaline and silane treatment on the mechanical properties of the biocomposites. From the experimental work, it has been reported that both silane-treated fibre reinforced composites and alkaline treated fibre reinforced composites offered superior mechanical properties compared to untreated fibre reinforced composites (Huda *et al.*, 2008).

2.2.1 Alkali Treatment

Alkali treatment of natural fibres, also called mercerization, is the common method to produce high-quality fibres. The scheme of the reaction is:

$$\text{FIBRE-OH} + \text{NaOH} = \text{FIBRE-O-Na+} + H_2O \qquad 2.1$$

Mercerization leads to fibrillation which causes the breaking down of the composite fibre bundle into smaller fibres. Mercerization reduces fibre diameter, thereby increases the aspect ratio which leads to the development of a rough surface topography that results in better fibre/matrix interface adhesion and an increase in mechanical properties (Kalia *et al.*, 2014). Moreover, mercerization increases the number of possible reactive sites, allows better fibre wetting and gets an effect on the chemical composition of the hemp fibres, degree of polymerization and molecular orientation of the cellulose crystallites due to cementing substances like lignin and hemicelluloses which were removed during the mercerization process. As a result, mercerization had a long-lasting effect on the mechanical properties of hemp fibres, mainly on fibre strength and stiffness. If the treatment is done at high percentage of NaOH there could be an excessive extraction of lignin and hemicelluloses which can results in damage of the ultimate cells walls. Similar reductions of mechanical properties after alkali treatment have been reported in the literature (Rodriguez *et al.*, 2012).

2.2.2 Acetylation Treatment

Acetylation was originally applied to wood cellulose to stabilize the cell walls against moisture, improving dimensional stability and environmental degradation and to introduce plasticization to cellulosic fibres by esterification. Acetylation is based on the reaction of cell wall hydroxyl groups of lignocellulosic materials with acetic or propionic anhydride at elevated temperature (Figure 2.1). Pre-treatment of fibres with acetic anhydride substitutes the polymer hydroxyl groups of the cell wall with acetyl groups, modifying the properties of these polymers so that they become hydrophobic (Anderson *et al.*, 2003; George *et al.*, 2001, 1998; Rowell, 1997). Hydroxyl groups that react with the reagent are those of lignin and hemicelluloses (amorphous material), whereas the hydroxyl groups of cellulose (crystalline material) are being closely packed with hydrogen bonds, prevent the diffusion of reagent and thus result in very low extents of reaction (Rodriguez, *et al.*, 2017).

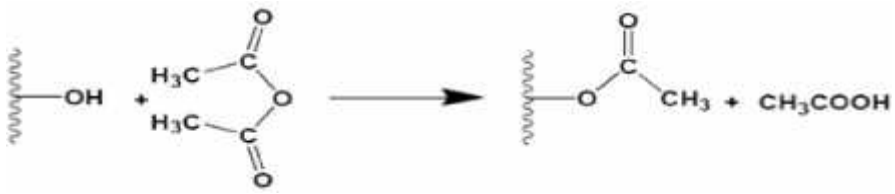


Figure 2.1 Scheme of acetylation reaction (Source: Rodriguez, *et al.*, 2017).

2.3 Polypropylene as a Thermoplastic

Plastics are categorized into four main groups namely; thermoplastics, elastomers, thermosets and polymer compounds. Macromolecular structures distinguish the class of any plastic material as well as its physical properties. Elastomers and thermosets have soft and hard elasticity, respectively; and their resins cannot be melted for recycling purposes. However, thermoplastics are either amorphous or semi-crystalline. Amorphous resins are disordered statistical oriented macromolecules whereas semi-crystalline resins macromolecules are nearly ordered since they are embedded with crystalline phases. Typical amorphous resins are

polycarbonate (PC), polystyrene (PS) and polyvinylchloride (PVC) where typical semi-crystalline resins includes polyamide (PA) and polypropylene (PP) (Klein, 2011).

Polypropylene (PP) has an excellent chemical resistance and can be processed through many converting methods such as injection molding and extrusion. Polypropylene is a polymer prepared catalytically from polypropylene. It is major advantage is related to the high temperature resistance which makes PP particularly suitable for items such as trays, funnels, pails, bottles, carboys and instrument jars that have to be sterilized (cleaned) frequently for use in a clinical environment. Polypropylene is a free-color material with excellent mechanical properties and it is better than polyethylene for the previous reasons **(**Hisham and Maddah, 2016**)**.

Polypropylene is a vinyl polymer in which every carbon atom is attached to a methyl group and can be expressed as shown in Figure 2.2. Polypropylene is a free-color material with excellent mechanical properties and it is better than polyethylene for the previous reasons (Hisham and Maddah, 2016). Polypropylene is a downstream petrochemical product that is derived from the olefin monomer polypropylene. The polymer is produced through a process of monomer connection called addition polymerization. In this process, heat, high-energy radiation and an initiator or a catalyst are added to combine monomers together. Thus, polypropylene molecules are polymerized into very long polymer- molecules or chains. Polypropylene is a vinyl polymer in which every carbon atom is attached to a methyl group and can be expressed as shown in Figure 2.2 (Hisham and Maddah, 2016).

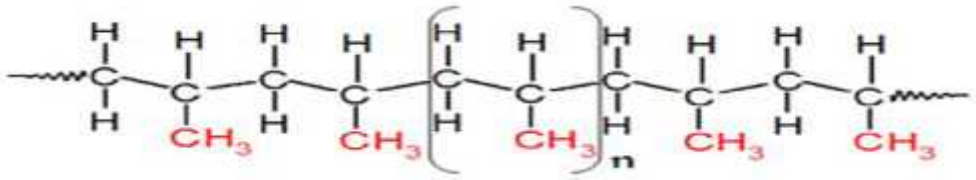


Figure 2.2 polypropylene structure (Source: Hisham and Maddah, 2016)

There are three major sources of polypropylene: from steam cracking of naphtha, gasoline refining process and propane dehydrogenation technology (Shubhra *et al.,* 2011). Polypropylene is the most important material among polyolefins due to three main reasons. First, great properties of PP such as low density, high melting temperature and chemical inertness with low cost making PP optimum for long-life applications. Second, polypropylene is a highly versatile material meaning that diversity in structural designs and mechanical properties are achievable. Third, different morphological structures of PP are possible by using fillers or reinforcing agents and blending PP with other polymers which yield to have superior characteristics. Special and reinforced polypropylene grades include elastomer-modified PP, elastomer modified filled PP, glass fibre reinforced PP, filled PP, esthetic filled PP, flame-retardant PP and thermoplastic elastomers (Galli *et al.*, 1984).

2.3.1 Polypropylene Properties and Types

In order to understand the different types of polypropylene, one needs to dig in and understand thermoplastics categories with a different point of view. Thermoplastics are categorized into two groups: commodity thermoplastics, this group covers the major plastics such as polyethylene, polypropylene, polystyrene and polyvinyl chloride. They have further sub-divisions such as PP-homo-polymers and Co-polymers, PVC-Rigid and Plasticized, polyethylene (PE)-High density, low density and linear low density. Engineering thermoplastics is the second thermoplastics group and products in this class are related to electrical and mechanical engineering applications. Using these plastics may replace other materials like metals and load-bearing components. These include polysulfone, nylons, polycarbonates, acetal and acrylonitrile butadiene styrene (ABS) terpolymers (Shubhra *et al.,* 2011)

However, thermoplastics are characterized by softening upon heating and hardening by cooling which is an advantage in processing procedures such as extrusion or injection

molding where discarded materials can be recycled. Polypropylene is found in three stereo specific configurations: isotactic, methyl groups on one side of polymer backbone, syndiotactic, methyl groups alternate on both sides and atactic, irregular arrangement of methyl group. Melting point of perfectly isotactic PP is 171 ^{0}C, but syndiotactic PP (30 % crystallinity) has a melting point of 130 ^{0}C (Shubhra *et al.*, 2011).

Polypropylene is attractive to petrochemical companies because of its great properties. For instance, polypropylene is semi-rigid, translucent, a good chemical resistance, tough, a good fatigue resistance and a good heat resistance. Moreover, PP has high softening or glass-transition point, high resistance to flexing stress, low water absorption, good electrical resistance, a lightweight, dimensional stability, high impact strength and a non-toxicity property. PP is stiffer than high density polyethylene (HDPE) and biaxial orientation of PP results in films and containers with superior optical and barrier properties (British Plastics Federation, 2011).

There are three different types of polypropylene. First, polypropylene containing only polypropylene monomer in a semi-crystalline solid form; which is called a homo-polymer *PP* (HPP). Second, polypropylene containing ethylene as a co-monomer in the PP chains at levels in the range of 1-8 % and this is referred to as a random copolymer (RCP). Third, HPP containing a co-mixed RCP phase that has an ethylene content of 45-65 % is referred to as an impact copolymer (ICP). In general, polymers consisting of identical monomers are called homo-polymers where polymeric compounds with more than one type of monomer in their chains are known as co-polymers (HMC Ploymer, 2019).

Impact polymers are optimal at low temperatures with higher impact resistance. The RCP part of the mixture is designed to have ethylene contents in the order of 40-65 % ethylene and it is called the rubber phase. The rubber-like reinforcement greatly improves impact strength

particularly at low temperatures (below 20 ^{0}C). However, stiffness is retained resulting in excellent stiffness/impact balance. ICP product as well as the impact resistance varies with respect to size, shape and distribution of the rubber particles. A comparison between homo-polymers and copolymers in their advantages and disadvantages of PP, in general, is illustrated in Table 2.3 (HMC Polymers, 2019).

Table 2.3 Advantages and Disadvantages of polypropylene

ADVANTAGES		DISADVANTAGES
Homopolymer	Copolymer	Degrade by ultraviolet (UV) light
Process ability, good	Process ability, high	Flammable, but retarded grades available
Impact resistance, good	Impact resistance, high	Attacked by chlorinated solvents and aromatics
Stiffness, good	Stiffness, high	Several metals accelerate oxidative degrading
Food contact, acceptable	Food contact, not preferable	Low temperature impact strength is low

(Source: HMC Polymer, 2019)

Generally, different PP grades are available depend on the required application. Commercial grades are available in a variety of molecular weight distributions, and co-monomer types as well as contents and additives. Enhanced physical properties allow polypropylene to be the core material in most demanding applications such as films, fibres, tapes, sheets, thermoforming, injections, and blow molding (HMC Polymers, 2019).

Some mechanical and thermal properties of commercial polypropylene plus a comparison of thermal conductivity of different plastics are shown in Table 2.4 and Table 2.5, respectively (Brydson, 1999; Andrady and Mike, 2009).

Table 2.4 Mechanical and Thermal Properties of polypropylene

Property	Homopolymer			Copolymer	
Melt flow index	3	0.7	0.2	3	0.2
Tensile Strength (MPa)	34	30	29	29	25
Elongation at break (%)	350	115	175	40	240
Flexural modulus (Mpa)	1310	1170	1100	1290	1030
Brittleness temperature (^{0}C)	+15	0	0	-15	-20
Vicar softness point (^{0}C)	154-150	148	148	148	147
Rockwell Hardness (R-Scale)	95	90	90	90	88.5
Impact strength (J/m^2)	10	25	34	34	42.5

(Source: Brydson, 1999)

Table 2.5 Thermal Conductivity

Polymer	Thermal conductivity (WmK^{-1})
Expanded polystyrene	0.035
Polyurethane foam	0.025 - 0.035
Phenolic	0.035
Polypropylene	0.17
Polyethylene	0.17

(Source: Andrady and Mike, 2009)

2.4 Fabrication of Pineapple Leaf Fibre (PALF) Reinforced Composites

There are various approaches in which fabrication process of the PALF composites have been discussed; these include processing method based on matrix materials such as thermoplastic, thermoset, rubber as well as based on techniques such as melt-mixing, compression molding or solution mixing. In this section, however, available fabrication process of PALF reinforced composites are discussed based on the fibre architecture, particularly its geometry, which is classified as short and continuous long fibres, with the latter having length of more than 100 mm.(Asim *et al.*, 2015)

2.4.1 Short Fibre PALF Reinforced Composites

Short fibre PALF reinforced composites can be produced using various methods depending on the types of matrix materials. In general, thermoplastic matrix composites can be produce by adopting one or two techniques such as solvent casting such as prepregging, melt mixing (e.g. extrusion) and melt forming such as injection molding, compression molding, thermoforming and etc (Zhou *et al.*, 2012)

Extrusion process is often used for melt mixing the raw materials such as resin/ matrix with the reinforcement being in the form of particulate or short fibres. During the extrusion process, raw materials (often supplied in pellet form) and reinforcement are fed into the hopper and the motor-driven screw will then extrude the material through the nozzle. Shape of the extruded materials can be controlled by carefully selecting the type of die required. The temperature of the extrusion head is specifically controlled and the temperature profile typically increases from the feed zone to the die. This is to allow sufficient melting time and prevent from thermal degradation of the mixer (Zhou *et al.*, 2012).

Injection molding process is a well-known process for thermoplastic-based resin; normally use to produce plastic materials with no reinforcement. However, this method can be adopted to produce short fibres composites when stiffness is of important requirement. Generally, this

process starts with the resin in the pellet form containing short fibres is fed into the hopper and passed through to the barrel of the machine. In return, the screw pushes the materials are further forward into the barrel and squeezing it to remove any entrapped gasses. The resin is often transformed into liquid form due to friction and shear induced by the screw heats before it reaches the injection chamber. Mechanical shearing cause splitting of the fibres and reduced their length. Following this, the materials are pushed forward by the screw and injected into the mold. The mold is then cooled to solidify the molded component before it is being injected out (Cui *et al.*, 2019)

Another method that is quite popular to form the final shape of the composites is using compression molding. The process begins with placing the mixture containing matrix and reinforcement materials onto the bottom half of preheated cavity mold. This process also enables production of laminated short fibre to be carried out. The mold then is closed and top half is lower and the pressure is increase to the preset level. With increasing pressure, the materials start to melt and flow into the cavity. The mold then is then cool down and the product is removed from the mold (Asim *et al.*, 2015)

Often, two-step methods are adopted to produce composites. The first stage is mixing method which can be done through melt mixing using an internal mixer or rotor mill or via solution mixing where the matrix is dissolve in solvent. This is followed by forming method such as injection molding or compression molding to form the composites at the desired shape (Asim *et al.*, 2015)

George *et al.*, (2014) has successfully produced short pineapple-leaf-fibre-(PALF)-reinforced low-density polyethylene (LDPE) composites using melt-mixing and solution-mixing methods. Prior to mixing process, short fibres with different length of 2, 6, and 10 mm were cleaned with water and dried in oven for 24 hours at 70 °C. The process of melt mixing was carried out using an internal mixer at different rotor speed, mixing time and chamber

temperature. Meanwhile, for the solution-mixing method, the LDPE were dissolved in toluene to form viscous slurry. The short fibres were then added to the slurry and stirred to ensure a good coating and were later dried at room temperature to evaporate off the solvent. Both of the composites were extruded at 120 °C. The profile were directly extruded into the mold for random fibres orientation composite, while for controlled fibre orientation composite, the extruded profile were carefully aligning in a mold followed by compression molding at 120 °C (George *et al*.,1995).

They also reported that for the melt mixing method, the optimum fabrication conditions were achieved at mixing time of 6 minutes with the rotor speed of 60 rpm, and mixing temperature of 130 °C. Morphology analysis revealed that a higher degree of damage such as splitting and peeling to the fibres occurred at higher rotor speed resulting in declining of the mechanical properties (George *et al*..1995). They argued that such observation is possibly due to better dispersion of the fibres in the matrix, low fibres damage and better adhesion were achieved with solvent mixing. They also reported that only 5 % of 6 mm of fibres length were retained using melt mixing in comparison to the 70 % produced by solution mixing. Reductions in fibre length are the direct result of damage occurred during mixing which lead to lower mechanical properties (George *et al.,* 1995)

In another study, Liu *et al.,* (2005) considered two processing methods to produce soy-based bioplastic and pineapple leaf fibre composites, using twin-screw extrusion followed by injection molding, with the focus on assessing the effect of different fibre loading and polyester amide grafted glycidyl methacrylate (PEA-g-GMA) as compatibilizer on the properties of pineapple leaf fibre reinforced soy based bio-composites. Morphological study using SEM revealed two important observations; Morphological change in the PALF fibre bundles as an effect of the processing which changes the fibre diameter hence resulting in an improved fibre dispersion in matrix and the improved fibre reinforcement efficiency, and dispersion of the

fibres is poorer at high fibre loading (30 weight %), however this is not in the case when compatibilizer was used. They suggested that such observations are possibly due to interactions between epoxy groups in PEA-g-GMA and hydroxyl groups in the pineapple leaf (Liu *et al.*, 2005).

Similar techniques were used by Threepopnatkul *et al*. (2009) to produced PALF reinforced composite with fibres length of 2 mm. Prior to the fabrication process, the fibres surface were treated using 1 % w/w silane (weight percentage compared to the fibre) in which was dissolved for hydrolysis in methanol solution with pH was adjusted to 3.5 using acetic acid. During the surface treatment, the fibres were soaked in the solution for 6 hours followed by air dried at room temperature. Both untreated and silane-treated PALFs were mixed with PC using diisononyl phthalate 3 % w/w (weight percentage compared to PC) internal mixer, at temperature of 230 °C with rotor speed of 10 rpm for 3–6 min. In this study, four different fibre concentration (0, 5, 10 and 20 weight %) were used. The mixtures were then injected using injection molding to produce the specimen for mechanical testing (Threepopnatkul *et al.*, 2009).

In another study, Kengkhetkit and Amornsakchai (2014) produced PALF reinforced polypropylene composite using two steps process. Initially, the matrix and fibres were mixed using two-roll mill for 15 min by keeping temperatures of the front and back rollers at 185 °C and 175 °C, respectively. The mixture then was stretched to form unidirectional prepreg. Later, the prepreg was then compression molded at a temperature of 195 °C under a pressure of 3.5 MPa for 5 minutes, fol-lowed by cooling under the pressure of 7.0 MPa for 3 minutes to form sheets with thickness of 1 and 3 mm respectively (Kengkhetkit and Amornsakchai, 2014)

Short fibre reinforced rubber composite have exceptional mechanical properties due to unique combination of fibre rigidity and rubber elasticity. More recently, Prukkaewkanjana *et al.*, (2015) developed rubber composites that exhibit a very high modulus at low elongation, high

elongation at break and strong. In this study, they produced hybrid composites by combining short fine pineapple leaf and carbon black.

Smitthipong *et al.,* in 2015, manufactured the PALF reinforced thermoplastic starch (TPS)/PLA composites via blending the component using single screw extrude. Prior to blending, the TPS was prepared by mixing of cassava starch, glycerol and water as a plasticizer with ratio of 65 weight % cassava starch, 26 weight % glycerol, and 9 weight % water manually. PALF short fibres of 1-mm length were then added at 2–10 weight % of the total TPS. The blend was extruded and pelletized. Consequently, the PALF/TPS was blended with PLA (0, 20, 40, 60 and 80 weight %) using single screw extruder at 180 °C and 180 r/min. The extruded profiles were then hot compression molded at 95 °C and 180 °C, respectively, with a pressure load of 15 MPa. Viscosity, water solubility as well as tensile properties of the composite were measure. The results showed that using short pineapple fibres in thermoplastic starch (TPS) and PLA blends improved the mechano-static properties as well as water resistance of the composites (Smitthipong *et al.,* 2015).

2.4.2 Long Fibre PALF Reinforced Composite

To date, there is still limited amount of published work on the continuous long PALF fibre reinforced composites. Arib *et al.,* (2006) manufactured continuous PALF fibre reinforced polypropylene composites using compression molding technique by laying down one layer of PALF fibres between two layers of thin polypropylene films in parallel array onto a stainless steel mold platen using a carver press machine with a temperature and pressure control. Here, heating was started immediately and a pressure of 12.4 MPa was introduced when the temperature reached 180 °C, with a soaking time of 5 minutes (Arib *et al.,* 2006)

Following this, the stainless steel mold platen was removed quickly from the press for cooling process to take place, with an aid of a cooling fan to expedite the cooling process. Consequently, 3-mm thick composite laminates produced from this process were characterized

mechanically via tensile testing as per ASTM-D638 and three-point bending testing as per ASTM- D790, as well as surface analyzed using a scanning electron microscope (SEM). It has been observed that even with small fibre loading (approximately 2.7 by volume fraction) in the composite system showed enhancement in both the tensile and flexural properties in comparison to that of the plain polymer. However, further work on improving the fibre-matrix bond strength and achieving homogeneous fibre distribution are required to significantly improve the overall composite performance as potential substitute to synthetic polymer composites such as glass fibre (Arib *et al.,* 2006).

Chollakup *et al.,* (2011) studied the effects of fibre length and fibre content on the PALF reinforced thermoplastic composites. In their study, both the short and long PALF fibres, with fibre final length being 40 mm and 140 mm respectively were considered as reinforcement for LDPE and PP thermoplastic materials. fibre mats with different directions, in which the fibres were aligned along the leaf length direction were produced. The long PALF fibre was arranged separately in parallel arrays which covered a 100 mm x 100 mm stainless steel plate, whereas the short PALF fibres were randomly arranged by means of a mini card machine to form a non-woven mat (Chollakup *et al.*, 2011)

For the plain thermoplastic polymer matrices, both the LDPE and the PP thin films with nominal thickness of 3 mm were prepared by a heat press machine at temperatures of 180° and 240° respectively, with an applied pressure of 12.5 MPa for 3 minutes. To minimize manufacturing defects such as voids and air bubbles, the specimens were repeatedly depressurized and pressurized at each melting temperature for 3 minutes. Following these, slow cooling to room temperature at a pressure of 12.5 MPa for duration of 30 minutes, to produce thin films with nominal thickness of 0.25 mm. Composite laminates with thickness of 0.5 mm were produced by laying up one layer of the fibre mat between two layer of either the LDPE or the PP sheets at the melting temperature of 160 °C and 185 °C respectively. It was

observed that the long PALF fibres rein-forced composites exhibit superior tensile strength in comparison to those of the short fibre reinforced composites. In addition, SEM analysis showed evidence of good dispersion of the long fibre in the composites (Chollakup *et al.,* 2011) Yaacob in 2015, manufactured continuous long alkaline-treated PALF fibre reinforced PLA composites via compression molding process in which the pineapple leaf fibres (extracted from *Josapine* pineapple) with fibre weight fraction of 30 weight % and fibre length of more than 100 mm were pre-treated using 5 weight % sodium hydroxide. Here, care was taken while handling the PALF fibres to ensure significant improvement in the mechanical properties of the reinforced PLA composites. The treated PALF fibre bundles were air dried for 48 hours before stored in a desiccator prior to usage and brushed to ensure good fibre alignment prior to lamination process in which the PALF fibres were laid down in between (Yaacob, 2015)

2.4.3 Epoxy Based PALF Reinforced Composites

Epoxy resin has excellent properties like adhesion, strength, low shrinkage, corrosion protection, and many other properties. Although it is expensive resin, its mechanical and chemical properties are very good. Natural fibres like jute, flax, sisal, and bamboo fibres with epoxy reinforced have been studied by Van de Weyenbery *et al.,* (2006).

PALF-epoxy composites will exhibit a positive result in interfacial bonding when combination of alkalization and DGEBA solution will be used. Such kinds of surface modification will enhance the flexural, tensile, and impact properties of epoxy composite as reported by Lopattananon *et al.,* (2008).

2.4.4 Polyethylene based PALF Reinforced Composites

A pineapple leaf fibre reinforced with polyethylene exhibits high performance composites as reported by Muniral *et al.,* (2006). In comparison to other natural fibres, pineapple leaf fibre (PALF) shows excellent mechanical and physical properties but the hydrophilic nature of

PALF causes a negative impact. This, a chemical treatment such as alkali, isocyanate, saline, and permanganate was carried out to improve the water resistance. Peroxide modification is very helpful to reduce the hygroscopicity of fibres as reported by George *et al.*, (1998).

2.4.5 Polypropylene based PALF Reinforced Composites

Pineapple leaf fibres (PALF) are renounced as possible and plentiful substitutes for the high-priced and nonrenewable synthetic fibres. PALF enhances the mechanical properties of the polymer matrix through its own high specific strength. PALF is multicellular, lignocellulosic and has very good mechanical properties. In study of stress behaviour of PALF reinforced polyethylene composite, stress is inversely proportional fibre content. Mechanical properties of polypropylene pineapple leaf fibre reinforced composites are reported. The tensile and flexural properties of composites are depending on volume fraction as reported by Arib *et al.*, (2006).

2.4.6 Vinyl ester based PALF Reinforced Composites

Now natural fibres are widely used in the research as a substitute of glass fibre (GF) in fibre reinforced plastics (FRP). In comparison to glass fibre, these natural fibres have lower densities, are economical, consume lesser energies during production, cause less or no abrasion to machines, and are not hazardous to health when inhaled as reported by Mallick, (2008). In spite of these properties, pineapple leaf fibres are untouched in research areas especially for reinforcing plastics although this application is now becoming an important research area. Now polymers composite is focused on using pineapple leaf fibres for developing value added applications. Despite several merits, PALF possesses inherent demerits such as poor interfacial fibre-matrix adhesion and absorbing water. In the last two decades, a lot of researches have been carried out to optimize the problem of the interfacial adhesion between natural fibres and polymer matrices as reported by John and Anandjiwala, (2008).

Moreover, interfacial shear stress (IFSS) is the measurement of fibre-matrix adhesion which is always higher for natural fibre-vinyl ester compared to those of other matrices as reported by Joffe *et al.,* (2003). Most of the work on PALF-reinforced thermoset composites used hand lay-up method in sample preparation and very few if any reported the use of liquid compression molding process. As reinforced matrix, both unmodified and bleached PALF are using in the form of random and unidirectional PALF mats. To evaluate the viability of PALF-vinyl ester eco-composites, there are many criteria of measurement, for instance, mechanical properties, water absorption, and thermal stability (John and Anandjiwala, 2008)

2.4.7 Polyester Based PALF Reinforced Composites

PALF is obtained from the pineapple plant's leaves. Major compounds of PALF are cellulose (70–80 %), lignin (5–12 %), and ash (1.1 %). The recent study proved that by using different surface modified pineapple leaf fibres as reinforcing material can be used for polyester matrix. PALF fibre loading up to 30 % by weight with polyester showed significant increment in flexural strength, tensile strength, and impact strength. Toughness of composite material is reached up to the benchmark of engineering materials. Surface modification by chemical treatment can enhance the strength of individual fibres and it can help to develop better mechanical strength PALF/polyester composite for commercial purpose as reported by Mohammed *et al.,* (2010).

2.4.8 Low Density Polyethylene based PALF Composites

Melt mixing and solution mixing techniques have been used in preparation of PALF reinforced LDPE composites. Solution mixed technique shows a better tensile strength than melt mixed technique. Relation of fibre size, loading %, and orientation with mechanical properties has been studied. Though fibre distribution curve and scanning electron micrographs, it is possible to analyze fibre rupture and damage during composite making. Fibre length of 6 mm length

was found to be suitable for PALF reinforced with LDPE. Mechanical properties are found to be improved and elongation at break is inversely proportional to fibre loading. In comparison to random and transverse orientation, longitudinal orientation of fibres showed better mechanical properties of composites. PALF-LDPE composites are ecofriendly, biodegradable and exhibit superior performance than any other cellulose-fibre reinforced LDPE systems. George *et al.*, (1999).

2.4.9 PALF based Hybrid Composites

Various combinations of natural lignocellulosic composite are promising interest of researchers. It provides wide range of results and properties which is very difficult to achieve through a single type of reinforcement. This type of matrix is generally used for the fibre having good interaction between matrix and fibres and together gives a better mechanical performance as reported by Idicula *et al.*, (2006).

This, hybrid composite is the mixture of two different types of fibres reinforced into a matrix. It has various improved qualities which help to make it best composite. Individual strength of fibres is combined to achieve improved composite with better efficiency. Many researches are in progress for partially or fully replacement to glass fibres (GF) by natural fibres. GF has very good quality of reinforcement along with natural fibres like sisal, jute, pineapple, hemp, and so forth as reported by Ahmed and Vijayarangan (2006); Panthapulakkal and Sain (2007).

2.5 Some PALF/PP Composites Characterization Equipment

2.5.1 Fourier Transmission Infrared Spectroscopy (FTIR)

Fourier-transform infrared (FTIR) spectroscopy is based on the idea of the interference of radiation between two beams to yield an interferogram. The interferogram is a signal produced as a function of the change of path length between the two beams. The two domains of distance and frequency are inter-convertible by the mathematical method of Fourier-transformation.

The radiation emerging from the source is passed through an interferometer to the sample before reaching a detector. Upon amplification of the signal, in which high-frequency contributions have been eliminated by a filter, the data are converted to digital form by an analog-to- digital converter and transferred to the computer for Fourier-transformation (Stuart, 2005).

2.5.2 Scanning Electron Microscopy (SEM)

The Scanning electron Microscope (SEM) has allowed researchers to examine a much bigger variety of specimens. The scanning electron microscope has many advantages over traditional microscopes. The SEM has a large depth of field, which allows more of a specimen to be in focus at one time. The SEM also has much higher resolution, so closely spaced specimens can be magnified at much higher levels. Because the SEM uses electromagnets rather than lenses, the researcher has much more control in the degree of magnification (University, 2014)

Traditional microscopes are dwarfed by the scanning electron microscope when resolution, depth of view and multiple specimen magnification is concerned. The high-resolution imagery produced by the SEM and the use of magnet over lenses provide superior control and a higher degree of magnification. All of these advantages, as well as the actual strikingly clear images, make the scanning electron microscope one of the most useful instruments in research today (University, 2014).

2.5.3 Energy Dispersive X-ray (EDX)

EDX or EDS makes use of the X-ray spectrum emitted by a solid sample bombarded with a focused beam of electrons to obtain a localized chemical analysis. All elements from atomic number 4 (Be) to 92 (U) can be detected in principle, though not all instruments are equipped for 'light' elements ($Z < 10$). Qualitative analysis involves the identification of the lines in the spectrum and is fairly straightforward owing to the simplicity of X-ray spectra. Quantitative

analysis (determination of the concentrations of the elements present) entails measuring line intensities for each element in the sample and for the same elements in calibration Standards of known composition (University, 2014).

By scanning the beam in a television-like raster and displaying the intensity of a selected X-ray line, element distribution images or 'maps' can be produced. Also, images produced by electrons collected from the sample reveal surface topography or mean atomic number differences according to the mode selected. The scanning electron microscope (SEM), which is closely related to the electron probe, is designed primarily for producing electron images, but can also be used for element mapping, and even point analysis, if an X-ray spectrometer is added. There is thus a considerable overlap in the functions of these instruments (University, 2014).

2.5.4 Transmission Electron Microscopy

A transmission electron microscope (TEM) forms an image of an object by firing a beam of electrons through the specimen. The TEM has a high-voltage electricity supply that powers a heated filament called the cathode. The cathode is part of the electron gun. This produces a beam of high energy electrons. The first set of lenses of the TEM, known as a magnetic lens, concentrates the electrons into a powerful beam. This beam is focused onto specific parts of the specimen via a set electromagnetic coil. These coils are called the beam deflection coils. The specimen is usually placed on a copper grid and the beam is allowed to pass through it. After the image has been collected it is magnified by a third set of electromagnetic coils, the projection lens. At the base of the machine, a fluorescent screen, the imaging plate, is positioned so that when the beam from the third coil interacts with it an image is formed (Kong, 2013).

The electron source consists of a cathode and an anode. The cathode is a tungsten filament which emits electrons when being heated. A negative cap confines the electrons into a loosely focused beam. The beam is then accelerated towards the specimen by the positive anode. Electrons at the rim of the beam will fall onto the anode while the others at the centre will pass through the small hole of the anode. The electron source works like a cathode ray tube (Mashego, 2016).

2.6 PALF Applications and Future Prospects

PALF is generally used in making threads for textile fabrics from several decades. Present application of PALF for various purposes is textile, sports item, baggage, automobiles, cabinets, mats, and so forth. Surface modified PALF is introduced for making machinery parts like belt cord, conveyor belt cord, transmission cloth, air-bag tying cords, and some cloths for industry uses. PALF is very good for carpet making because of its chemical processing, dyeing behaviour, and aesthetically pleasing fabric. The use of pineapple leaf fibre can be considered relatively as new in the paper manufacturing industry in Malaysia. PALF can be suitable for various other applications such as cosmetics, medicine, and biopolymers coating for chemicals. (Yusof *et al.*, 2013).

The pineapple leave fibre is one of the natural fibres, having highest cellulosic content nearly 80%. Its density is similar to the other natural fibres while Young's modulus shows highest tensile strength when compared to other natural fibres. These properties are suitable for its application as building and construction materials, automotive components, and furniture. From this review it is clear that limited work has been done on thermal, electrical, dynamic, and mechanical properties. Till now, PALF has been studied as being reinforced with PP and unsaturated polyester only, so it is required to understand its behaviour with other resins also in relation to fabricated bio-composites and hybrid composites. PALF is widely accepted in

textile sector and already used in our daily life materials but we attribute that further study will enhance the application in various other exiting products (Yusof *et al.*, 2013).

2.6 Nano PALF Fibrils

Nanocellulose is usually defined as the cellulosic material that precisely having at least one dimension in the range of 1 to 100 nm. However, it is worth mentioning that there is still a significant incongruity in the terminology and classification of these nano-dimensional cellulose products dictated by the large variability of starting lignocellulosic biomass (origin) and extraction procedures (preparation methodologies and conditions). The unstandardized nomenclature presents in the literature results in some ambiguity and misunderstanding. In general, there are three main structures of nanocellulose, namely nanocrystalline cellulose (NCC), nanofibrillated cellulose (NFC) and bacterial nanocellulose (BNC). They have essentially different in term of morphology, regardless of its nanoscale dimensions. Because of its nano-scale dimensions, nanocellulose exhibits various outstanding and excellent physico-chemical properties compared with typical cellulose material, such as large specific surface area, high porosity, high aspect ratio, excellent tensile strength and modulus, and biodegradability (Cao *et al.*, 2015).

In recent years, many studies have been carried out on the synthesis of nanocellulose fibres as reinforcement agents in polymer nanocomposites. Compared with inorganic reinforcements, the main advantages of this naturally-derived nanostructured cellulosic material are: (i) a wide variety worldwide; (ii) renewable and economic feasible; (iii) low density, light material and less energy consumption during processing; and (iv) high specific strength, modifiable surface and reactive surface that can be graft with others polymers easily (Jonoobi *et al.*, 2015).

2.6.2 Basic Principle on the Isolation/Production of Nano Cellulose

Although the heterogeneous catalyst is widely used for cellulose conversion, the fact that transfer resistance between solid acid and insoluble (or partially soluble) cellulose will eventually restrict the catalytic activity should be taken into account (Cabiac *et al.*, 2011). Thus, it is important to promote the mass and heat transfer for enhancing the activity of solid acid catalysts for the cleavage of glycosidic linkage in cellulose. Among these, hydrothermal condition (H_2O as reaction medium) is a good choice for enhancing the accessibility of solid catalyst to cellulose matrix. Other than acting as the mass transfer medium, H_2O can also play a significant role as the catalyst for auto-hydrolysis process. The hydronium ions (H_3O^+) formed on the surface of catalyst could further promote the cellulose hydrolysis process (Cabiac *et al.*, 2011).

2.6.3 Morphology and Dimensions of Cellulose Nanocrystals

The geometrical dimensions (length, *L*, and width, *w*) of CNCs vary greatly, depending on the source of the cellulosic material and the conditions under which the hydrolysis is performed. Cellulose nanocrystals show a notable decrease in dimensions and an increase in crystallinity when the hydrolysis time is increased. With excessive increase in the hydrolysis time and temperature, degradation of the CNCs is observed. A continuous and progressive decrease in the thermal stability of the nanoparticles occurs as the hydrolysis time increased, probably because of the high sulfunation caused by the sulphuric acid on the surface of the nanocrystals (Sheltami *et al.* 2012).

Size uniformity can be promoted by carefully monitoring the filtration, differential centrifugation or ultracentrifugation steps. The size of CNCs can be studied by microscopy TEM, AFM, FE-SEM or light scattering techniques. Due to the drying step. TEM images usually show agglomerated CNC particles making it difficult to measure accurately measure the size of individual crystals (Sheltami *et al.* 2012).

2.6.4 Applications of Nano Cellulose Reinforced Composites

Biocomposites consisting of the polymer matrix and natural cellulose fibres are environmentally-friendly materials which can replace glass fibre-reinforced polymer composites, and are currently used in a wide range of fields such as the automotive and construction industries, electronic components, sports and leisure (Thakur, 2015).

Nanocellulose can also be used to make aerogels and foams, either homogeneously or in composite formulations. Nanocellulose-based foams are being considered for packaging applications as an alternative to polystyrene-based foams (Thakur, 2015).

Paper and Paperboard

CNC have potential application in the paper and paperboard industry where they can increase the fibre-fibre bond strength and thereby increasing the strength of the paper (Ahola *et al.*, 2008; Eriksen *et al.*, 2008; Taipale *et al.* 2010). CNCs can also be used as a barrier in grease-proof type of papers and as a wet-end additive to enhance retention, dry and wet strength in commodity type of paper and board products (Hubbe *et al.* 2008; Syverud and Stenius 2009; Aulin *et al.*, 2010; Lavoine *et al.* 2013).

Food Processing

As a food thickener, nanocellulose can be used as a low-calorie replacement for carbohydrate additives, as a flavour carrier and suspension stabilizers. It can also be used to produce fillings, crushes, chips, wafers, soups, gravies, puddings etc. The food applications of CNCs were one of the earliest applications of nanocellulose due to the rheological behaviour of the nanocellulose gel (Lavoine *et al.*, 2013)

Hygiene and Absorbent Products

Different applications in this field include but are not limited to, super water absorbent (e.g. material for incontinence pads material), nanocellulose in tissue, non-woven products or absorbent structures and antimicrobial films (Ahola *et al.*, 2008).

Medical, Cosmetic and Pharmaceutical

The use of nanocellulose in cosmetics and pharmaceuticals was also early recognized. A wide range of high-end applications have been suggested which include but not limited to; freeze-dried nanocellulose aerogels used in sanitary napkins, tampons, diapers or as wound dressing, as a composite coating agent in cosmetics e.g. for hair, eyelashes, eyebrows or nails. A dry solid nanocellulose composition in the form of tablets for treating intestinal disorders, nanocellulose films for screening of biological compounds and nucleic acids encoding a biological compound, filter medium partly based on nanocellulose for leukocyte free blood transfusion, a buccodental formulation, comprising nanocellulose and a polyhydroxylated organic compound. Powdered nanocellulose has also been suggested as an excipient or bulking agent in pharmaceutical compositions. An excipient is a natural or synthetic substance formulated alongside the active ingredient of a medication, included for the purpose of bulking-up formulations that contain potent active ingredients, nanocellulose in compositions of a photoreactive noxious substance purging agent, elastic cryo-structured gels for potential biomedical and biotechnological application (Syverud and Stenius, 2009).

CHAPTER THREE

MATERIALS AND METHODS

3.1 Background

This chapter describes the details of the characterization of the pineapple leaf fibre extracted. Also, the method used for determination of the microbial load of the pineapple leaf fibre, which was for fungi and bacteria, fabrication of the mold used in the processing of the composites, steps used in achieving particle size reduction of the pineapple leaf fibre from macro to micro and then to nano-particle sizes; the characterization of the PALF micro fibrils and PALF nano fibrils procedure; the tests for physical (water absorption), mechanical (Tensile strength and Young´s modulus using ASTM D638-11, Flexural strength and flexural modulus using ASTM D256-11, impact strength using ASTM D790-17) and thermal conductivity property (ASTM E1530-11) of the composites produced.

3.2 Materials

3.2.1 Reagents Used

Some of the include HCl, NaOH, ZnCl, H_2SO_4, $C_3H_6O_3$, HNO_3, e.t.c.

3.2.2 Equipment Used

Some of the equipment used include; JEOL JEM 2100 High Resolution Transmission Electron Microscope (HRTEM), Integral Systems Turbo Ultrasonicator UD 8054-2L, JEOL JSM 7500F Scanning Electron Microscope (SEM), Emitech K950X Carbon Evaporator (for carbon and gold coater)

3.2.3 Raw Material

The polypropylene used in this research was purchased from the Eleme petrochemicals, Port-Harcourt, Nigeria. The polypropylene used in this research work has characteristics as given in Table 3.1.

Table 3.1 Characteristics of the Polypropylene used in this research work

Product name	Flexural modulus	Properties	Processes/Applications
ELPROP	1500	Nucleated	Injection molding and extrusion coating-thin walled food and cosmetic packaging, housewares and appliances, caps and closures

The pineapple leaves used for this research were collected from a private pineapple plantation (San Carlos), in Ihe village, Agwu Local Government Area of Enugu State, Nigeria during the harvest period. Awgu is located approximately between latitudes 06 00‘and 06 19‘North of the Equator and longitudes 07 23 ‘and 07 35’ East of the Greenwich Meridian (Nwankwo, 2014).

3.3 METHODOLOGY

3.3.1 PALF Extraction

The fibres were extracted by mechanical means (scraping the thin outer layers of the spiky leaves) that is, manually from the semi-dried leaves (this is considered on the process of extracting the fibre from the leaves to give maximum yield) fibre extraction was achieved by the use of sharp broken tile edge as tool for the extraction, the process.

The fibre extracted were then cleaned, this was achieved by washing the fibre thoroughly in 2 % detergent solution at 70 ^{0}C then rinsed with very clean water. Basically, this procedure removed most of the foreign objects and impurities that could contaminate the fibre as a result of the extraction process.

The now clean fibre were then dried in an oven at 70 °C for 24 hours. Thus, preparing the fibre for characterization, chemical treatment (surface modification), microbial load test, Fourier Transform Infrared Spectroscopy, particle size reduction, and composite compounding.

3.3.2 Yield of PALF and Classification in Different Particle Sizes

This was achieved by adopting the mechanical scrapping method, on the course of this research, other fibre extraction methods such as retting were tried with low output and also, the retting method was time consuming, thus, it was abandoned and the mechanical scrapping method was utilized all thru the research period. This method gave a yield of 32-37 % which is more that the yield via the retting method which averaged around 12-14 %.

The PALF went through particle size reduction stages, broadly classified into the macro (2- 6 mm), micro (70 - 300 µm) and nano (20 - 500 nm). The method adopted in the research that gave good results is actually novel and it is termed chemo-mechanical method. In this method, the PALF undergo alkalization, followed by a bleaching process and the acid hydrolysis, the method's concluding part is the milling process with lead to micro/nano fibrils. For a 100 g of macro PALF, the yield is as summarized in this order; PALF modified with NaOH gave a yield of 44.0 % (44.0 g) of nano fibrils, PALF modified with $C_3H_6O_3$ yielded 54.9 % (54.9 g), the PALF modified with $HN0_3$ gave a yield of 59.9 % (59.5g) and he PALF modified with Zncl gave a yield of 49 % (49.0 g).

3.4 Pineapple Leave Fibre (PALF) Surface Modification

The raw biomass used is the PALF that were extracted and divided into five (5) different portions by weight. One portion was set aside as the control for this research work, the other four (4) portions were used for surface modification or enhancement using sodium hydroxide, acetic anhydride, nitric acid and with zinc chloride respectively, without prejudice to the order of selection of the chemicals used in this research work. The procedures adopted for surface modification are as documented subsequently. The removal of surface impurities on plant fibres is advantageous in fibre-matrix adhesion because it facilitates both mechanical interlocking and bonding reactions.

Equal weights of the PALF samples to be surface modified were each taken using an electronic balance and the results recorded.

3.4.1 Treatment with Sodium Hydroxide

The procedure used is the method adopted by Nurul and Ishak (2012); with slight modifications. The PALF was modified with 6 % NaOH. The fibre was immersed in the alkali solution for 50 minutes, then neutralized with acetic acid and washed with distilled water repeatedly until all sodium hydroxide was eliminated. Finally, the fibre was washed with distilled water and dried at room temperature for 48 hours. It is known that the alkalization treatment removes impurities and increases the fibre surface adhesion characteristics with the resin.

3.4.2 Treatment with Acetic Anhydride

The acetylation process used is the method adopted by Bledzki *et al.,* (2009), with slight modifications. The PALF was soaked in distilled water for an hour, filtered and placed in a round bottom flask containing 10 % acetic acid solution for 30 minutes. The fibre was then transferred into flask containing 14 % acetic anhydride solution. The process te mperature of acetylation was 175 ^{0}C and the residence time was 70 minutes. The fibre was then washed periodically with distilled water until acid free- The distilled water was drained off the PALF using a tray sieve. Lastly, the modified fibre was air dried for 48 hours.

3.4.3 Treatment with Nitric Acid

The nitric acid treatment was according to the method used by Vautard *et al.,* (2013); with modifications. The PALF fibre was oxidized with 6 % nitric acid. The prepared oxidized solution was heated to a temperature of 60 ^{o}C and the fibre immersed in the solution at

maintained said temperature for 50 minutes. It was then neutralized with NaOH solution and washed with distilled water repeatedly until all the nitric acid was eliminated.

3.4.4 Treatment with Zinc Chloride

The treatment with Zinc chloride was done based on the method used by Nadanthangam *et al., (2013*), with modification. The fibre was soaked in 3 % ZnCl solution for 70 minutes after which it was washed with distilled water until the washing solution became chloride free. The fibre was washed with distilled water and dried at room temperature for 48 hours. Figure 3.10 shows the PALF after it was modified with ZnCl

3.5 Pineapple Leaf Fibre Characterization

3.5.1 Preparations of Test Samples

Before the characterization took place the pineapple leaf fibre were chopped to particle sizes of 2- 6 mm. The chopped fibre was milled. The residues after this milling were used for the compositional analysis.

3.5.2 Compositional Analysis of the Pineapple Leaf Fibre (PALF)

The pineapple leave fibre was subjected to compositional analysis using the gravimetric method. Chemical composition of PALF was measured as follows: acid insoluble lignin (ASTM E1758-01, 2015), cellulose and hemicellulose (ASTM D1105-98, 2001) as reported by Natalie *et al.,* (2016). The schematic representation of the step-by-step compositional analysis is as shown in Figure 3.1.

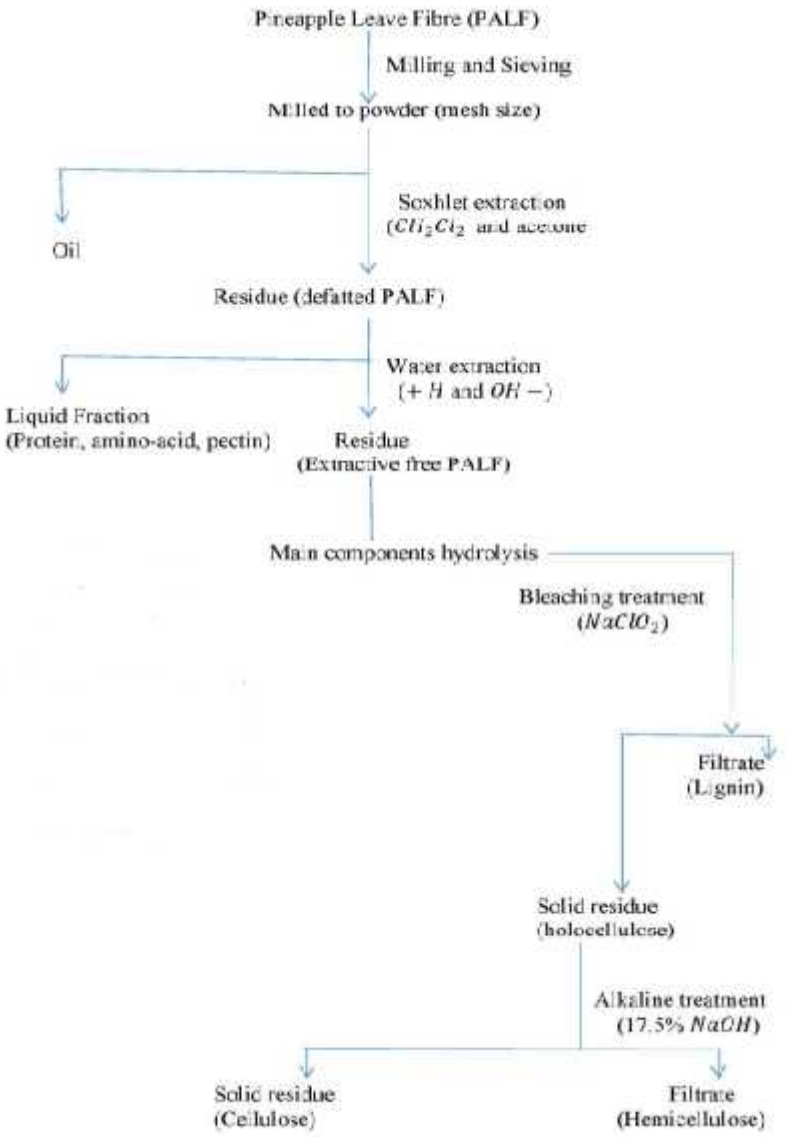


Figure 3.1 Schematics of the compositional analysis of the PALF

Extractives

The procedure used in this research work is as adopted by Aswanida, (2015) and James *et al.*, (2014). 0.5 g of dried PALF was loaded into a thimble. With the Soxhlet extractor set up as shown in figure 3.14, 150mL of acetone was used as solvent for extraction. Residence time for the boiling and rising stages were carefully adjusted to 70^0C and 25 min respectively on the heating mantle for a 4-hour run period. After extraction, the sample was air dried at room temperature for few minutes. Constant weight of the extracted material was achieved in a

convection oven a 105 ^{0}C. The % (w/w) of the extractives content was evaluated as the difference in weight between the raw extractive-laden biomass and extractive-free biomass.

Hemicellulose

1 g of extracted dried biomass was transferred into a 250 ml Erlenmeyer flask. 150 ml of 500 mol/m^3 NaOH was added. The mixture was boiled for 3.5 hours with distilled water. It was filtered after cooling through vacuum filtration and washed until neutral pH. The residue was dried to a constant weight at 105 ^{0}C in a convection oven. The difference between the sample weight before and after this treatment is the hemicellulose content (% w/w) of dry biomass (Ayeni *et al.,* 2013, Blasi *et al.,* 1999 and Lin *et al.,* 2010).

Lignin

The method used is as reported by Shuiter *et al*, (2008) where 0.3 g of dried extracted PALF was weighed in glass test tubes and 3 ml of 72 % H_2SO_4 was added. The sample was kept at room temperature for 2 hours with careful shaking at 30 minutes intervals to allow for complete hydrolysis. After the initial hydrolysis, 84 ml of distilled water was added. The second step of hydrolysis was made to occur in an autoclave for 1 hour at 121 ^{0}C. The slurry was then cooled at room temperature. Hydrolyzates were filtered through vacuum using a filtering crucible. The acid insoluble lignin was determined by drying the residues at 105 ^{0}C and accounting for ash by incinerating the hydrolyzed samples 375 ^{0}C in a muffle furnace.

Cellulose

The cellulose content (% w/w) was calculated by difference, assuming that extractives, hemicellulose, lignin, ash, and cellulose are the only components of the entire biomass as reported by Blasi *et al*, (1999) and Lin *et al.,* (2010).

3.6 Proximate Composition of the PALF

Minerals were extracted by wet ashing methods as reported by Sopie *et al.,* (2011). Total ash was obtained from 10 g dry matter calcinations at 550 °C and left until constant weight. The sample (0.5 g) was placed into beaker containing 10 mL of hydrochloric acid and filtered. The filtrate was adjusted to 50 ml with 1 % hydrochloric acid. After recovering the minerals solution, the phosphorus (P) content was evaluated by colorimetric with the vanadomolybdic reagent. Aluminum (Al), Calcium (Ca), plumb (Pb), potassium (K), Sodium (Na) and zinc (Zn) were determined using flame atomic absorption spectrophotometer (Jenway PFP7) with standard range of each element.

3.7 Microbial Load Analysis

This analysis was carried out at the department of pharmacology, Faculty of Pharmacy, Nnamdi Azikiwe University, Awka.

Stock solution and dilution of test samples

0.1g each of the fibre samples were cut into smaller sizes and weighted into the sterile 50ml conical flask aseptically and labeled accordingly. The sample were soaked with sterile distilled water for 20 min. The sample stock solutions were diluted using ten-fold dilution with sterile distilled water to ensure countable colonies.

Preparation and sterilization of media and samples

The media used were nutrient agar (NA) and Sabouraud agar (SA) for enumeration of bacteria and fungi, respectively. The nutrient agar (28 g/l) and sabouraud dextrose agar (SDA, 65g/l) used were prepared following manufacturer's specification and sterilized in an autoclave at 121 ^{0}C for 15 min. The dried plant samples were ground into fine particles under aseptic conditions in a surface sterilized laboratory bench. The grater was washed, dried and sterilized before use. After grinding, the samples were placed in different sterile McCartney bottles and labeled accordingly.

In vitro estimation of bacteria and fungi viable cell count

The pour plate method was used to cultivate serially diluted portions of the fibre samples under investigation. Enumeration was carried out on nutrient agar (NA) for bacteria and on Sabouraud agar (SA) for fungi. Triplicate plates of appropriate dilutions were prepared. The NA plates were incubated at 37 ^{0}C for 24 - 48 hours for bacterial growth while SA plates were incubated at room temperature (28 ± 2 ^{0}C) for 48 – 72 hours for fungal growth. The developed microbial colonies were counted and computed as colony forming units per gram (cfu/g) of plant material. The colonies were purified, isolated and stored for morphological and biochemical characterization. These were further identified with to the aid of Bergey's Manual of Determinative Bacteriology for bacteria and Illustrated Genera of Imperfect Fungi for fungi. The experiment was carried out over a period of 12 months; the results are as presented in Chapter 4 of this research work.

Number of Viable Cell Count

The number of the viable count on the agar surface were counted and determined as follows

$$\text{Colony forming unit} = \frac{\text{Number of colony}}{\text{Volume per drop}} \times \text{dilution factor (CFU/ml)} \qquad 3.1$$

3.7.1 Identification of Bacterium Genera Present in the Pineapple Leaf Fibre (PALF)

Colony Characterization of the Test Organisms

The 24-hour culture of the test organisms were characterized by direct observation on the agar plate where conclusion was drawn based on the following characters on the general-purpose media (Nutrient agar); shape, entire, chromogenesis, size, opacity, elevation, consistency, surface etc. All this were characterized in order to facilitate and authenticate the test organisms through the staining character and possible confirmatory (biochemical) test, of all these characteristic studies, the observations were recorded as result of colony characterization.

Staining and Gramm Reaction of the Test Organisms

The simple and Gramm staining were carried out to review the shape and morphology of each organism used before further confirmation. The simple staining was carried out by preparing smear of the organism on glass slide, allowed to air dry and heat fixed, the primary dye (gentian violet) was added for 60 seconds and then rinsed of with sufficient tap water, drained and thereafter, the preparation were added with oil immersion and then viewed under 100 X objective lens.

In this case, only the shape and morphology were determined. Similarly, Gramm stain was also carried in a similar way with extension of additional reagents at different time interval as follows; with primary stained smear preparation, Lugol's iodine solution was added for 45 to 60 seconds and this was decolorize using 70 % alcohol for 20 to 30 seconds and rinsed with gentle tap water. Counter stain of safranin (secondary dye) was added for 60 seconds and also rinsed with gentle tap water, drained with addition of oil immersion and viewed under 100X objective lens as well. Here, both shape/morphology, arrangement and Gramm character were determined and recorded

Biochemical Test

Starch hydrolysis is a qualitative test for identification of some spore formers of gram-positive bacteria rod, this is a complex polysaccharide which appear dark blue color upon the addition of a solution of iodine. Some bacteria have the gene for making the enzyme amylase. This test is used to identify bacteria that can hydrolyze starch (amylose and amylopectin) using the enzymes a-amylase and oligo-1, 6-glucosidase. This test is often used to differentiate species from the Bacillus and other anaerobic bacteria like Clostridium.

The starch is used as a carbon source by the bacteria which secrete a-amylase and oligo-1,6-glucosidase into the extracellular space. These enzymes break the starch molecules into smaller glucose sub-units which can then enter directly into the glycolytic pathway of

bacterial metabolism. Starch agar is a simple nutritive medium with starch added. Since no color change occurs in the medium when organisms hydrolyze starch, iodine was added to the plate after incubation. Iodine turns blue- black (depending on the concentration of iodine) in the presence of starch. A clearing zone around the bacterial growth indicates that the organism has hydrolyzed starch.

The isolate was streaked on the agar plate by surface streak method on the line down the center of the agar surface. The resultant product was incubated upside down at
37 ^{0}C for 48 hours. After incubation, the starch hydrolysis test was done by covering the surface of the agar plate with iodine and observe the colour change reaction after 10-20 seconds.

3.7.2 Fungi Characterization and Possible Identification

Aspergillus was also identified macroscopically, by identifying the white felt like colony turning black with conidia formation. Microscopically, the identity was confirmed by the presence of black, glucose conidia with very dark to black spores.

3.8 Fourier Transform Infrared Spectroscopy of the Pineapple Leaf Fibre (PALF)

Buck scientific M530 USA FTIR was used for the analysis. This instrument was equipped with a detector of deuterated triglycine sulphate and beam splitter of potassium bromide. The software of the Gram A1 was used to obtain the spectra and to manipulate them. An approximately 1.0g weight of samples respectively was properly placed on a salt pellet. During measurement, FTIR spectra was obtained at frequency regions of 4,000 – 600cm^{-1} and co-added at 32 scans and at 4cm^{-1} resolution. FTIR spectra were displayed as transmitter values.

3.9 Fabrication of Mold for the Mechanical and Thermal Property Tests of the Composites

To achieve high level of production of composite samples, it is imperative at this level to eliminate the conventional methods of making sample in box mold where by each test sample will be later cut to standard test sizes and shapes. The set-back on the normal practice is the fact on the process of cutting into the standard shapes and sizes; the grain arrangement of the composite gets affected as a result of the applied pressure on the process of cutting. To take care of this obvious set-back, the idea of fabricating individual molds for each property test samples be produced, such that the that issue of cutting the composite will be completely eliminated.

The molds were designed and fabricated at the Scientific Equipment Development Institute, Enugu, Nigeria, based on ASTM standards for each property to be tested on the composite to be produced. To achieve high level of precision, a Computer Numerically Controlled (CNC) Machine, called vertical Milling Centre (VMC), model 750, manufactured by BAO JI, Laber Precise Industries Co. Ltd was used.

Programs were written, using the CNC programming languages, which is basically G-CODES, the programs were fed into the CNC machine which served as the series of instructions with which the CNC functioned by taking each code in sequential format till parts of each mold were fabricated to the optimal level of precision.

3.10 Production /Isolation of Micro and Nano Particles from the PALF

The production/ isolation of micro and nano particles was carried out at the Department of Pharmacy Technology and Industrial Pharmacy, University of Nigeria, Nsukka.

About 100 g quantity of PALF with different treatment was added into 2 % w/v NaOH solution and digested at 80 ^{0}C for 3 hours using a thermostated hot plate. This removes lignin in the form of soluble complexes. The samples were then washed severally with distilled water and

filtered using sieve number 40 mm mesh size. The samples were bleached with 10% aqueous dilution of sodium hypochlorite for 30 minutes at 100 ^{0}C, washed and then filtered again. The samples were further modified with 17.5 % w/v sodium hydroxide at 80 ^{0}C for 1 hour and the resulting samples were washed thoroughly with water and subjected to whitening process with 10 % sodium hypochlorite for 15 minutes at 80 ^{0}C, they were washed with water until neutral. The samples were filtered, processed and reduced to small pieces and dried for 1 hour at 60 ^{0}C with a hot air oven.

The quantity of the material obtained was hydrolized with a solution of 2.5N hydrochloric acid at 100 ^{0}C for 15 minutes. The acid mixture was poured into water which was followed by vigorous stirring with a glass rod. The particles obtained were washed with water until neutral, sieved with sieve number 60 mm mesh size, pressed and dried at 60 ^{0}C in an oven. The dried samples obtained were milled using an end-runner mill until micro / nano particles were obtained and passed through sieve number 150 mm to get very fine powder.

3.10.1 Determination of Percentage Yield of micro and nano PALF fibrils

The percentage yield of the micro/nano particles obtained from plant materials of different treatment was determined by the formula below:

Percentage yield = $\frac{w_1}{w_2} \times \frac{100}{1}$ 3.2

Where; W_1 = initial weight of dried sample, W_2 = weight of micro/nano particles obtained

Initial weights of the samples are as follows:

PALF modified NaOH = 44.0g

PALF modified with acetic anhydride = 54.9g

PALF modified with Nitric acid = 59.5g

PALF modified with Zncl = 49.0g

3.11 Characterization of the PALF Micro Fibrils

The characterization was carried out at the National Center for Nanostructured Materials (NCNSM), Council for Scientific and Industrial Research (CSIR), Pretoria, South Africa.

A pinch of each of the PALF powder samples were collected and placed on the already cleaned sample(s) holders that were coated with carbon. Each of the sample(s) holder was placed into the Emitech K950X turbo carbon evaporator to remove excess carbon particles on the test samples to produce relatively fine coatings on the samples. This fine coating is to prevent the test samples from emitting current (charges) should in case when the samples will be analyzed in the SEM. After a 10 minutes spin in the equipment, the samples were finely coated and removed. The now coated samples were subsequently removed from the carbon evaporator and placed onto the SEM sample(s). All screws were tightened on the sample holder to ensure nothing falls out. The sample holder was then transferred into the main chamber, after waiting for vacuum inside the chamber to stabilize at 9.6 X 10E-5. Each sample was selected one after the other and analyzed. The right sample holder was selected on the top of the screen. The number of the sample to be viewed was then clicked and moved (the stage should be moved to Z= 8mm). The RIBE (reactive ion beam etching) was inserted, should in case the samples emit charges. The beam was switched to the required voltage in a step wise manner, in this case, it was set at 3.0KV, with a varied range of magnifications set at X10,000, X25,000, X50,000 and X100,000.

3.12 Characterization of the Nano Cellulose PALF

The characterization was carried out at the National Center for Nanostructured Materials (NCNSM), Council for Scientific and Industrial Research (CSIR), Pretoria, South Africa.

Small portions of the samples were collected on the spatula tip and dispersed into plastic cuvettes containing ethanol, this is to create very lightly dispersed solutions of each of the test samples accordingly. The labeled cuvettes were then placed into the Emitech X950K Turbo

Ultrasonicator at room temperature. A carbon coated Cu grid is then dipped into the solution and left to dry for 3 days (this is depended on the solvent used and the nature of the sample). After the samples were fully dried, they were loaded onto the sample holder. Efforts were made to ensure firm and secured grip. The sample(s) holder was inserted with the help of a guide pin into position inside the column, until it came to a stop. A `click` sound was heard indicating that vacuum can be pumped into the column. A green light appeared indicating that the appropriate pressure was reached. Adjustments were made to ensure that the sample holder was in the appropriate position, this is ascertained by a steady appearance of green light and `beam status ready on the readout. The anti-contamination chamber was then filled with liquid nitrogen.

3.13 EDX -SEM on PALF at the Micro and Nano Fibrils Dimensions

The characterization was carried out at the National Center for Nanostructured Materials (NCNSM), Council for Scientific and Industrial Research (CSIR), Pretoria, South Africa.

A pinch of each of the PALF powder samples were collected and placed on the already cleaned sample(s) holders that were coated with carbon. Each of the sample(s) holder was placed into the Emitech K950X turbo carbon evaporator to remove excess carbon particles on the test samples to produce relatively fine coatings on the samples. This fine coating is to prevent the test samples from emitting current (charges) should in case when the samples will be analyzed in the SEM. After a 10 minutes spin in the equipment, the samples were finely coated and removed. The now coated samples were subsequently removed from the carbon evaporator and placed onto the SEM sample(s) stubs. All screws were tightened on the sample holder to ensure nothing falls out. The sample holder was then transferred into the main chamber, after waiting for vacuum inside the chamber to stabilize at 9.6 X 10E-5. Each sample was selected one after the other and analyzed. The right sample holder was selected on the top of the screen. The

number of the sample to be viewed was then clicked and moved (the stage should be moved to Z= 8mm). The RIBE (reactive ion beam etching) was removed. The beam voltage was switched on at a voltage of 15.0KV and magnification of X3000. The spectra and tabular values were displayed on the screen and recorded accordingly.

3.14 Compounding of the PALF/PP Composites

The preparation of sample was done in such a way that the PALF/PP were firstly dry mixed in a blender before been poured into the injection molding machine.

The injection molding machine was used in the production of the different PALE/PP composites test simples. For each property test, its marching mold was placed in the injection molding machine.

The first step in this process is mounting of the mold for each test after another on the mold cavity of the injection mold machine. Each mold, male and female components were properly dumped and screwed into the machine.

After this stage, the injection molding machine was power and allowed to heat up for 1 hour 30 minutes, the temperature was set at 180 ^{0}C and the pressure was set at 400 Kpa.

The already mixed PALE/PP were then place into the machine vid the hooper, the leads to the screw press which transported the screw aids in further missing of the PALE/PP composites and melting the PP in the process into a molten form.

The hydraulic pressure device then by the use of mechanical force and hydraulic pressure forced the molten PALE/PP into the mold cavity through the injection nozzles.

The entire process take an average of 3- 4 minutes. The machine is then stopped and the mold cavity was opened to allow the now formed test samples cool off and be brought out of the mold cavity.

3.14.1 PALF/PP Composite Preparation at the Macro PALF Level

The PALF was sieved to obtained uniform particle sizes of an average range of 2 - 6mm. This particular size appears to be the most suitable processing size for melt mixing which gives effective reinforcement in Polypropylene as reported by George *et al.,* (2001) and Kalia *et al.,* (2011).

3.14.2 PALF/PP Composite Preparation at the Micro and Nano Cellulose Dimension

To achieve maximum compounding, the PP was reduced to 75µm- 290 µm, the PP was pulverized. Pictures of the pulverized PP are placed in appendix E4.

The melt mixing method was used to mix PALF and PP; various compositions of PALF in PP were compounded in an injection molding machine. Table 3.2 indicates different PALF loading that were compounded in the PP matrix.

Table 3.2 PALF/PP Composites weight load Ratio

PALF weight % ratio (g)	Polypropylene weight ratio (g)	Total % weight composition
40	360	400
80	320	400
120	280	400
160	240	400

3.15 Physical Property Test on the PALF/PP Composites

3.15.1 Water Absorption

The PALF/PP composites were cut into pieces of 100 mm^2, weighed (m_i), immersed in 100ml beaker containing distilled water and kept at 37 ^{0}C for 168 hours. After 24 hrs intervals, the samples were dried and weighed (m_f). The percentage of soluble mass was determined by the following equation.

$$\text{Solubility mass \%} = \frac{(m_i - m_f)}{m_i} \text{x100 Soluble mass (\%)} \qquad 3.3$$

All experiments were performed in triplicate, and standard deviation was calculated.

The data collected for the water absorption at the micro cellulose PALF and nano cellulose PALF contained no significant difference in water absorption, thus, they were discarded.

3.16 Mechanical Properties Tests of the PALF/PP Composites

This aspect of the research was carried out at the Engineering testing laboratory of the Standard Organization of Nigeria (SON), Enugu. All the mechanical testing methods used in this research were based on American Society for Testing and Materials (ASTM). There were three tests performed, namely Tensile Test (ASTM D638-11), Flexural Test (ASTM D256-11) and Impact Test (ASTM D790-17). The major mechanical properties tested in this research are as outlined below;

1. Tensile properties tests were performed to determine the tensile strength and Young's modulus of the composite samples.
2. Flexural properties tests were performed to determine the flexural strength and flexural modulus of the composite samples.
3. Impact strength test was performed to determine the impact strength of the composite samples

3.16.1 Tensile Properties Test

The ASTM-D638-11 method was adopted for this research work. The dumbbell shape (Type I) specimen guide was used for reinforced PALF/PP composite testing. Detailed dimension for this is shown in Table 3.3. The testing was done in standard laboratory atmosphere of 37 ˚C ± 2 ˚C. A computerized Universal Testing Machine

(TUE-C-100), manufactured by Fine Spavy Associates and Engineers PVT Miraj, India, was used at cross-head speed of 50 mm/minute. The specimens were positioned vertically in the grips of the testing machine. The grips were then tightened evenly and firmly to prevent any

slippage with gauge length kept at 50mm. An average of the 3 repetitive tests was taken and recorded.

The tensile strength was calculated from the stress-strain plots given by the UTM, the equation used is as shown in equation 3.4

Tensile strength (MPa) = (Load at break)/(original width)(original thickness)……..3.4

And the Young's modulus was calculated using equation 3.5 below.

$$\text{Young's modulus} = \frac{(\text{loadatpointontangent})/(\text{originalwidth})(\text{originalthickness})}{(\text{elongationatpointontangent})/(\text{initialgaugelength})} \quad \ldots\ldots\ldots\ldots\ldots 3.5$$

Table 3.3 Dumb bell-shaped specimen dimension for Type I in ASTM D638

Dimension	Unit of Measurement (mm)
Thickness <7mm, h	1.00 ± 0.4
Width of narrow selection, b_1	13
Length of narrow selection, l_1	57
Width overall, l_3	19
Length overall, l_3	165
Gauge length, l_3-l_2	50
Distance between grips, l_2	115

3.16.2 Flexural Properties Test

Flexural strength (FS) is the ability of the material to withstand bending forces applied perpendicular to its longitudinal axis. Sometime it is referred as cross-breaking strength where maximum stress developed when a bar-shaped test piece, acting as a simple beam, is subjected to a bending force perpendicular to the bar. The ASTM D790-11 method was adopted for flexural test in this research work. The three-point loading system applied on a supported beam was utilized.

In using Procedure A, of ASTM D790-11, width and depth of the specimen were measured to the nearest 0.03mm at the centre of the support span. The test samples were then placed on two supports and load will be applied. The distance of two supports span (L) was fixed at 100mm.

Flexural modulus is a measure of the stiffness of a material during the first or initial step of the bending process, often called modulus of elasticity or bending modulus.

Flexural properties test was performed using the computerized Universal Testing Machine (TUE-C-100), manufactured by Fine Spavy Associates and Engineers PVT Miraj, India at standard laboratory atmosphere of 23 ˚C ± 2 ˚C. The flexural properties were determined from the plots using equations 3.6 and 3.7 as shown below.

To determine flexural strength, equation 3.6 was used

$FS=PL/bd^2$……. …….3.6

Where

P= maximum applied load (N)

L= span length (mm), and

b, d = average width and depth of specimen (mm)

And the flexural modulus was calculated using equation 3.7 below.

$E= L^3F/4bh^3y$……. 3.7

Where L= length of span (mm)

y= distance covered by a load (mm)

F= load (in Newton)

b= width of test bar (mm)

h= thickness of test bar (mm)

3.16.3 Impact Strength Test

The impact properties of the material are directly related to the overall toughness which is defined as the ability to absorb applied energy.

The Izod notch method (ASTM D256-17) was used to determine the impact strength of the PALF/PP composites. The specimens were notched, notching was done because it provides a

stress concentration area that promotes a brittle rather than a ductile failure. Furthermore, notching also drastically reduces the energy loss due to the deformation of the composite. In performing the test, specimens were clamped vertically as a cantilever beam and then struck by a single swing of the pendulum released from a fixed distance from the specimen clamp. The line of initial contact is at a fixed distance from the specimen clamp and from the center line of the notch and on the same face of the notch. There are a few parameters that are set according to the standard they include; Hammer Velocity = 3.46 m/s and Hammer Weight = 0.905 kg. The equipment is manufactured by Samuel Denison Limited, England.

3.17 Thermal Property Test on the PALF/PP Composites

3.17.1 Thermal Conductivity Test

Thermal conductivity measurements are carried out under steady state condition. According to ASTM E1530-11, disc shaped specimens with diameter of 50 mm and thickness of 10 mm are used in the instrument for thermal conductivity measurements. A known constant heat is applied from one side of the specimen. When the thermal equilibrium is attained and the system approaches to steady state situation, the temperature of top bottom surfaces was measured by using thermocouples installed on top and bottom of the specimen. Knowing the values of heat supplied, temperatures, and thickness, the thermal conductivity was determined by employing one-dimensional Fourier's law of conduction. All measurements are carried out approximately in the similar temperature range, 25 - 90 ^{0}C. The test was performed using a thermal conductivity apparatus.

CHAPTER FOUR

RESULTS AND DISCUSSION

4.1 Background

This chapter contains the results obtained on the process of carrying out this research as well as the discussion on the result obtained. The results were compared with those obtained by other researchers and are found to be in close agreement.

4.2 Extraction of the Pineapple Leave Fibre (PALF)

The yield of the PALF at the macro size level was between 32-37 % per 100 g. For a 100 g of the micro/nano PALF, the yield is as summarized in this order; PALF modified with NaOH gave a yield of 44.0 % (44.0 g) of nano fibrils, PALF modified with $C_3H_6O_3$ yielded 54.9 % (54.9 g), the PALF modified with HNO_3 gave a yield of 59.9 % (59.5g) and the PALF modified with Zncl gave a yield of 49 % (49.0 g).

4.3 Chemical Compositions of the Pineapple Leave Fibre (PALF)

The pineapple leaf fibre as detailed earlier was classified into three different particle size, namely the macro sizes, micro sizes and the nano dimensions. This segment of this research contains the result of the composition of the pineapple leaf fibre (PALF) at the macro, micro and nano particle dimension.

Table 4.1 Chemical Composition of the PALF at the macro particle sizes

Cellulose	Lignin	Hemicellulose	Reagent used
58.15	5.06	13.16	NaOH
55.43	4.86	15.90	HNO_3
60.56	5.01	12.47	ZnCl
61.15	4.95	12.22	$C_4H_60_3$
70.87	5.34	13.92	Unmodified PALF

4.3.1 Cellulose

From Table 4.1, considering the Pineapple leaf fibre (PALF) modified with NaOH, the average value of cellulose is 58.15 %, the sample modified with nitric acid (HNO_3) has an average value of 60.56 %, the sample modified with ZnCl has a value of 55.43 %, the sample modified with acetic anhydride ($C_3H_6O_3$) has 60.56 %, a value of 61.15 % and the unmodified PALF sample has the highest value of 70.87 %.

From the results obtained, the sample modified with HNO_3 has the lowest value of 55.43 %, while the unmodified sample has the highest value of 70.87 %.

It can be seen that the value obtained are in close agreement with the values obtained by earlier researchers that conducted similar activities on PALF. Danladi and Shu áib (2014) got a value of 66.2 %, Yu (2015) got a value range of 56-62 %, Mishra *et al.,* (2004) got a value range of 70 - 82 %, Natalai *et al.,* (2016) got a value of 66.74 %, Moharty *et al.,* (2005) got a range of 70 - 72 %.

4.3.2 Lignin

The PALF sample that was modified with NaOH gave a lignin average value of 6.06 %, the sample modified with HNO_3 gave a value of 4.86 %. The sample modified with ZnCl has an average lignin value of 5.01 %, the sample modified with $C_3H_6O_3$ has a lignin value of 4.95 %. The unmodified sample has an average value of 5.34 %.

From the results obtained, the sample with HNO_3 has the lowest lignin content value of 4.86 % while the unmodified sample has the highest value of 5.34 %.

The results obtained are in close agreement with the results obtained by those that conducted research on PALF with respect to lignin content. Natalia *et al.,* (2016) got values within a range of 8.31-10.46 %, Rowell and Han (2000) got a range within 4.6-12 %, Danladi and Shu ‘aib (2014) got 5 %, Samidoss and Prasanth (2015) got a value of 4.2 %, Munirah *et al.,* (2007) got

4.78 %, Zawawi *et al.*, (2014) got 4.2 %, Uddin *et al.,* (2017) for value within the range of 4.4 - 15.4 %.

It has been established by earlier researchers that fibre with higher amount of residual lignin content leads to composites with lower tensile and impact strengths and increased degradability when subjected to accelerated weathering test as reported by Beg and Pickering (2008).

Also, the presence of higher lignin content in the fibre tends to lead to composite that has high thermal stability with slight reduction in thermal degradation temperatures, they also tend to have low degree of water absorption as reported by Nair *et al.,* (2017).

4.3.3 Hemicellulose

The PALF modified with NaOH gave an average for hemicellulose as 13.16 %. The sample modified with HNO_3 gave an average value of 15.90 %. The sample modified with ZnCl has a value of 12.47 %. The sample modified with $C_3H_6O_3$ has a value of 12.22 %, while the unmodified PALF gave an average value of 17.01 %.

From the results above, the sample modified with acetic acid have the lowest average value of 12.22 %, while the unmodified sample has the highest average value of 17.01 % for hemicellulose.

The results however are in close agreement with the results obtained by other researchers that conducted same test on PALF, Swamidoss and Prasanth (2015) got a value of 19.5 %, Natalia *et al.,* (2016) got an average value of 17.45 %, Udden *et al.,* (2017) got an average value of 9.45-18.80 %, Munirah *et al.,* (2007) got 9.45 %, Zawawi *et al.,* (2014) got a value of 19.5 % and Yu (2015) got a range of values between 16-19 %.

Table 4.2 Chemical Composition of the Micro Cellulose PALF

Cellulose	Lignin	Hemicellulose	Reagent used
68.20	2.98	8.21	NaOH
74.18	2.72	8.01	HNO_3
72.35	2.68	8.38	ZnCl
69.75	2.88	8.11	$C_4H_60_3$
74.47	3.58	9.09	Unmodified PALF

Table 4.3 Chemical Composition of the Nano Cellulose PALF

Cellulose	Lignin	Hemicellulose	Reagent used
70.50	2.73	7.84	NaOH
78.83	2.11	6.53	HNO_3
73.54	2.40	6.96	ZnCl
70.60	2.38	7.01	$C_4H_60_3$
72.20	3.10	7.99	Unmodified PALF

It is pertinent to discuss the compositions of the PALF before and after the isolation/ production into the micro/nano cellulose levels.

The bleaching process on the process of achieving micro and nanocellulose reduces the amount of lignin and hemicellulose in natural fibre cellulose. Similar trend was discovered in this research as the same test that was conducted to verify the percentage composition of the presence of main constituents of the PALF namely, Cellulose, lignin and hemicellulose was repeated again after isolating for micro and nanocellulose. This is so due to the removal of the amorphous content of the PALF which increased the crystalline fraction. Increase in the proportion of crystalline cellulose leads to increases in thermal stability as reported by Mahardika *et al.,* (2018).

The results obtained as shown in Tables 4.2 and 4.3 fall within the acceptable limits and are in close agreement with work done by Yuliasmi *et al.,* (2017) who reported in their study, of

making microcrystalline cellulose from pineapple leaf using nitric acid and sodium nitrite, which yielded results showed that alpha cellulose can be as much as 15.48 % of the 100-gram sample pineapple (*Ananas comosus* L. Merr.) leaves and microcrystalline cellulose could yield as much as 7.25 grams (7.25 %)

4.4 Proximate Analysis of the Pineapple Leave Fibre (PALF)

This aspect of the research was done in two part, in other words, initially, the conventional approach was adopted using Atomic Force Microscopy (AFM) and the results recorded.

The second part was done using a more accurate method, this was achieved by the use of EDX-SEM at the Council for Scientific and Industrial Research (CSIR), Pretoria, South Africa. The results are as shown in Plates I, II, III, IV and V. Also, the results in Plates I to V are also interpreted in tabular form for easy interpretation as shown in Table 4.5.

Table 4.4 Proximate Analysis of the PALF using AFM

C	O	Ca	Na	Fe	K	Cu	Reagent used
71.2	26.4	2.2	0.34	0.7	0.94	0.02	Unmodified PALF
66.6	23.9	0.90.9	0.32	0.01	0.17	0.01	NaOH
64.3	22.3	0.5	0.34	0.03	0.23	0.01	ZnCl
60.5	24.7	0.1	0.37	0.05	0.31	0.01	$C_3H_60_3$
68.3	24.4		0.36	0.03	0.49	0.01	HNO_3

From Table 4.4, the percentage composition of carbon for the unmodified PALF at the macro particle level is 71.27 %, oxygen is 26.4 %, calcium is 2.2 %, sodium is 0.34 %, iron is 0.7 %, potassium is 0.94 % and copper is 0.03; comparing the data with the data for the unmodified PALF from the EDX results as shown in table 4.5, same unmodified PALF at the micro/nano cellulose levels gives an average of 71.04 % for percentage of carbon, depicting a difference of 0.13 %, which is within the acceptable limits. Also, from table 4.5, the percentage composition of oxygen is 24.81 %, this gives a difference of 1.55 % from the composition of oxygen in Table 4.4, this too, is within the permissible limits.

Table 4.5 Proximate Analysis of the Micro/Nano PALF using EDX-SEM

C	O	Ca	Na	Al	Cl	N	Reagent used
71.04	24.85	0.10	0.34	0.09	0.43	3.05	Unmodified PALF
70.71	26.84	-	0.36	0.10	-	1.10	NaOH
61.77	37.97	-	0.31	-	2.28	-	ZnCl
63.57	32.12	-	0.31	0.09	0.36	0.72	$C_3H_60_3$
68.45	27.16	-	0.33	0.23	-	2.90	HNO_3

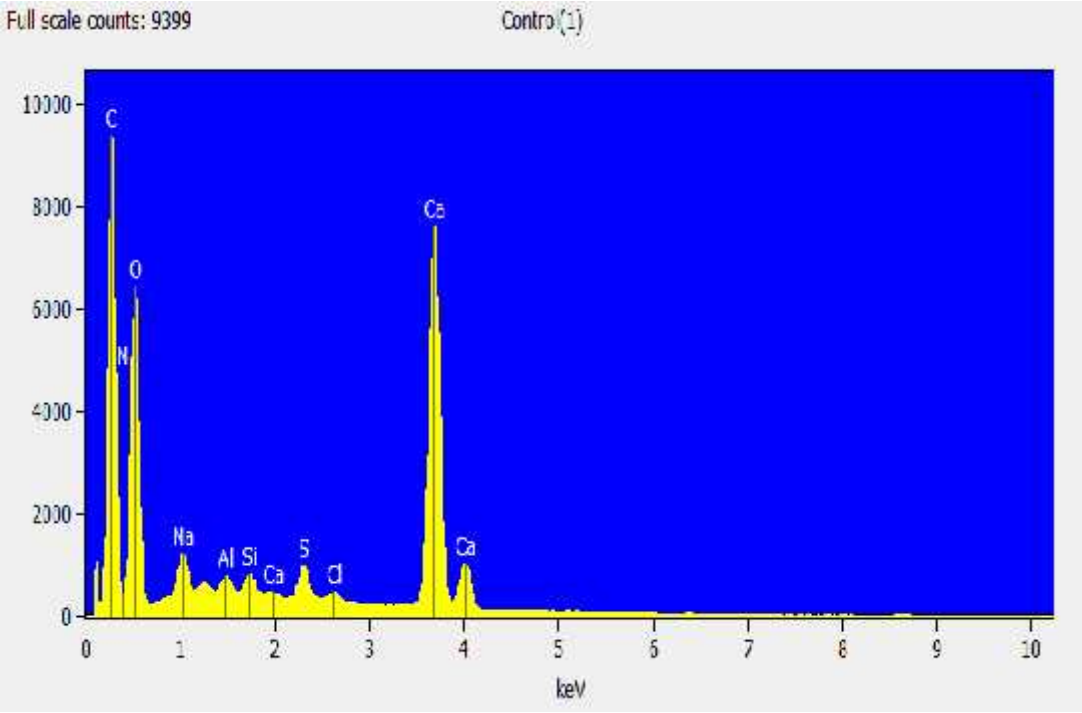


Plate I. EDX of the unmodified PALF

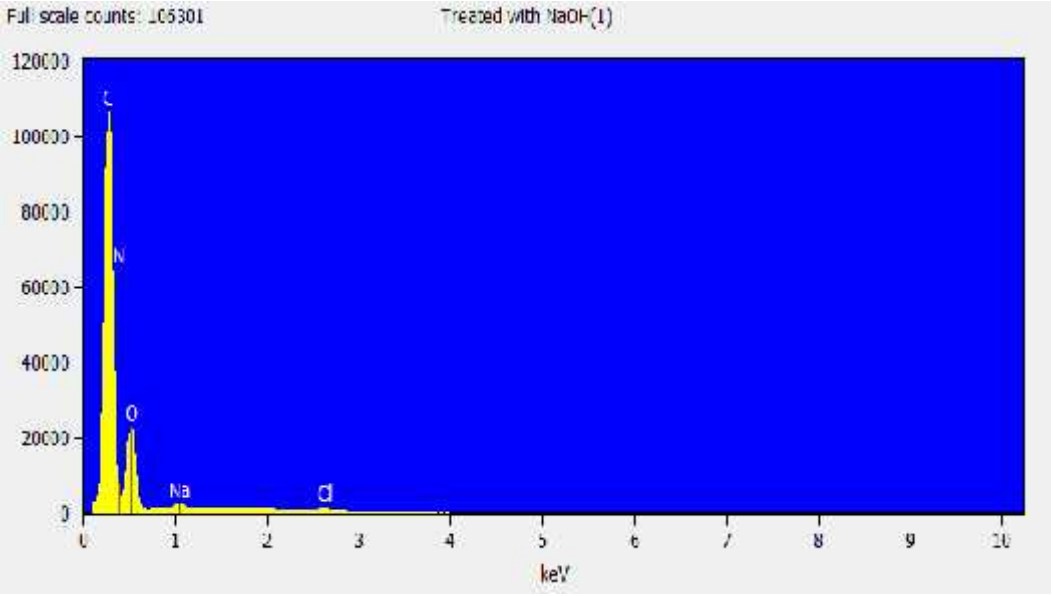


Plate II. The EDX of the PALF modified with NaOH

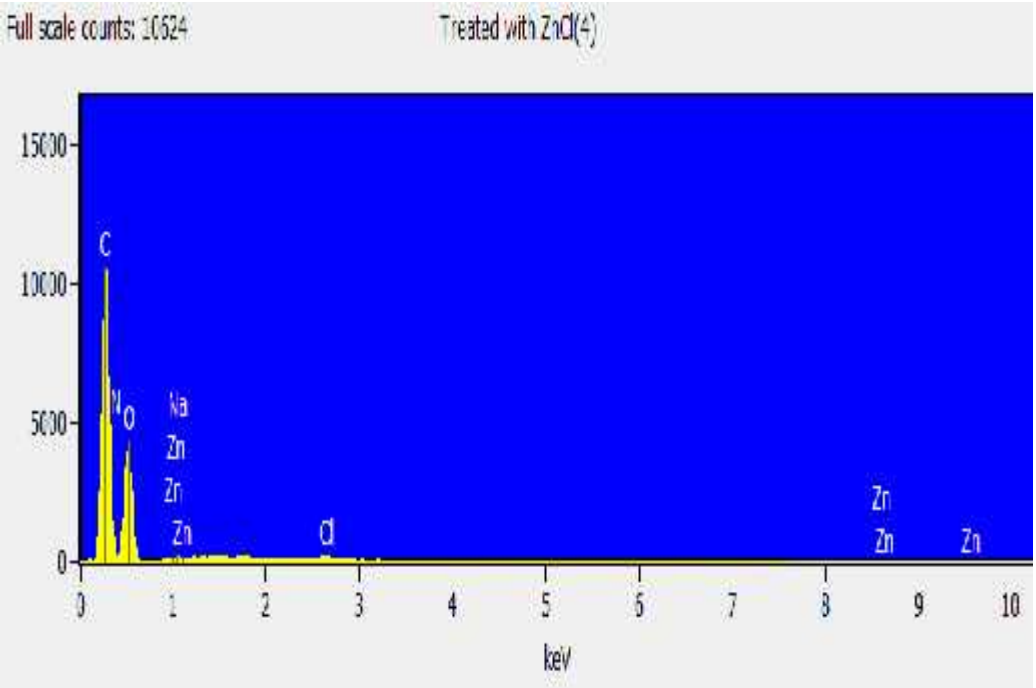


Plate III. The EDX of PALF modified with ZnCl

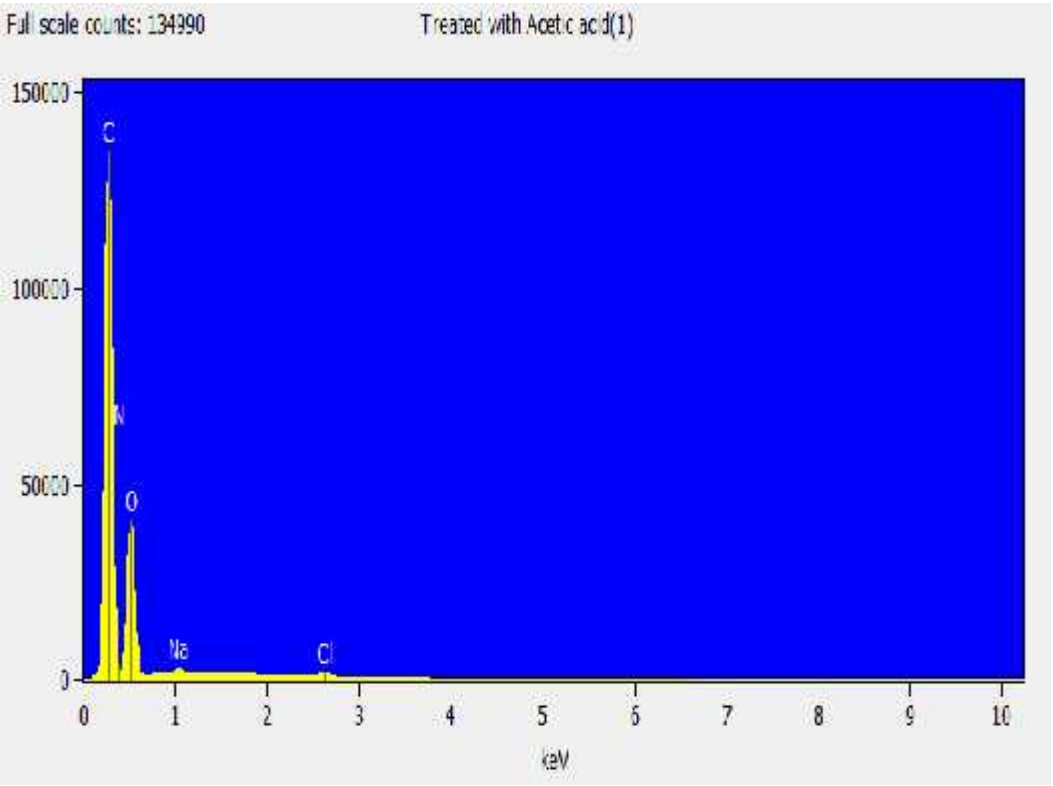


Plate IV. The EDX of the PALF samples modified with $C_3H_6O_3$

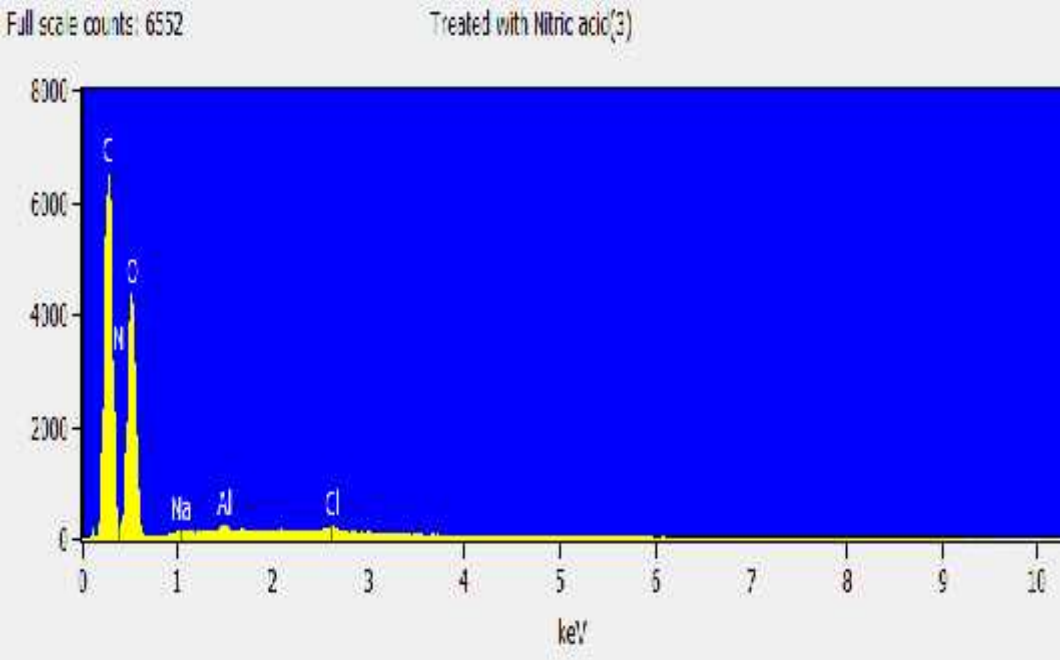


Plate V. The EDX of the PALF modified with HNO_3

From Table 4.5, the percentage composition of calcium is 0.10 %, this gives a difference of 2.10 %, sodium has a percentage composition of 0.34 %. aluminum is 0.09 %, chlorine is 0.43 % and nitrogen is 3.05 %.

From the above data, it can be said that for the unmodified PALF in the macro, micro and nano particle levels, there is no significant differences in the elemental composition of the samples and the results are in close agreement with those obtained by earlier researchers as reported by Asim *et al.*, (2015), in their study, the percentage composition of unmodified PALF is 73.18 %, oxygen is 24.17 %, nitrogen 2.27 % and calcium is 2.88 %.

For the samples modified with NaOH, the percentage composition of Carbon at the macro, micro/nano levels is 66.6 % and 70.26 % respectively. Clearly, there is a difference of 4 % between the two methods, however, this is within the acceptable limits. The percentage composition of oxygen in table 4.4 and 4.5 is 26.4 % and 26.84 % respectively from the two methods, the results from the EDX shows a higher percentage of oxygen, however, a difference of 0.80 % is highly acceptable.

For the samples modified with ZnCl, the percentage composition of carbon is 64.3 % and 61.7 % from Tables 4.4 and 4.5 respectively, there is a difference of 2.6 % which is within acceptable limit.

For the samples modified with $C_3H_6O_3$, the percentage composition of carbon is 60.5 % and 63.57 % from Tables 4.4 and 4.5 respectively, there is a difference of 3.69 %, between the two methods and the result is within acceptable limits.

From Table 4.4, the sample modified with HNO_3 has a percentage composition of carbon as 68.3 %, from table 4.5 the samples modified with HNO_3 gave a percentage composition of 68.45 % for carbon at the micro/nano particle level. Here, we observed a difference of 0.15 %. Similarly, percentage composition of oxygen at the macro level from table 4.4 is 24.4 % while using the EDX at the micro/nano levels, from Table 4.5, the percentage composition of oxygen is 27.16 %.

4.5 Identification of Bacterium and Fungi on the PALF

The experiment was carried out for a 12 months calendar period. Below are the experimental data collected during the period under investigation.

Table 4.6 Result of the fungal load on the PALF after 24 hours Observation

Sample codes	Dilution factor			
	10^1	10^2	10^3	10^4
	No of colonies (cfu/ml)			
A	1.2	0.0	0.0	0.0
B	1.1	0.0	0.0	0.0
C	6.8	6.6	3.5	1.1
D	1.1	0.0	0.0	0.0
E	1.1	0.0	0.0	0.0
Distilled water	0.0	0.0	0.0	0.0

Table 4.7 Result of the Bacterial Load on the PALF after three Months Observation

Sample codes	Dilution factor			
	10^1	10^2	10^3	10^4
	No of colonies (cfu/ml)			
A	6.6	0.0	0.0	0.0
B	0.0	0.0	0.0	0.0
C	0.0	0.0	0.0	0.0
D	0.0	0.0	0.0	0.0
E	0.0	0.0	0.0	0.0
Distilled water	0.0	0.0	0.0	0.0

For the bacterial load tests, data from Tables 4.7 shows bacteria growth on the samples treated with ZnCl after a 24 hours experiment. The results obtained in Table 4.7 however shows that the samples treated with ZnCl after 24 hours of observation have bacterial content of 6.6 X 10^1 cfu/ml, this however diminished to 0.0 after further investigations.

Table 4.8 Result of the Fungal Load on the PALF after three Months Observation

Sample codes	Dilution factor			
	10^1	10^2	10^3	10^4
	No of colonies (cfu/ml)			
A	0.0	0.0	0.0	0.0
B	0.0	0.0	0.0	0.0
C	1.1	1.1	1.1	1.1
D	0.0	0.0	0.0	0.0
E	0.0	0.0	0.0	0.0
Distilled water	0.0	0.0	0.0	0.0

Table 4.9 Results on Fungal Load on PALF after Six Months

Sample codes	Dilution factor			
	10^1	10^2	10^3	10^4
	No of colonies (cfu/ml)			
A	0.0	0.0	0.0	0.0
B	0.0	0.0	0.0	0.0
C	1.1	1.1	1.1	1.1
D	0.0	0.0	0.0	0.0
E	0.0	0.0	0.0	0.0
Distilled water	0.0	0.0	0.0	0.0

Table 4.10 Result of the Fungal Load on the PALF after Three Months Observation

Sample codes	Dilution factor			
	10^1	10^2	10^3	10^4
	No of colonies (cfu/ml)			
A	0.0	0.0	0.0	0.0
B	0.0	0.0	0.0	0.0
C	1.1	1.1	1.1	1.1
D	0.0	0.0	0.0	0.0
E	0.0	0.0	0.0	0.0
Distilled water	0.0	0.0	0.0	0.0

Table 4.11 Result of the Fungal Load on the PALF after Twelve months Observation

Sample codes	Dilution factor			
	10^1	10^2	10^3	10^4
	No of colonies (cfu/ml)			
A	0.0	0.0	0.0	0.0
B	0.0	0.0	0.0	0.0
C	1,1	1.1	1.1	1.1
D	0.0	0.0	0.0	0.0
E	0.0	0.0	0.0	0.0
Distilled water	0.0	0.0	0.0	0.0

For fungal load test, no growth was observed after the one month period. From Tables 4.6, 4.8, 4.9, 4.10 and 4.11, significant presence of microbes was not observed under the experimental conditions. However, from Table 4.7, after a 24 hours observation, the samples modified with ZnCl, HNO_3, $C_3H_6O_3$, NaOH and the untreated samples contained 1.2 $X10^1$, 1.1 $X10^1$, 6.8 $X10^1$, 1.1.$X10^1$, and 1.1$X10^1$ cfu/ml respectively. After a 3 months observation as seen in Table 4.11, significant amount of fungi was noticed only on samples modified with $C_3H_6O_3$ at 1.1$X10^1$ to 1.1.$X10^4$ cfu/ml.

Aspergillus was also identified as the specie of fungus present in the PALF. This was identified macroscopically, by identifying the white felt like colony turning black with conidia formation

and microscopically, it was also confirmed by the presence of black, globose conidia with very dark to black spores, as shown in Figure 4.1



Figure 4.1 An experimental set-up showing aspergillum as the fungus identified on the PALF

4.6 Fourier Transform Infrared Spectroscopy of the Pineapple Leaf Fibre (PALF)

Fourier Transform Spectroscopy (FTIR) is used to detect characteristic chemical functional groups in fibre.

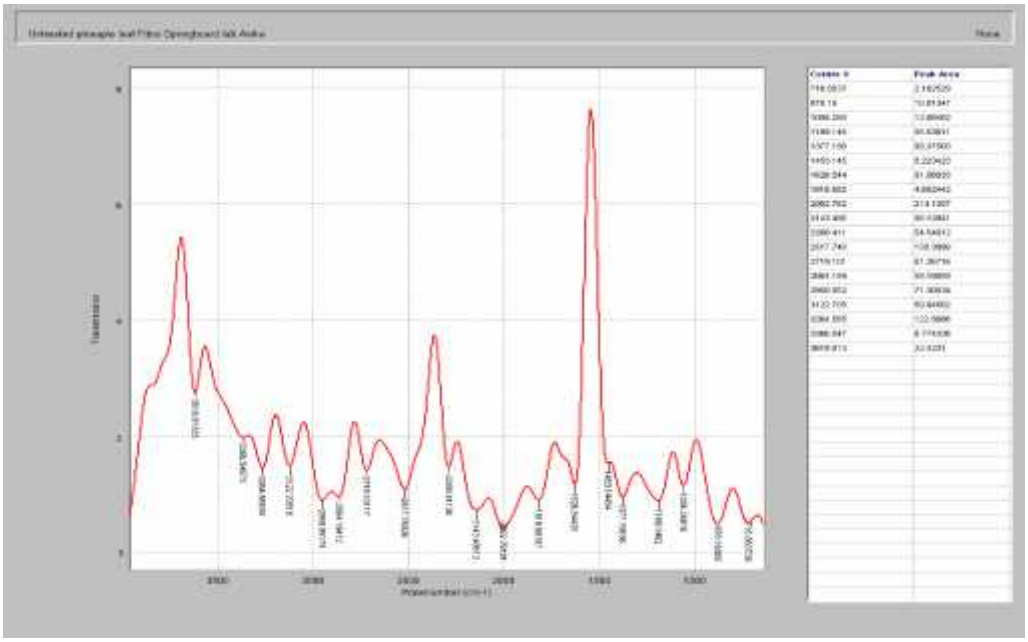


Plate VI. The FTIR spectrum of the unmodified PALF

Plate VI which illustrates the FTIR spectrum of unmodified PALF sample has a total of 19 well defined peaks as observed, there are peaks at 3618.81cm^{-1}, 3366.55, 3264.59, 3122.71, 2950.85, 2864.19, 2719.1, 2517.75, 2288.41, 2143.49, 2002.76, 1816.68, 1526.54, 1453.15, 1377.20, 1188.15, 1056.27, 878.16 and. 716.86 cm^{-1}

The peak observed at 3366.55 cm^{-1} corresponds to the stretching vibration mode of intra- and intermolecular hydroxyl (–OH) bond of cellulose which is in agreement with what was obtained by Prasanna *et al., (*2017) and the peak 2950.85 cm^{-1} corresponding to the asymmetric and the symmetric stretching of methylene (-CH_2-) groups in long alkyl chains. These peaks prove the presence of waxes in the PALF as reported by Abidi *et al.,* (2018). The vibration located at 1816.68cm^{-1} is attributed to C=O stretching vibration and could originate from esters or amide as asserted by Akerholm *et al.,* (2004). The C-C stretching vibrations are observed at 1526.54 cm^{-1} in the FTIR spectrum as earlier reported by Deepak and Vedha (2013). The peak 453.12 cm^{-1} indicates C=C aromatic symmetrical stretching of PALF, and 1453.15 cm^{-1} showing the presence of aromatic group C=C as studied by Deepak and Vedha (2013). The band at the 1377.20 cm^{-1} represented the CO. The peak 1377.20 cm^{-1} proved the presence of alcohols, carboxylic acids, esters, ethers and aliphatic compounds as studied by Yamunadevi (2012). The crystalline structure and the band at 878.16 cm^{-1} is attributed to CH deformation in the amorphous region of the cellulose as reported by Deepak and Vedha (2013).

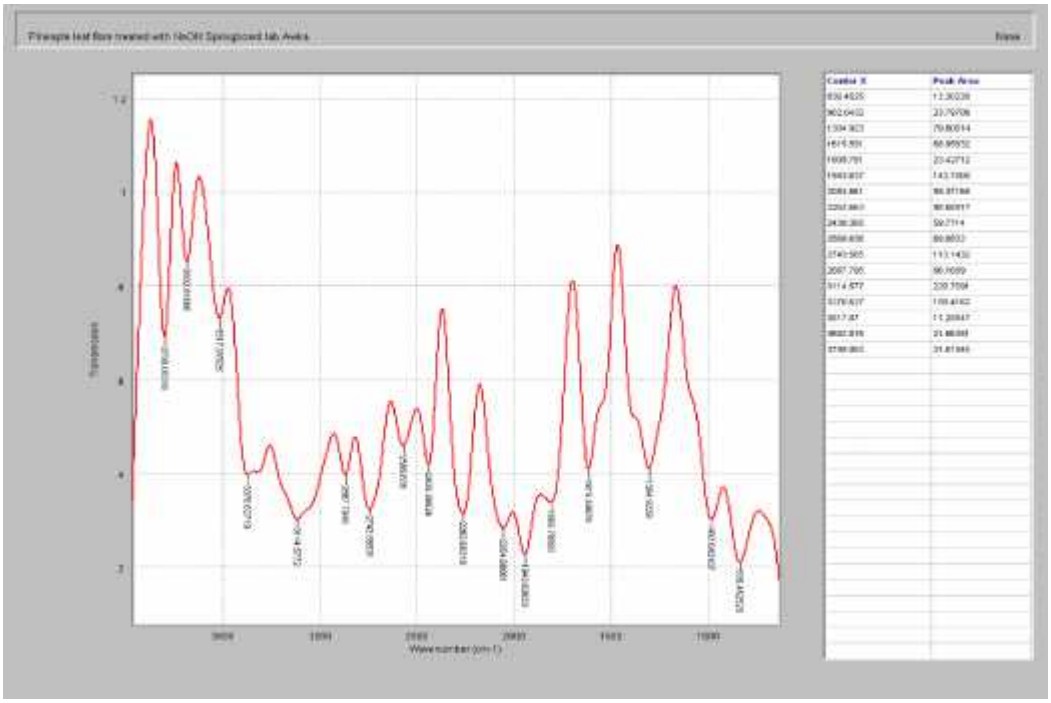


Plate VII. The FTIR spectrum of the PALF modified with sodium hydroxide

Plate VII which illustrates the FTIR spectrum of PALF sample modified with NaOH has a total of 17 well defined peaks as observed, there are peaks at 3799.08 cm^{-1}, 3682.82, 3517.07, 3370.63. 3114.56, 2867.80, 2743.57, 2569.64, 2439.39, 2262.67, 2054.66, 2054.68, 1943.64, 1809.78, 1615.59, 1304.92, 982.64 and 836.48 cm^{-1}.

Plate VII shows the FTIR spectrum of PALF modified with NaOH. The peak 3517.17 cm^{-1} is assigned to the stretching vibrations of hydroxyl groups present in the PALF. In the double bond region, the peaks at 1943.64 cm^{-1} and 1808.78 cm^{-1} are assigned to the carbonyl (C=O) stretching from ester linkage of cellulose, hemicelluloses or lignin. The peak at 1615.59 cm^{-1} is reflected for amide. The bands at 1304.92 cm^{-1} is due to the bending vibration of -CH_3- group. The peak ranges from 982.64 cm^{-1} to 836.48 cm^{-1} represents of -CH- bending vibrations.

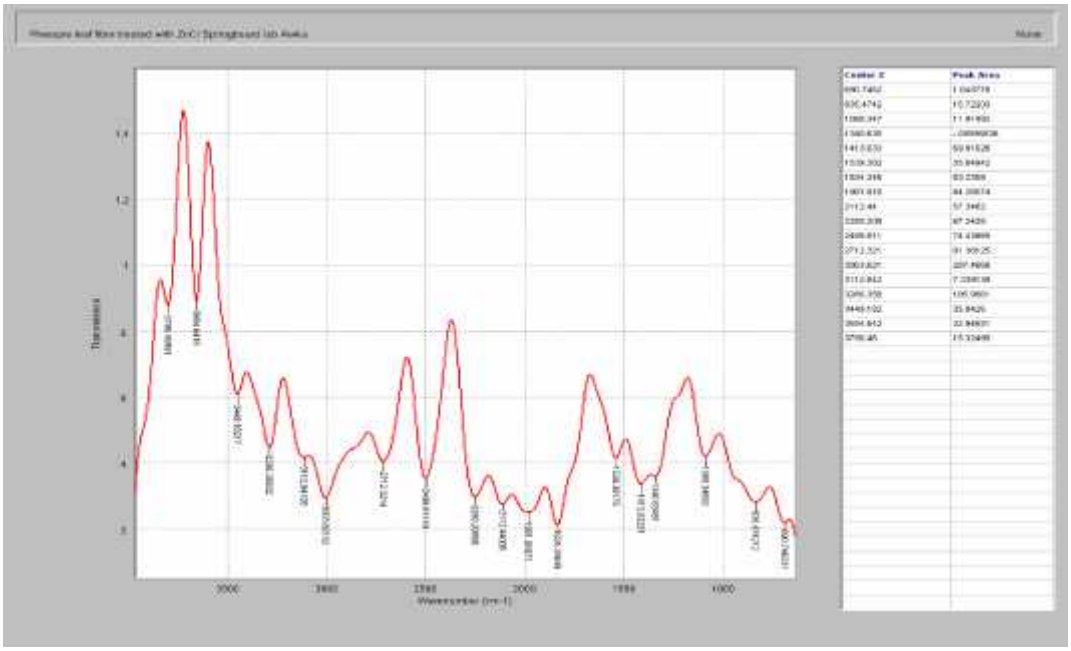


Plate VIII. The FTIR spectrum of the PALF modified with zinc chloride

Plate VIII which illustrates the FTIR spectrum of PALF sample modified with ZnCl has a total of 18 well defined peaks as observed, there are peaks at 3798.46 cm^{-1}, 3654.64, 3449.18, 3286.36, 3112.84, 3003.62, 2712.32, 2498.81, 2258.21, 2112.44, 1981.92, 1834.35, 1539.38, 1413.03, 1340.63, 1088.35, 825.47 and 690.75 cm^{-1}.

The peaks observed at 3449.18 cm^{-1} and 3286.26 cm^{-1} corresponds to the stretching vibration modes of intra- and intermolecular hydroxyl (-OH) bond of cellulose as studied by Prasanna *et al.*, (2017) and the peaks observed at 1534.38 cm^{-1} and 1413.3 cm^{-1} corresponds to the presence of aromatic group (C=C) as reported by Deepak and Vedha, (2013). The band at 1340.63 cm^{-1} represents the CO group. The peak at 1340.63 cm^{-1} proved the presence of alcohols, carboxylic acids, esters, ethers and aliphatic compounds as reported by Yamunadavi, (2013).

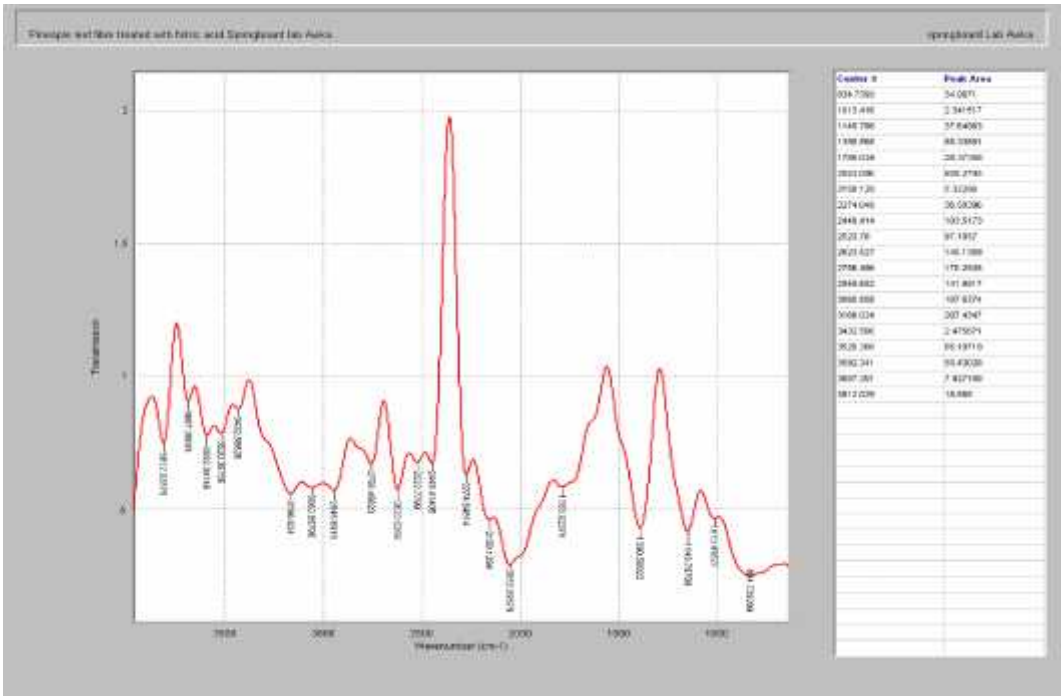


Plate IX. The FTIR spectrum of the PALF modified with nitric acid

Plate IX which illustrates the FTIR spectrum of PALF sample modified with HNO_3 has a total of 20 well defined peaks as observed, there are peaks at 3812.03 cm^{-1}, 3687.3, 3592.34, 3520.37, 3432.59, 3166.02, 3060.86, 2945.69, 2756.47, 2623.53, 2523.78, 2448.41, 2274.05, 2158.13. 2053.10, 1788.02, 1390.57, 1149.79, 1013.42, and 834.74 cm^{-1}.

The peaks observed at 3572.34 cm^{-1}, 3520.27 cm^{-1} and 3432.59 cm^{-1} correspond to the stretching vibration mode of intra- and intermolecular hydroxyl (-OH) bond of cellulose as reported by Prasanna *et al.*, (2017) and the peak 2945.69 cm^{-1} corresponding to the asymmetric and the symmetric stretching of methylene (-CH_2-) groups in long alkyl chains. These peaks prove the presence of waxes in PALF as reported by Abidi *et al.*, (2018). The vibration located at 1788.02 cm^{-1} is attributed to C=O stretching vibration and could originate from esters or amide as reported by Akerholm *et al.*, (2004). The peak 1390.57 cm^{-1} proved the presence of alcohols, carboxylic acids, esters, ethers and aliphatic compounds as reported by Yamunadevi *et al.*, (2013). The peak seen at 1149.79 cm^{-1} indicates the in-plane bending vibrations of the -CH_2 and -CH groups of cellulose as reported by Prasanna *et al.*, (2017). The -CO group

stretching in hemicelluloses was observed at 1014.42 cm^{-1} as reported by Annapoonani and Divya, (2017). The crystalline structure and the band at 834.7 cm^{-1} is attributed to CH deformation in the amorphous region of the celluloses it was similarly reported by Deepak and Vedha, (2013).

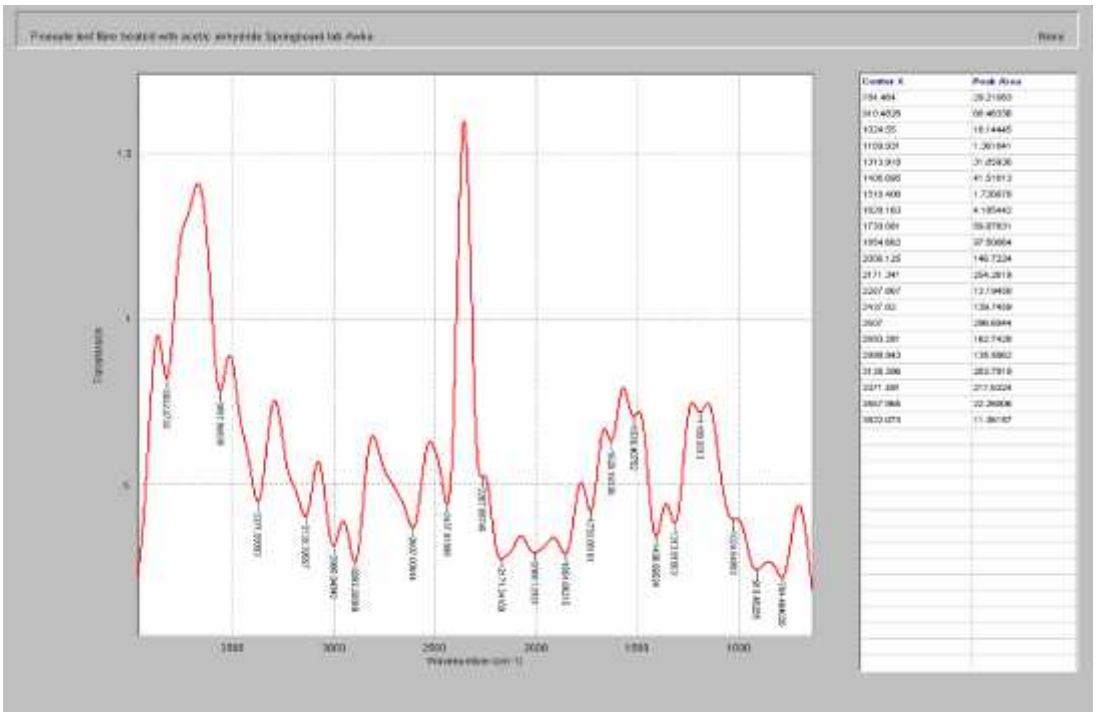


Plate X. The FTIR spectrum of the PALF modified with acetic anhydride

Plate X which illustrates the FTIR spectrum of PALF sample modified with $C_3H_6O_3$ has a total of 21 well defined peaks as observed, there are peaks at 3822.07 cm^{-1}, 3557.97, 3371.59, 3138.40, 2998.94, 2893.28, 2607, 2437.82, 2267.87, 2171.34, 2006.13, 1854.66, 1730.08, 1628.16, 1516.41, 1408.70, 1313.92, 1189.93, 1024.55, 910.48 and 744.46 cm^{-1}.

The peak observed at 3371.59 cm^{-1} corresponds to the stretching vibration mode of intra- and intermolecular hydroxyl (-OH) bond of cellulose as reported by Prasanna *et al.,* (2017) and the peak 2998.94 cm^{-1} corresponding to the asymmetric and the symmetric stretching of methylene ($-CH_2-$) groups in long alkyl chains. These peaks prove the presence of waxes in PALF as reported by Abidi *et al.,* (2018). The vibration located at 1730.08 cm^{-1} is attributed to C=O stretching vibration and could originate from esters or amide as reported by Akerholm *et al.,*

(2004). The C-C stretching vibrations of the PALF are observed at 1516.41cm^{-1} in the FTIR spectrum as reported by Deepak and Divya, (2013). The band at the 1408.7cm^{-1} represented the CO as reported by Sangeeta and Dinesh (2016). The peak 1313.92 cm^{-1} proved the presence of alcohols, carboxylic acids, esters, ethers and aliphatic compounds as reported by Yamunadevi *et al.,* (2004). The peak seen at 1628 cm^{-1} indicates the in-plane bending vibrations of the -CH_2 and -CH groups of cellulose as reported by Prasanna *et al.,* (2017). The CO group stretching in hemicelluloses was observed at 1189.93 cm^{-1} as reported by Annaponani and Divya (2017).

4.7 Production of Molds for the production of PALF/PP Composites

The molds were designed and fabricated at the Scientific Equipment Development Institute, Enugu. The molds after fabrication were hardened in a furnace. The molds were tested and certified fit for use in the injection molding machine for the production of the composites.

4.8 Production / Isolation of PALF Micro and Nano fibrils

4.9.1 Characterization of the PALF Micro Fibrils

4.9.2 Scanning Electron Microscopy (SEM) of the PALF micro fibril

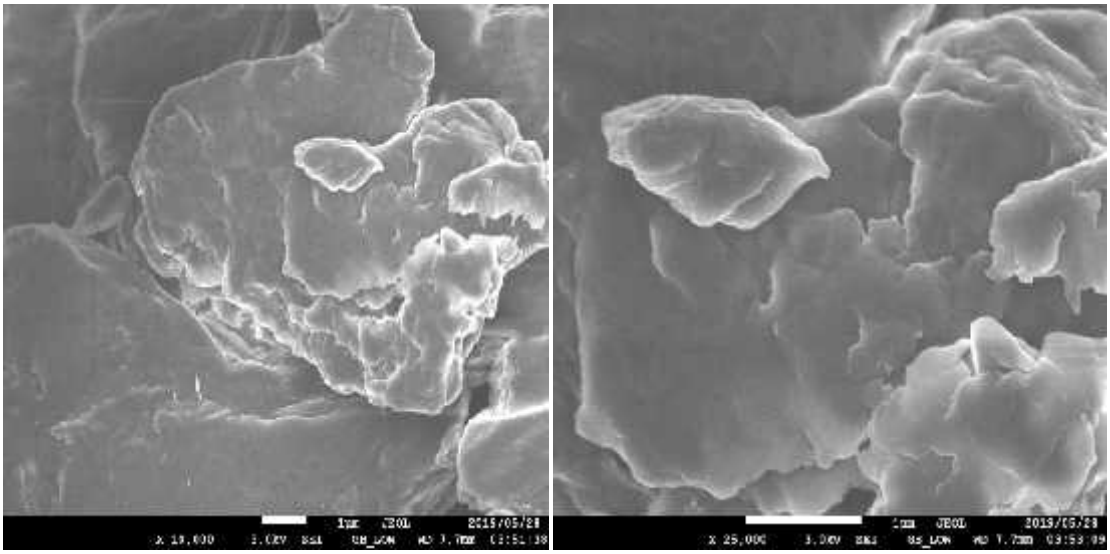


Plate XI. SEM of the unmodified PALF micro cellulose at different magnifications

The unmodified PALF at the micro cellulose level is considered amorphous in nature. The micrographs of the SEM of the unmodified PALF micro cellulose are as shown on Plate XI, the

particles are exhibiting close agglomerates of the micro cellulose, depicting the already established fact that unmodified natural fibres are hydrophobic in nature. This also indicate that there will be improper or inhomogeneous mixing between the matrix and the filler, in this case, the PP and PALF respectively. Plate XI to the left shows the unmodified PALF micro cellulose at 1µm voltage of 3.0 kv and a magnification of X10,000, the micrograph to the right shows same image at a higher magnification of X25,000.

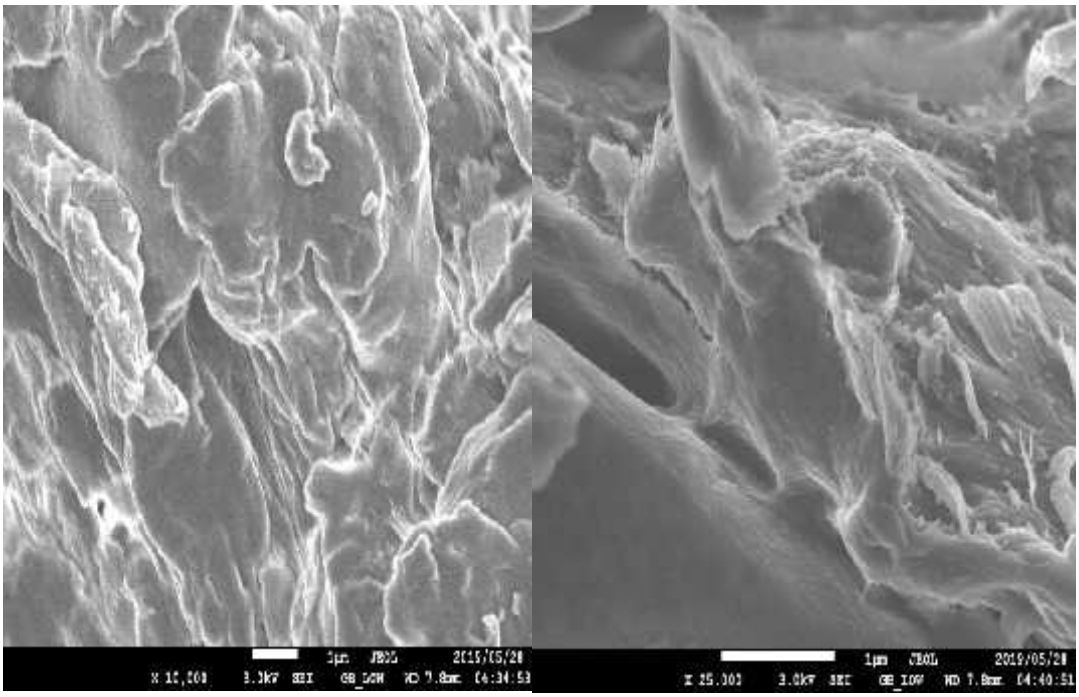


Plate XII. SEM of the PALF micro samples modified with NaOH at different magnifications

Plate XII shows the micrograph of the micro cellulose of the PALF modified with NaOH, the micrograph to the left shows the micro cellulose that depicts an exposed surface, in another words, showing a sample that has a surface that is readily available to read with another surface, suffice to say that the reaction between the hydrophobic PALF and NaOH produces a micro cellulose sample that has a hydrophilic tendency. Plate XII shows the SEM micrograph of the PALF micro cellulose modified with NaOH taken at 3.0KV and 1µm with magnification of X10,000 and X25,000 magnification to the right.

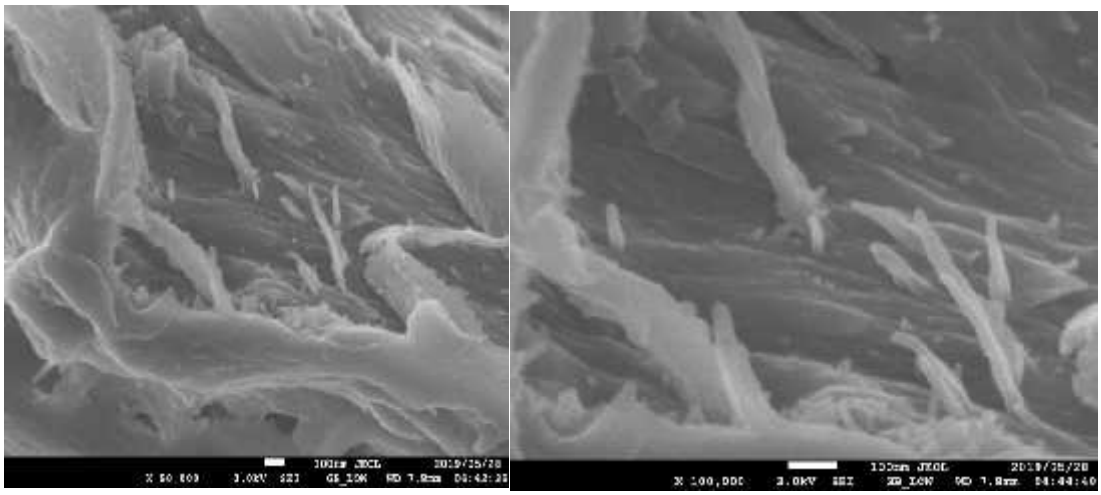


Plate XIII. SEM of the PALF micro samples modified with NaOH at X50, 000 and X 100, 000 magnifications

Plate XIII shows the SEM micrographs at higher resolutions of X50,000 and X100,000 of the modified PALF with NaOH, from Plate XIII, it can be seen that the surface of the modified micro cellulose are flagella in nature, and this compares favorably with micrographs from other researchers.

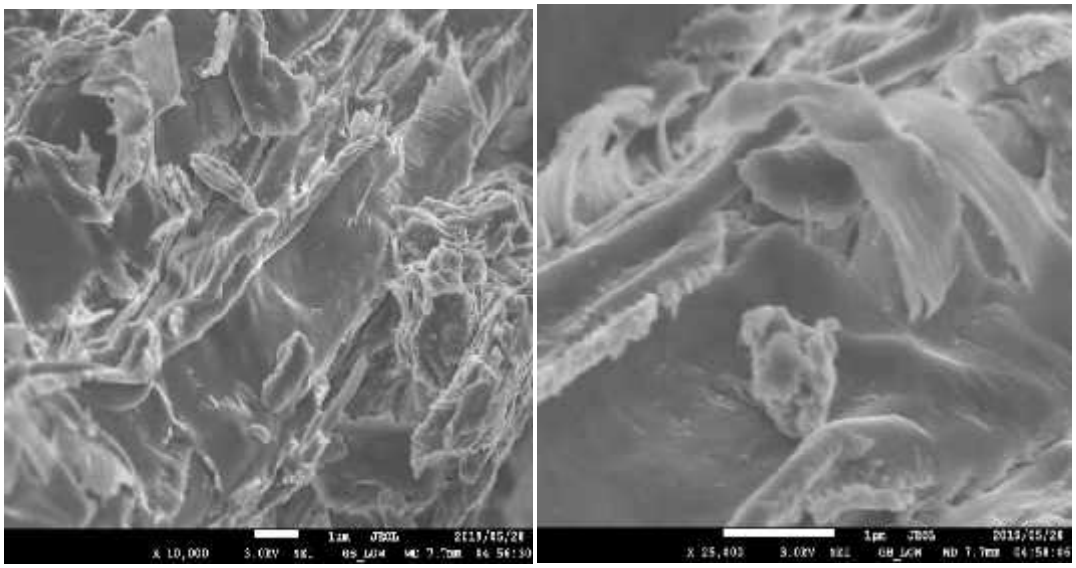


Plate XIV. SEM of the PALF samples modified with acetic anhydride

Plate XIV shows the SEM micrograph of the PALF micro cellulose modified with acetic anhydride, at 1µm at 3.0 KV and a magnification of X10,000 and X25,000, respectively, compared to Plate XI and XII, it can be seen that the micro cellulose modified with acetic anhydride exhibits are more exposed surface area.

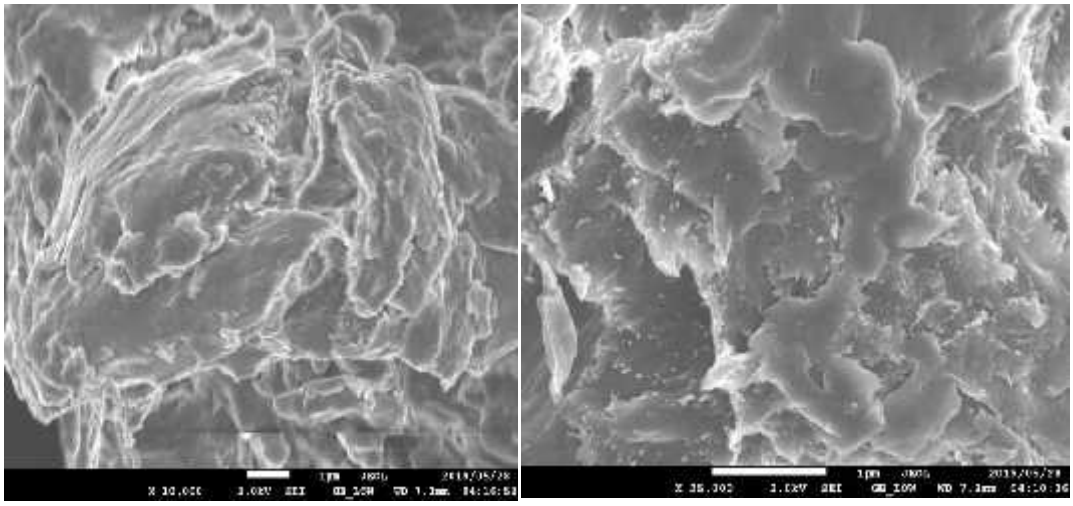


Plate XV. SEM of the PALF micro samples modified with Zinc Chloride at different magnifications

Plate XV and XVI show the micrographs of the PALF micro cellulose modified with Zinc chloride. Plate XV shows the micrographs at magnifications of X10,000 and X25,000 respectively. Plate XVI shows a set of more enhanced micrographs at magnifications of X50,000 and X100,000 respectively.

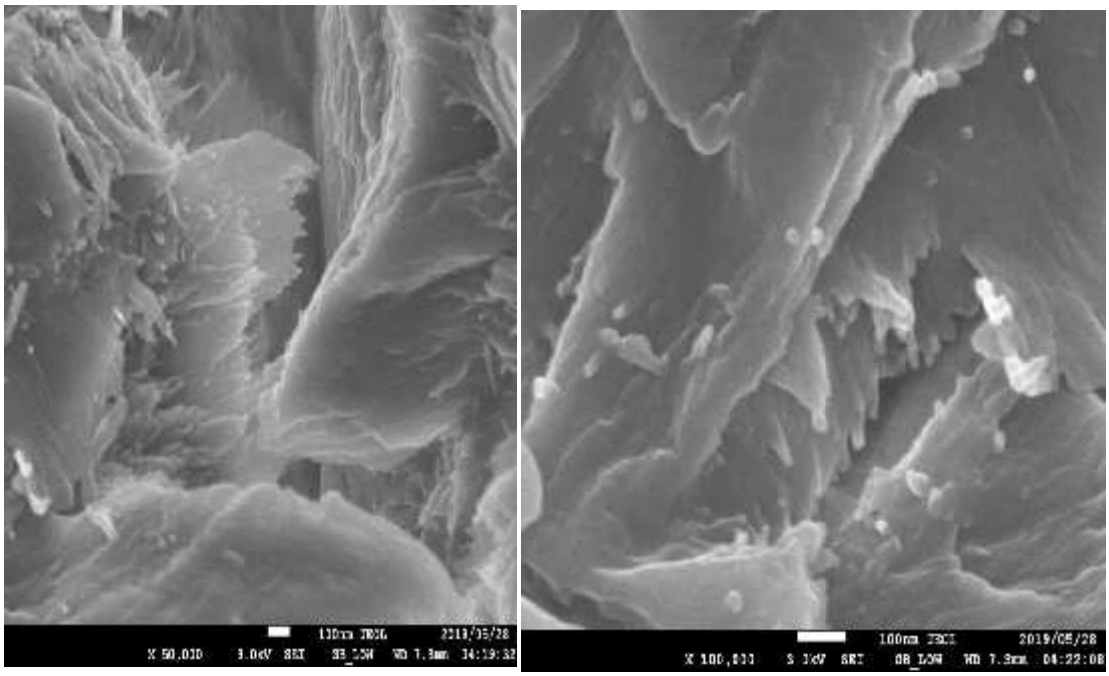


Plate XVI. SEM of the PALF micro samples modified with Zinc Chloride at X50,000 and X100,000 magnifications

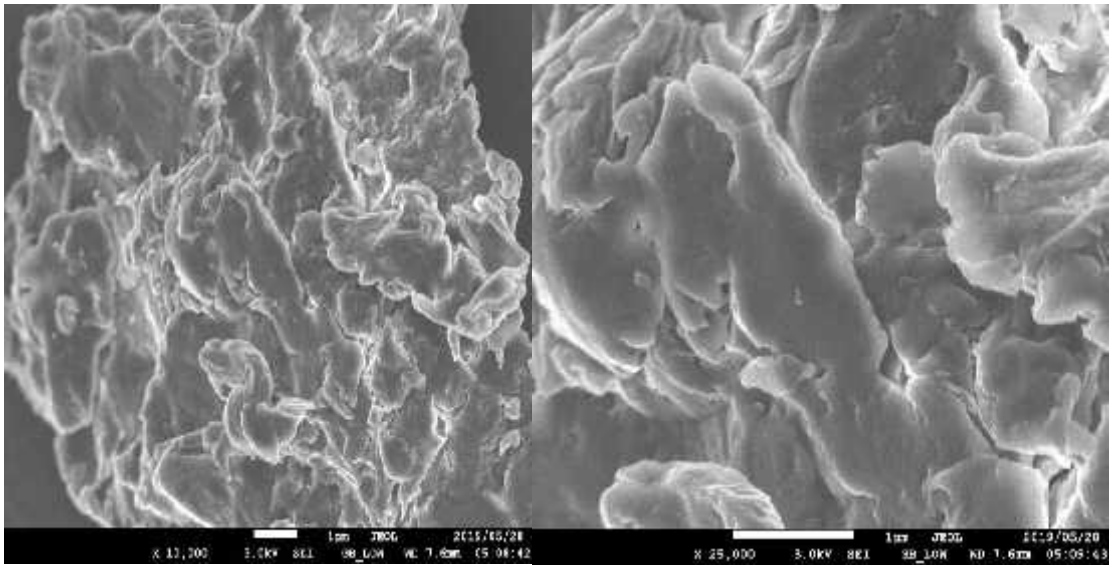


Plate XVII. SEM of the PALF micro samples modified with Nitric acid at X10,000 and X25,000 magnification

Plate XVII shows the SEM micrographs of the PALF modified nitric acid, to the left is the micrograph of micro cellulose at a magnification of X10,000 and to the right same samples at enhanced magnification of X25,000.

Putting Plate XI to XVII into perspective, in order of seemly exposed surface area, in order of anticipated enhanced mechanical, chemical and physical property of the PALF micro cellulose, it could be summarized that the PALF modified with HNO_3 > PALF modified with $C_3H_6O_3$ > PALF modified with NaOH > PALF modified with ZnCl > unmodified PALF. The average PALF micro cellulose obtained are within the range of 150 - 300 µm

4.9.3 Characterization of the PALF Nano Fibrils

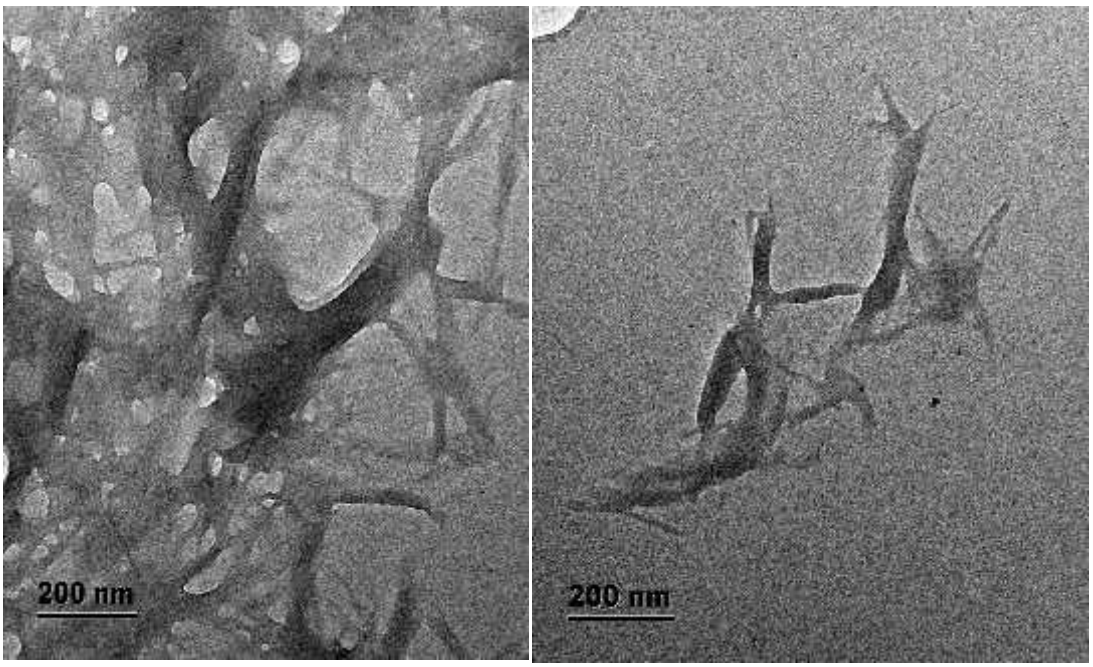


Plate XVIII. TEM of the unmodified (control) PALF nanocellulose agglomerate at different magnifications

Plate XVIII shows TEM agglomerate of unmodified PALF, the agglomerate is due to drying as a result of sample preparation. The attraction is due to the interactions of the abundant hydroxyl group on the surface of the crystals on the TEM equipment. Sample views are obtained when the samples are placed on carbon substrate exposed by a copper gel.

Plate XXIX shows the TEM of the unmodified PALF agglomerate at 200 nm, Plate XXIX shows the TEM of the unmodified PALF agglomerate at 500 nm, the view to the left shows a well dispersed agglomerate while the view to the left shows a dense agglomerate.

Plate XXIX shows the TEM of PALF nano cellulose agglomerate at a magnification of 200 nm. Here, it is clear that the agglomerates are more dispersed when compared to those of the unmodified PALF nano cellulose. The view to the right shows nano cellulose with average dimensions of 34.37 nm in diameter and 280.47 nm in length.

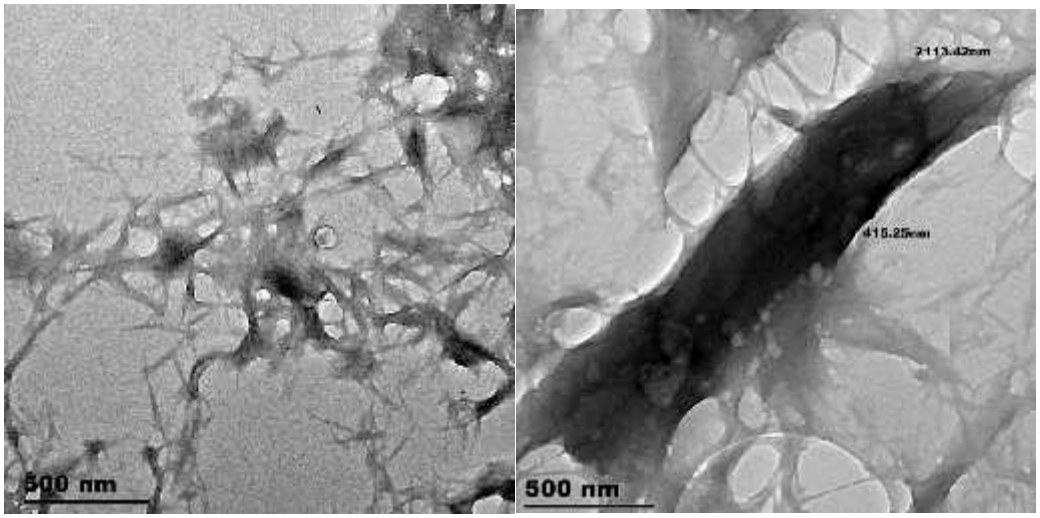


Plate XIX. TEM of the unmodified (control) PALF nanocellulose agglomerate at higher magnification of 500 nm

Plate XIX shows TEM agglomerate of unmodified PALF, the agglomerate is due to drying as a result of sample preparation. The attraction is due to the interactions of the abundant hydroxyl group on the surface of the crystals on the TEM equipment. Sample views are obtained when the samples are placed on carbon substrate exposed by a copper gel.

The dispersion of some of the nano cellulose samples is a result of ultrasonication which assist in preventing agglomeration. Agglomerations are as a result of the Van der Waals attractive forces between the nano particles.

Plate XXXII shows the TEM of the unmodified PALF agglomerate at 200 nm, Plate XXXIII shows the TEM of the unmodified PALF agglomerate at 500 nm, the view to the left shows a well dispersed agglomerate while the view to the left shows a dense agglomerate.

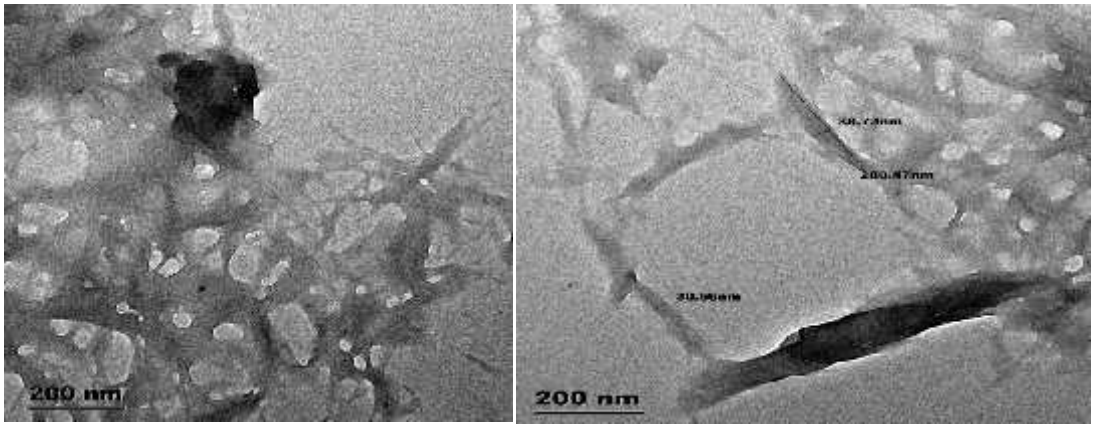


Plate XX. TEM of the PALF nanocellulose agglomerate modified with NaOH

Plate XX shows same PALF nanocellulose samples modified with NaOH from a different view at a higher resolution of 500 nm. Plate XX shows the TEM of PALF nano cellulose agglomerate at a magnification of 200 nm. Here, it is clear that the agglomerates are more dispersed when compared to those of the unmodified PALF nano cellulose. The view to the right shows nano cellulose with average dimensions of 34.37 nm in diameter and 280.47 nm in length.

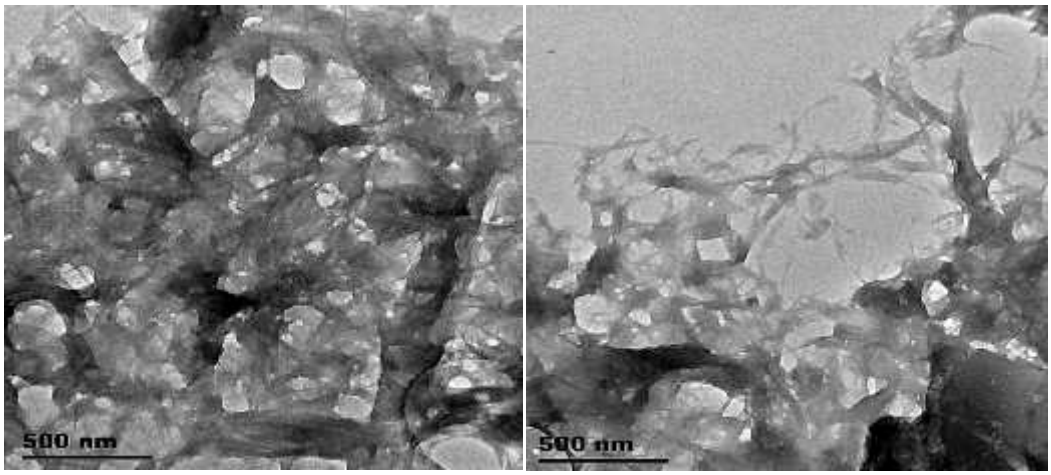


Plate XXI. TEM of the PALF nanocellulose agglomerate modified with NaOH at higher resolution of 500 nm

Plate XXI shows same PALF nanocellulose samples modified with NaOH from a different view at a higher resolution of 500 nm.

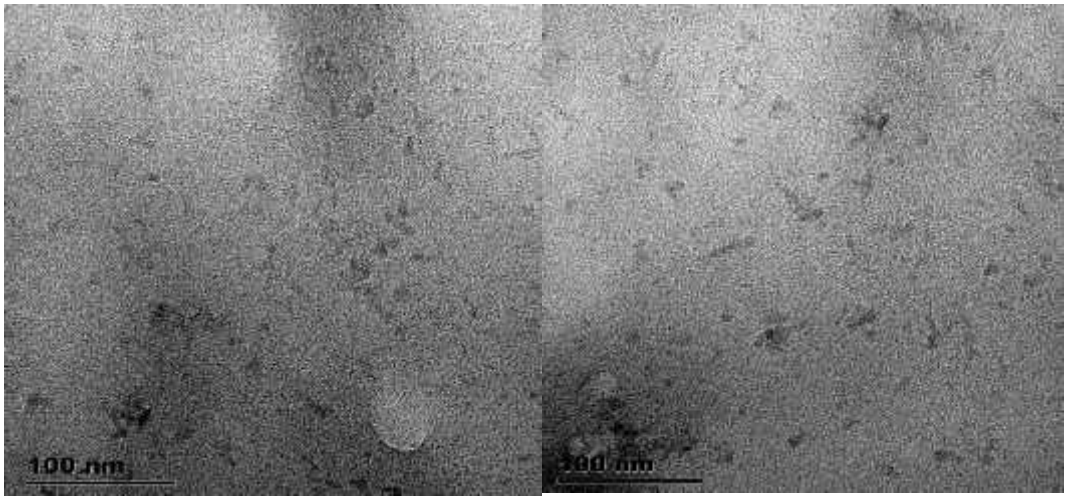


Plate XXII. TEM of the PALF nanocellulose agglomerate modified with acetic anhydride (depicting a more readily dispersed agglomerate)

Plate XXII shows the TEM nanocellulose agglomerate of PALF modified with $C_3H_6O_3$ at a magnification of 100 nm, this gives a view of a more dispersed nanocellulose agglomerate.

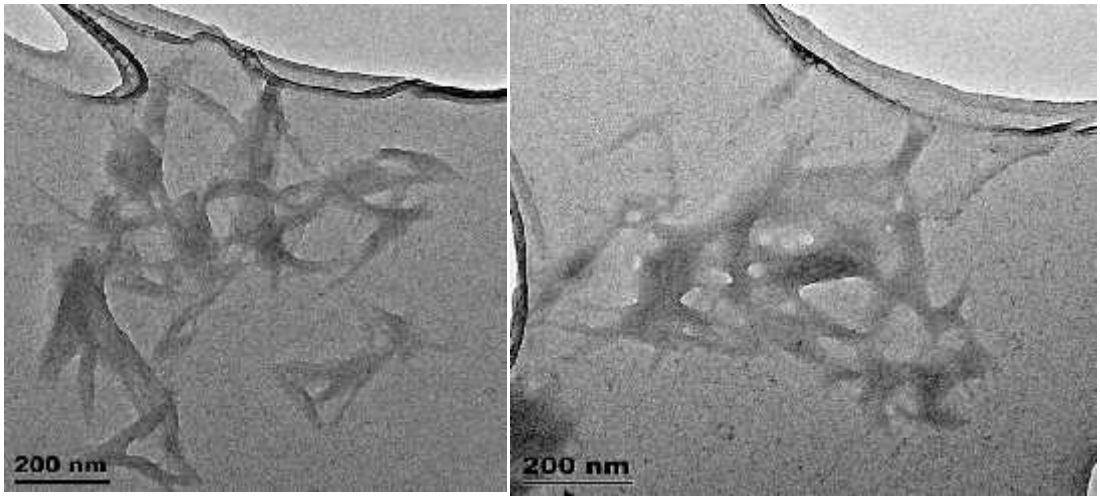


Plate XXIII. TEM of the PALF nanocellulose agglomerate modified with acetic anhydride (depicting a more readily dispersed agglomerate) at a magnification of 200 nm

Plate XXIII and XXIV shows similar result, this time at higher resolutions of 200 nm and 500 nm respectively

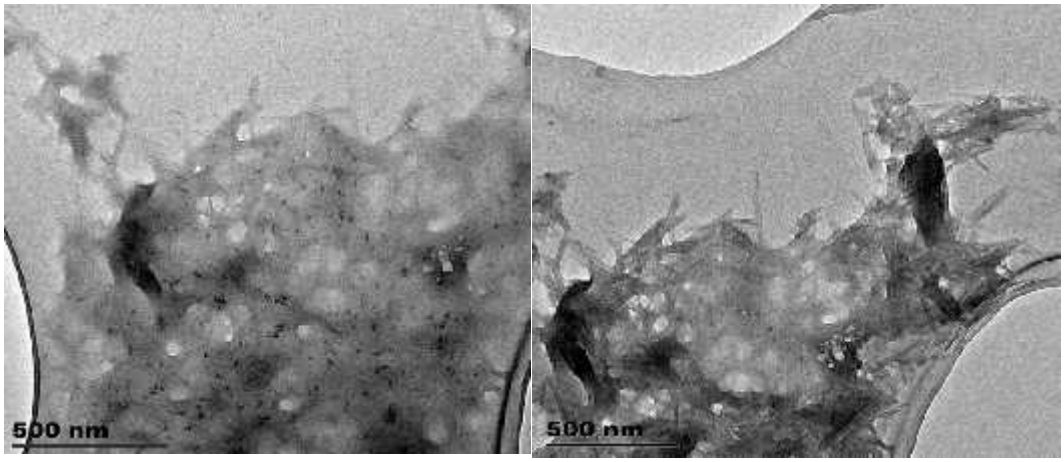


Plate XXIV. TEM of the PALF nanocellulose agglomerate modified with acetic anhydride (depicting a more readily dispersed agglomerate) at a magnification of 500 nm

Plate XXIII and XXIV shows similar result, this time at higher resolutions of 200 nm and 500 nm respectively

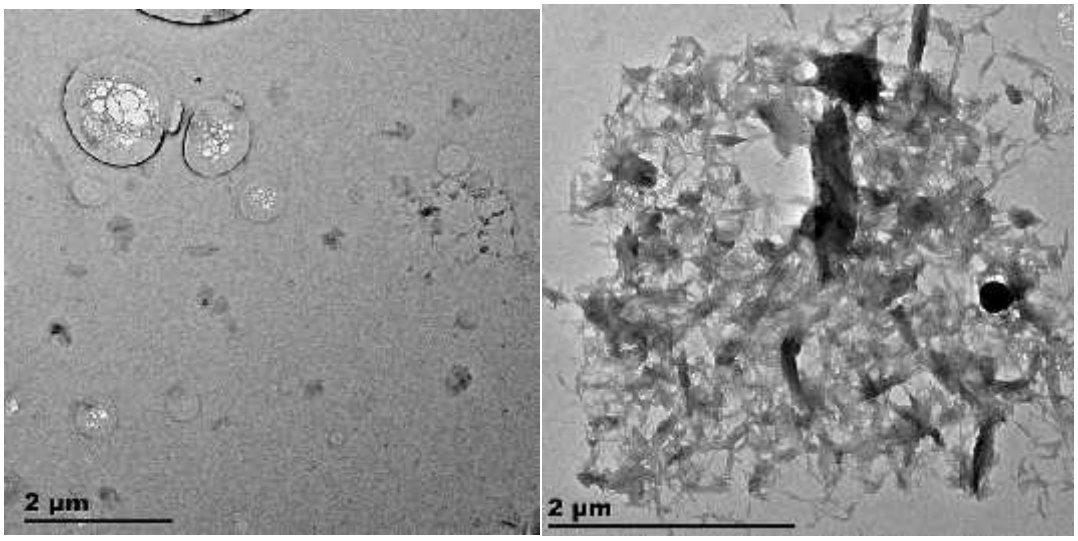


Plate XXV. TEM of the PALF nanocellulose agglomerate modified with ZnCl (depicting a more readily dispersed agglomerate) at a magnification of 2 µm

Plate XXV shows the TEM well dispersed agglomerate of PALF nanocellulose modified with ZnCl at lower resolution of 2 µm. at the magnification of 2 µm the PALF nano fibrils samples give a highly dispersed agglomerate in a spider-web like network as reported by other researchers. The composites produce from this samples gave more adhesion between the filler and matrix.

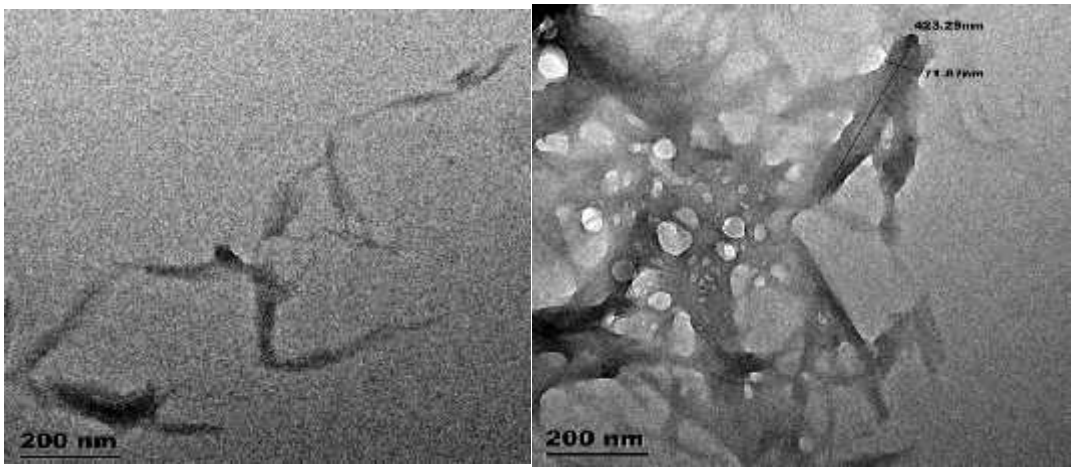


Plate XXVI. TEM of the PALF nanocellulose agglomerate modified with ZnCl (depicting a more readily dispersed agglomerate) at a magnification of 200 nm

Plate XXVI shows a well dispersed agglomerate compared to those modified with $C_3H_6O_3$. Plate XL shows same sample, this time on a higher resolution of 200 nm. The average size of nanocellulose here is 71.67 nm in diameter and 423.20 nm in length.

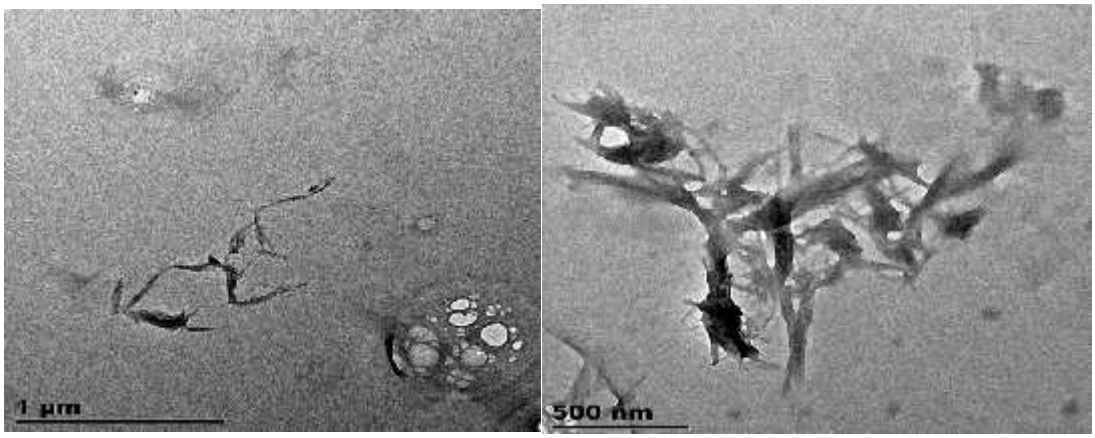


Plate XXVII. TEM of the PALF nanocellulose agglomerate modified with ZnCl (depicting more readily dispersed agglomerate) at a magnification of 1µm and 500 nm

This Plate shows the PALF nano fibril modified with Zinc chloride at a magnification of 1 microns and 500 nm respectively

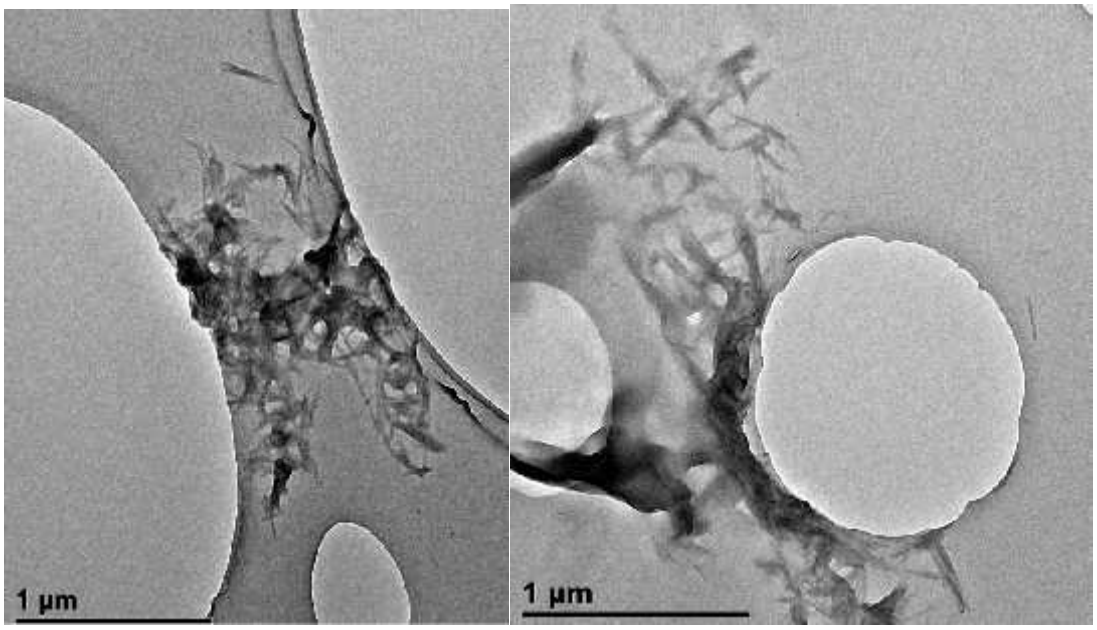


Plate XXIII. TEM of the PALF nanocellulose agglomerate modified with nitric acid (depicting a more readily dispersed agglomerate) at a magnification of 1µm

Plate XXIII to Plate XXX show the TEM agglomerate of the PALF nanocellulose modified with HNO_3, the samples here are at lower magnification of 1µm, these results depict a better more dispersed set of nanocellulose agglomerate.



Plate XXIX. TEM of the PALF nanocellulose agglomerate modified with nitric acid (depicting a more readily dispersed agglomerate) at a magnification of 200 nm

Plate XXIX and Plate XXX shows same samples of nanocellulose modified with HNO_3, this time at higher resolutions of 200 nm and 500 nm respectively. The average nanocellulose dimensions here is around 22 nm in diameter and 250 nm in length.

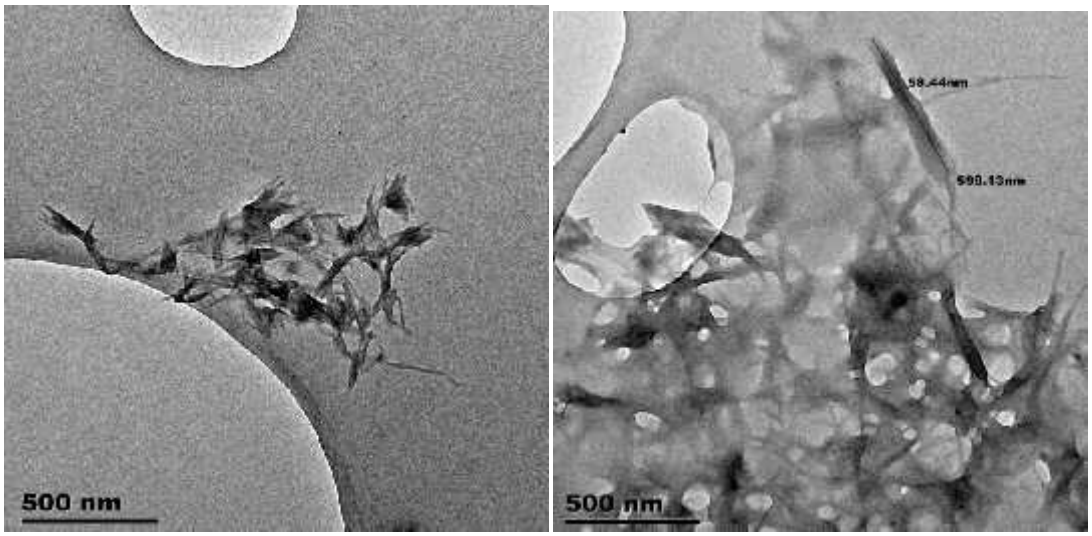


Plate XXX. TEM of the PALF nanocellulose agglomerate modified with nitric acid (Depicting a more readily dispersed agglomerate) at a magnification of 500 nm

The dimensions of nanocellulose are dependent on the sources of cellulose microfibrils, the circumstances of acid hydrolysis process, and ionic strength. Normally, the average length of nanocellulose varies from 200 nm to 600 nm, while the width varies from 3nm to 50nm. In some cases, the diameters would be higher due to the aggregation of nanoparticles (Johnsy and Sabapathi, 2015). In here is an overview for dimensions of nanocrystalline cellulose depending on the sources and preparation methods. Beck-Candanedo, (2005), used H_2SO_4 hydrolysis on wood fibre and got nanocellulose within the range of 100-300nm length and average diameter of 3-5 nm. Araki *et al.* (2001), used HCl hydrolysis on cotton fibre and got nanocellulose with particle length of 100-150 and average diameter of 10 - 30 nm. Kasim *et al.*, (2016) used H_2SO_4 hydrolysis on ramie and got 70 - 200 nm length and 5 - 15 nm average diameter. Kimura *et al*. (2005), used H_2SO_4 hydrolysis on tunicates and got an average size > 1000 nm length and diameter of 10 - 20 nm. Mahadrika *et al*. (2018), used H_2SO_4 on bacteria and got an average

size of 100-1000 and diameter of 10-20 nm. Cui *et al.*, (2019) used HCl hydrolysis on bacteria and got average length of 160 - 420 nm and average diameter of 15 - 25 nm.

Nanocellulose with high length to diameter ratio have the better mechanical performances and stronger reinforcing ability due to the formation of percolated networks in the polymers (Johnsy and Sabapathi, 2015).

Putting into perspective the results of the TEM characterization of the nanocellulose isolated in this research, in order of dispersion, PALF modified with HNO_3 > PALF modified with $C_3H_6O_3$ > PALF modified with NaOH > PALF modified with ZnCl > unmodified PALF.

The results of this research fall with the acceptable limits of nanocellulose particles as reported by Liu *et al,* (2011), they did a study on banana fibre nanocellulose which gave them nanocellulose with average diameter of < 100 nm, Teixera *et al.*, (2011), studied the nanocellulose from sugarcane bagasse and obtained nanocellulose with average diameter of 255 nm, Chen *et al.*, (2017) worked on potato peel fibre and isolated nanocellulose with average diameter of 411nm, Yu *et al*, (2012) worked on isolation of nanocellulose from bamboo and got an average diameter of 200 - 500 nm. Santos *et al.*, (2013), isolated nanocellulose from PALF and got average cellulose diameter of 210 - 240 nm, Silveria *et al.*, (2013) worked on corncob and isolated nanocellulose with average diameter of 283.7 nm, Zheng *et al.*, (2015) worked on softwood and got values average of 100nm, Sofia *et al.*, (2016) studied on sugarcane bagasse and got nanocellulose with diameter within the range of 240 nm, Nurrudin *et al.*, (2016) worked on kenaf and wheat straw and isolated nanocellulose within the diameter range of 100 nm. Lastly, Phanthong *et al.*, (2018) worked on cellulose powder and were able to isolate nanocellulose within the value range of 10 - 25 nm, Mahardika *et al.*, (2018) studied the production of nanocellulose from PALF via high shear homogenization and

ultrasonication, and were able to obtain nanocellulose with an average diameter of 68 nm and length between 88 - 1100 nm.

4.11 Physical Property Analysis of the PALF/PP Composites

4.11.1 Water Absorption Data of the PALF/PP Composites

Figures 4.2 to 4.6 give the results of the chemical property test (water absorption) of the PALF/PP composite. This aspect of the analysis only reports for water absorption of the PALF/PP composites at the macro level, the reason is that the PALF micro cellulose/PP composites and the PALF nanocellulose/PP composites show no reasonable gain in weight after performing the experiment on their individual samples for same period as the PALF/PP composites.

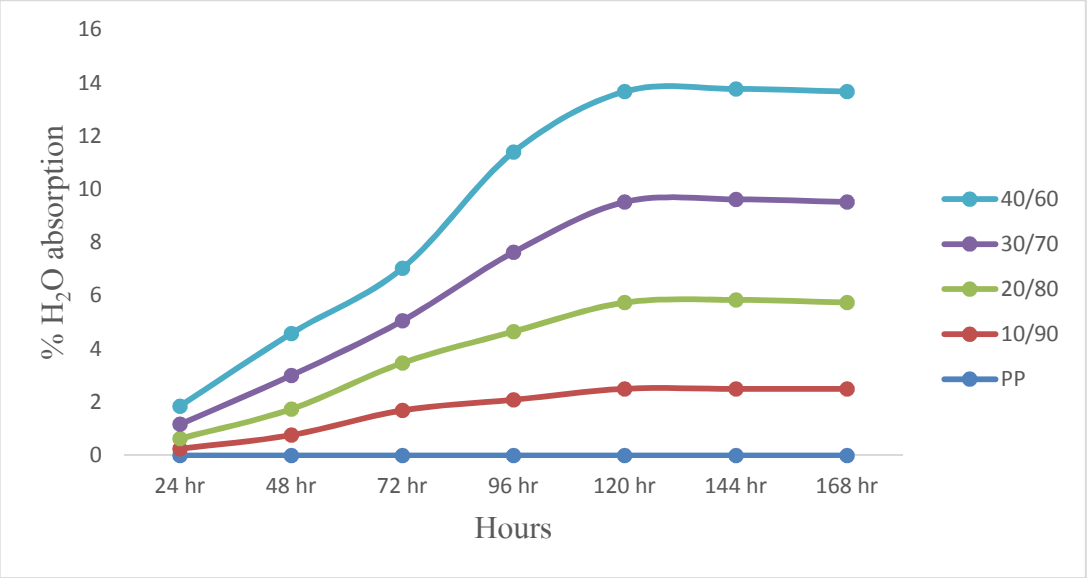


Figure 4.2 Water absorption property of the reinforced unmodified PALF/PP Composites

From Figure 4.2, it can be observed that there is a gradual increase in the rate of water absorption of the PALF/PP composites samples after 24 hours, there seems to be a steady growth after 48 hours and 72 hours, stagnation in growth was observed after 96 hours, same was seen till after 168 hours and the experiment was terminated.

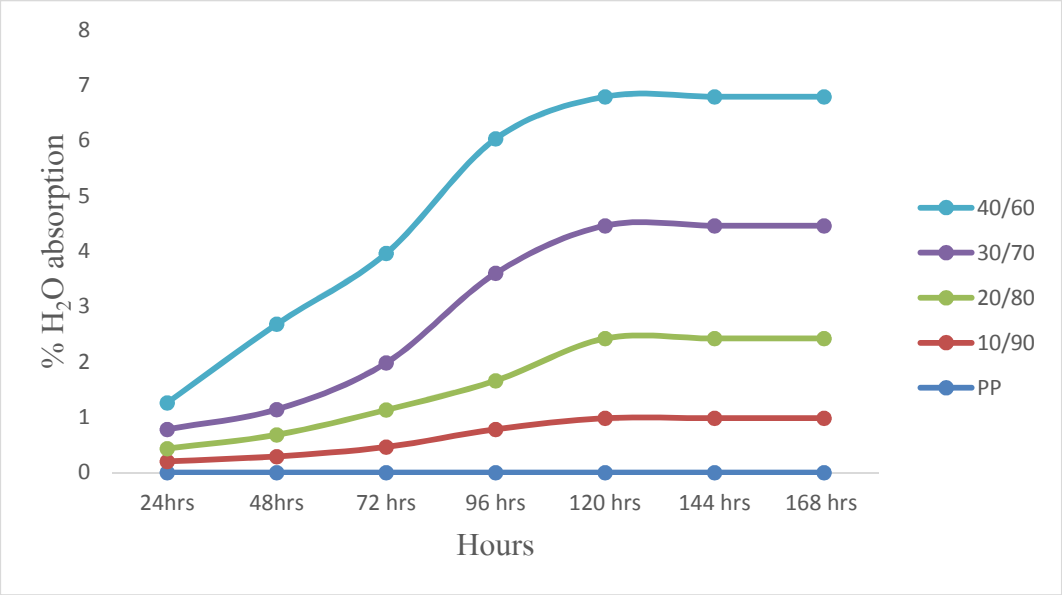


Figure 4.3 Water absorption property of the reinforced PALF/PP Composite modified With NaOH

From Figure 4.3, it can be observed that there is a gradual increase in the rate of water absorption of the PALF/PP composites samples after 24 hours, there seems to be a steady growth after 48hours and 72 hours, stagnation in growth was observed after 96 hours, same was seen till after 168 hours and the experiment was terminated.

The ability of water to penetrate into fibre composites is a great disadvantage as this eventually lowers the life span of the composites, because the microorganisms present in water can attack the cellulose of the pineapple fibre and let to possible degradation as reported by Danladi and Shuaib, (2014).

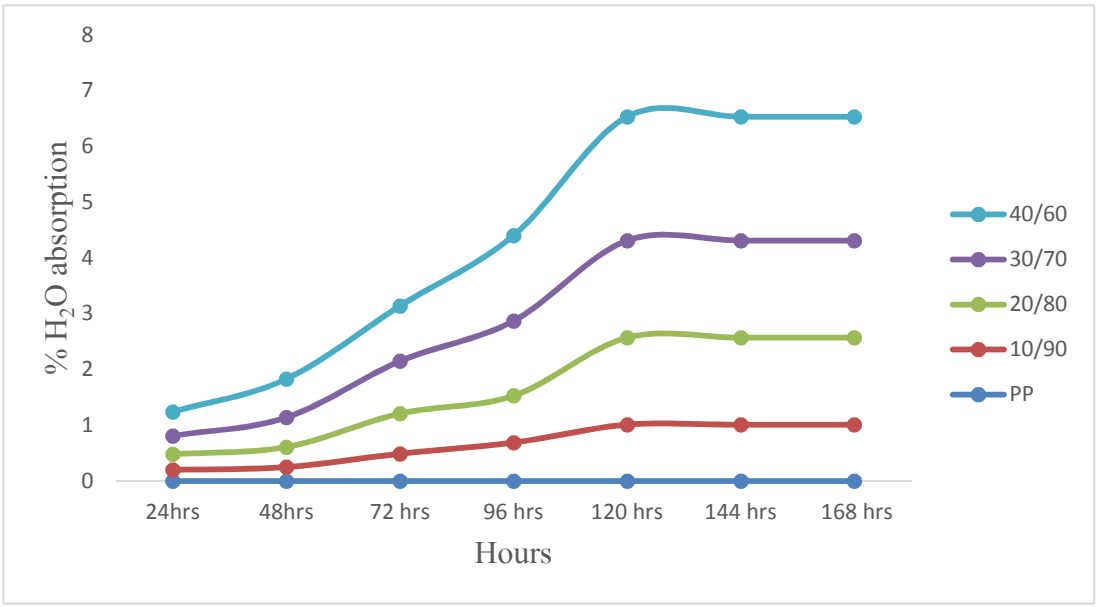


Figure 4.4 Water absorption property of the reinforced PALF/PP Composite modified with ZnCl

A similar phenomenon was observed in figures 4.4. The significant difference here is that the highest rate of water absorption was recorded in the unmodified PALF/PP composites, The rate of water absorption can be summarized this way; water absorbed by unmodified PALF/PP composites > PALF/PP composites modified with NaOH > PALF/PP composites modified with ZnCl > PALF/PP composites modified with $C_3H_6O_3$ > PALF/PP composites modified with HNO_3.

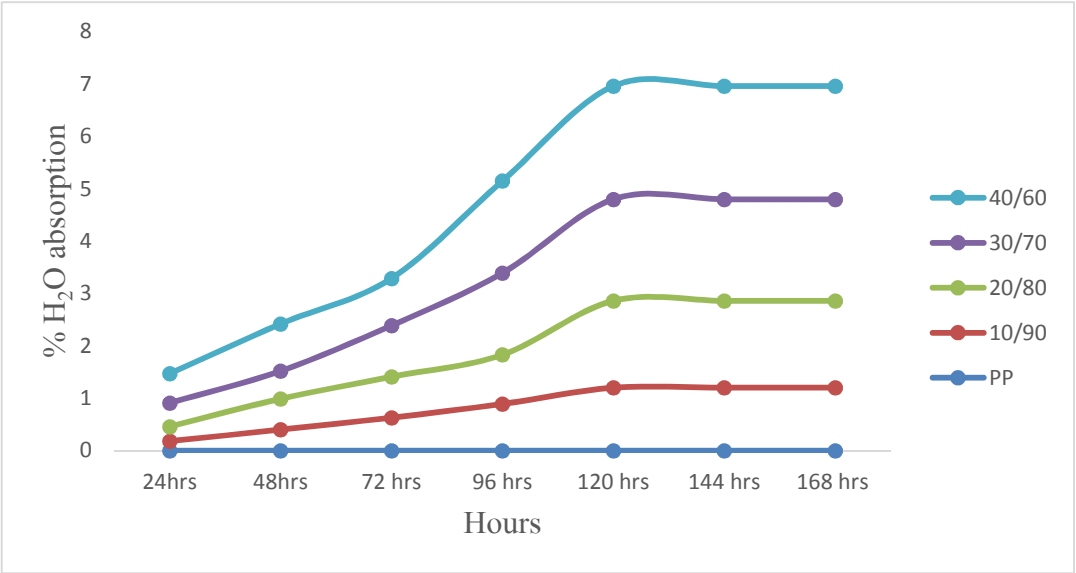


Figure 4.5Water absorption property of the reinforced PALF/PP Composite modified with $C_3H_6O_3$

From Figure 4.5, it can be observed that there is a gradual increase in the rate of water absorption of the PALF/PP composites samples after 24 hours, there seems to be a steady growth after 48 hours and 72 hours, stagnation in growth was observed after 96 hours, same was seen till after 168 hours and the experiment was terminated. A similar phenomenon was observed in Figures 4.2, 4.3, 4.4 and 4.5.

The significant difference here is that the highest rate of water absorption was recorded in the unmodified PALF/PP composites, The rate of water absorption can be summarized this way; water absorbed by unmodified PALF/PP composites > PALF/PP composites modified with NaOH > PALF/PP composites modified with ZnCl > PALF/PP composites modified with $C_3H_6O_3$ > PALF/PP composites modified with HNO_3.

Santosh *et al,* (2015) reported that water absorption mainly depends on the presence of natural fibre and immersion time, the longer immersion time resulted in higher water uptake. Daramola *et al*., (2017) in their reported immersed composites in distilled water at room temperature for about 336 hours. They observed that the water absorption by the composite increased with immersion time although the rate of absorption decreases with increased time. It was also observed that the composite attains equilibrium after 336 hours.

Patti and Acierno *et al*., (2018) reported that the amount of water absorbed increases with fibre content. The water absorption property of PALF/polyester reinforced with natural fibres and their derivatives is dependent on the amount of the fibre, fibre orientation, immersion temperature, area of the exposed surface to water; also, the permeability of fibres, void content, and hydrophilicity of the individual components (in this case the PALF and the polyester

matrix). The swelling stresses that develop under these circumstances can result in composite failure.

Kasim *et al*., (2016) in their study reported that the 40 weight % composition of the fibre has the highest maximum water absorbed. The fibre content contributes to its absorptivity rate. At the beginning, it absorbs water at an increased rate before it attains the maximum, the rate drops drastically until reaches saturation point. The 40 weight % of the fibre attains saturation earlier than the rest specimen.

Daramola *et al.*, (2017) worked on the Pineapple peal fibre (PAPF) and reported that the modified PAPF reduced the water absorption because of better interfacial bonding. To promote the adhesion between the fibre and the matrix, chemical treatment or modifications are considered. Chemicals activate the hydroxyl groups or introduce new moieties that can effectively interlock with the matrix. Alkali treatment has two effects on the fibre which are increasing the surface roughness resulting in better mechanical interlocking; and increasing the amount of cellulose exposed on the fibre surface, thus increasing the number of possible reaction sites. Alkali treatment also reduces the polarity of the PAPF which increased the crystallinity and reduced the sorption capacity of the fibre. The chemically modified LDPE/PAPF exhibited a reduction in water uptake.

Sofia *et al*. (2016) reported that micro/nano cellulose highly ordered crystalline regions of nanocrystalline cellulose could reduce the accessibility of organic solvents and water uptake, thus decreasing the binding water molecules at equilibrium of the composite and creating the difficult path for gas and water penetration. Therefore, CNCs with tightly-packed crystalline

structure could increase the stiffness and enhance the barrier properties significantly and utilized as an excellent reinforcement in bio-polymer composition materials.

It can categorically be stated here that the results of this test are in close agreement with those obtained by other researchers and are within the acceptable limits.

4.12 Mechanical Properties Analysis Data of the PALF/PP Composites

The mechanical properties test which includes the (1) the tensile properties test (2) the flexural properties and (3) the impact strength of the composites produced were all carried out at the Engineering laboratory of the Standards Organization of Nigeria (SON), Emene, Enugu. The results of the test carried out at room temperature and pressure are as given below in form of charts.

Tensile strength (TS), tensile modulus (TM), flexural strength (FS), flexural modulus (FM), and impact strength (IS) of the prepared composites were studied and the data are given from Figure 4.6 to Figure 4.25. The TS, TM, FS. FM and IS of the PALF/PP composites are as discussed.

4.12.1 Tensile Strength Results of the PALF/PP Reinforced Composites

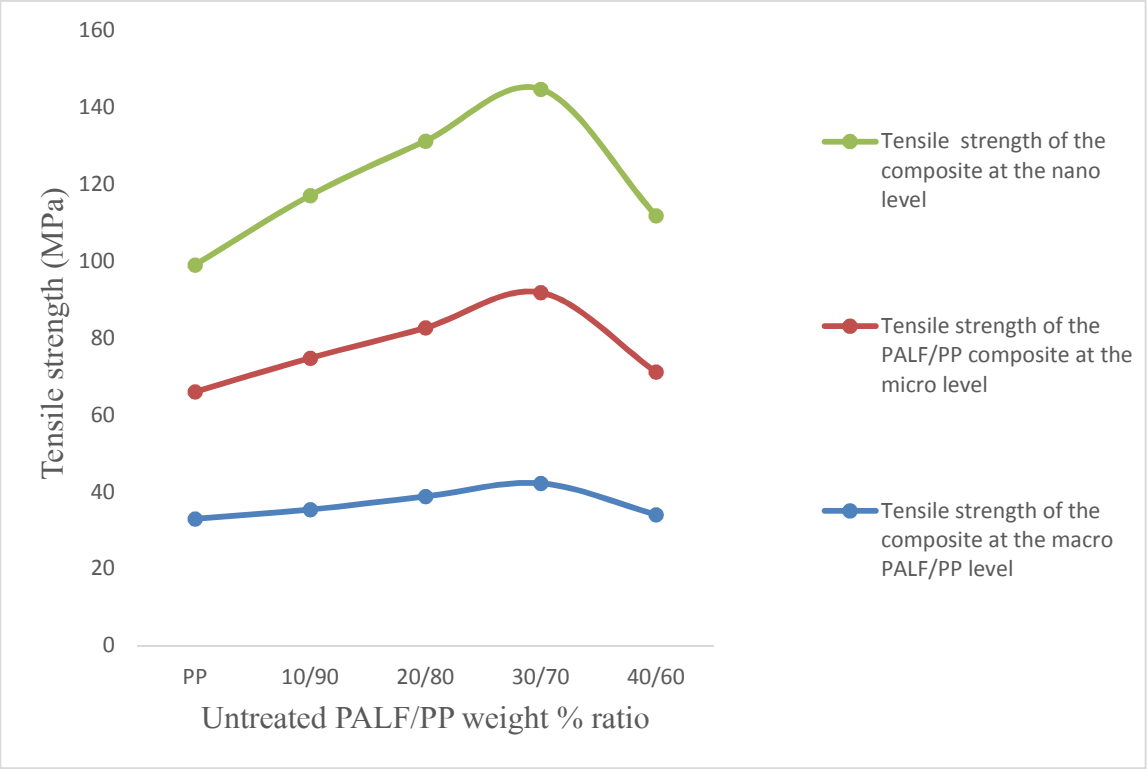


Figure 4.6 Tensile strength (MPa) of the unmodified reinforced PALF/PP composites against weight ratio

Figures 4.6 to 4.10 show the plots of the tensile strength (TS) of the PALF/PP composites depicting the TS of the PALF/PP composites with the PALF (reinforcing agent) at the macro. Micro and nano cellulose dimensions. The results show that at PALF 10 %, 20 % and 30 % weight ratio, there is a gradual increase in TS with maximum strength seen at PALF 30 % weight content. It also shows a gradual decline in TS as the fibre content increased beyond the 30 % weigh ratio. Comparing the TS at the maximum; for the PALF/PP reinforced with macro PALF at 30/70 of PALF/PP, the TS is 42.2 MPa, for the macro PALF/PP composite, the TS is 49.9 MPa and the TS for the nano PALF/PP composite is 52.9 MPa, there is an increase by 27.87 % at the macro reinforcement level to 70.65 % at the nano PALF dimension.

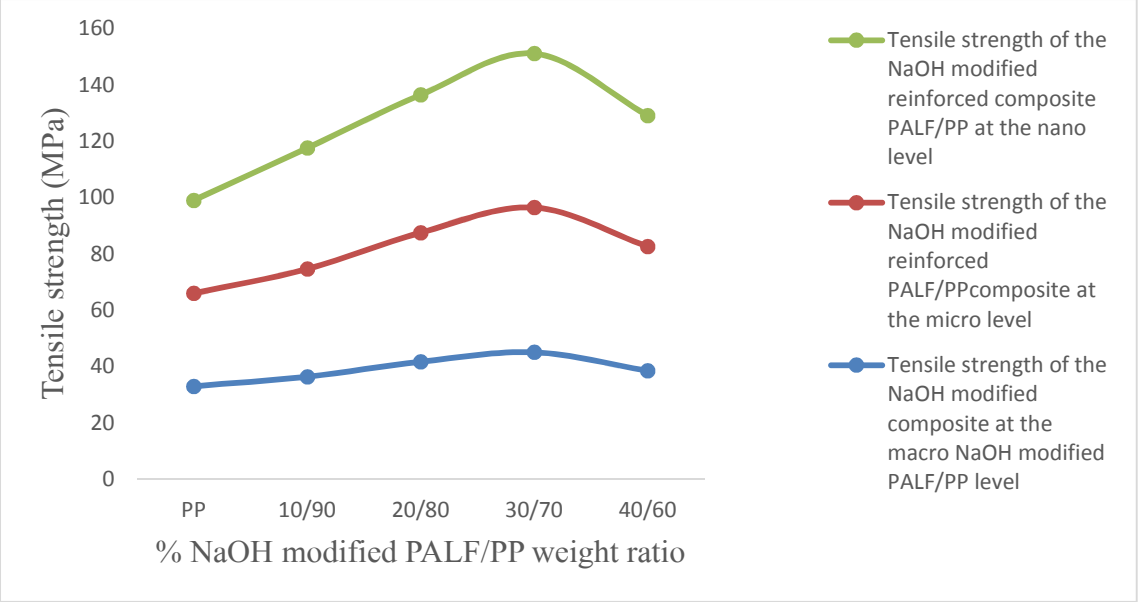


Figure 4.7 Tensile strength (MPa) of the NaOH modified reinforced PALF/PP composites against weight ratio

Figure 4.7 shows the PALF/PP composites of samples modified with NaOH; for the reinforced macro PALF/PP composites, there is an increase in the TS up to the 30 % PALF weight ratio, which is 36.65% to 65.58 % at the nano cellulose PALF/PP composites, this shows an enhanced TS by an increase of over 100% with the reinforcement change in dimensions.

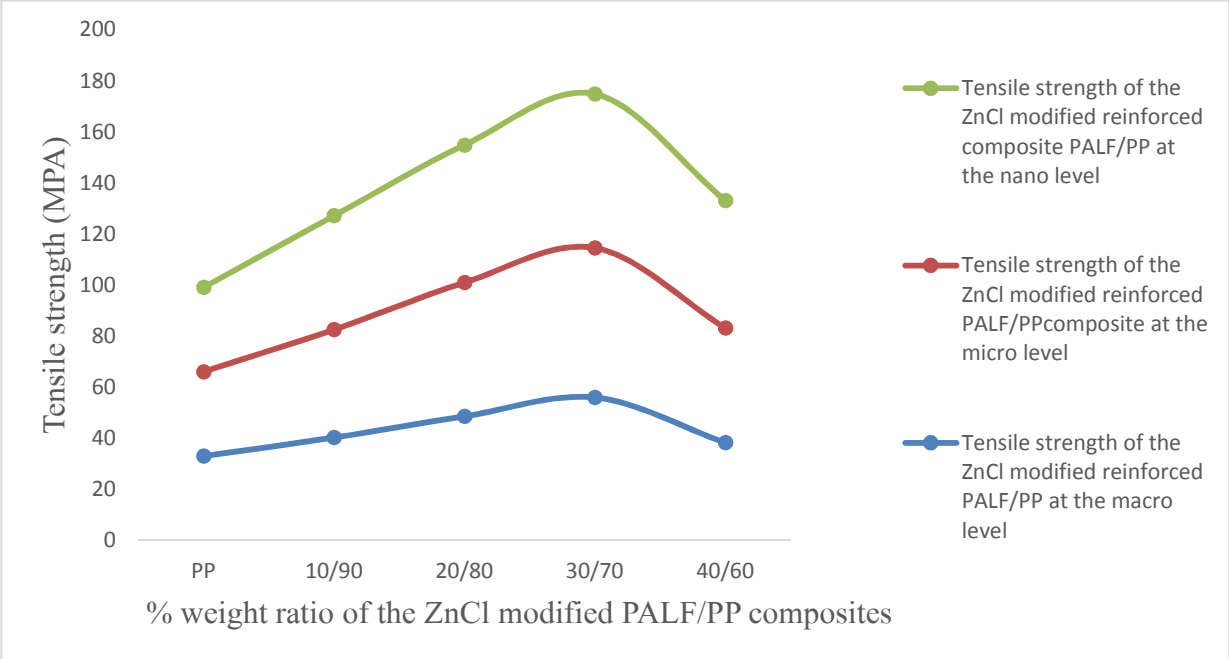


Figure 4.8 Tensile strength (MPa) of the ZnCl modified reinforced PALF/PP composites against weight ratio

Figure 4.8 shows the ZnCl modified reinforced PALF/PP composites, here also, there is an increase of 69.39 % in terms of TS at the 30 % PALF weight ratio at the macro PALF dimension to 90.09 % at the nano cellulose PALF dimension.

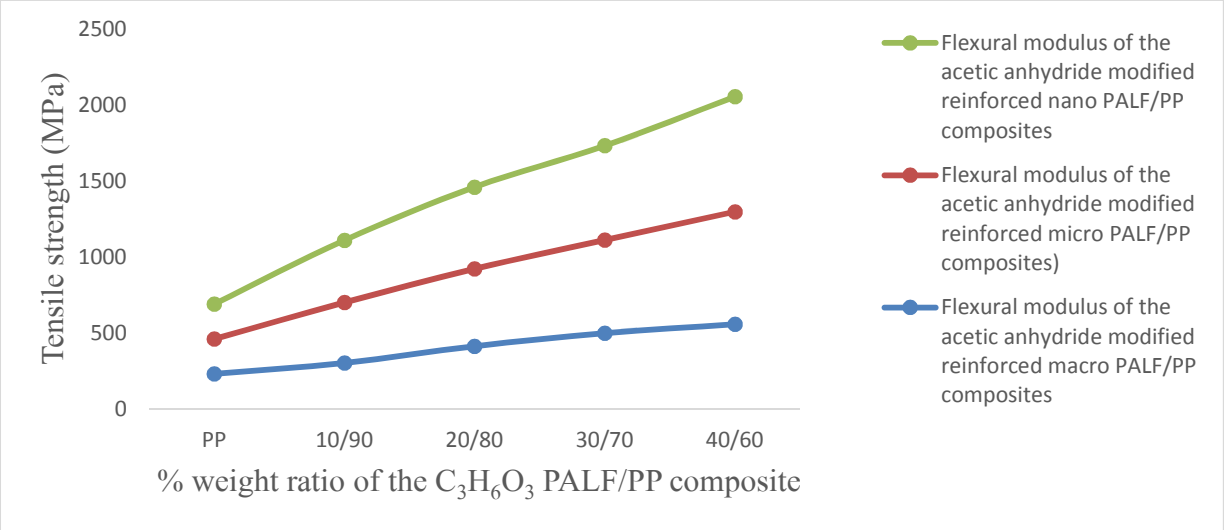


Figure 4.9 Tensile strength (MPa) of the $C_3H_6O_3$ modified reinforced PALF/PP composites against weight ratio

Figure 4.9 shows the $C_3H_6O_3$ modified reinforced PALF/PP composites; considering the TS at 30 % weight ration of the PALF at the macro PALF dimension, the TS is 36.06 %, 54.88 % and 63.63 % at the micro and nano cellulose dimensions respectively.

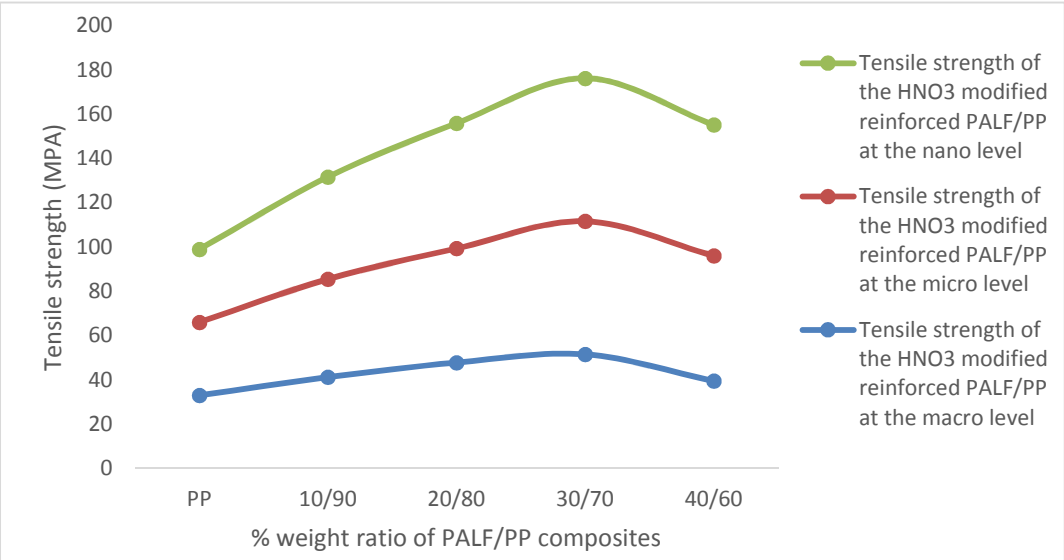


Figure 4.10 Tensile strength (MPa) of the HNO_3 modified reinforced PALF/PP composites against weight ratio

Figure 4.10, here, the HNO_3 modified PALF/PP composites depicts with TS of 52.5 MPa (56.06 %) at the 30 % PALF weight ratio macro cellulose dimension to 64.59 MPa (96.67 %) at the nano PALF cellulose dimension.

Nayan *et al.,* (2013) studied the effect of mercerization process on the structural and morphological properties of Pineapple Leaf Fibre (PALF) pulp and reported that then tensile strength of the un-mercerized PALF bundle corresponds well with previously reported works. Treatment with NaOH increases the tensile strength of mercerized PALF due to the removal of impurities and poor crystalline structure of hemicelluloses and lignin.

4.12.2 Young's Modulus Data of the PALF/PP Reinforced Composites

Figure 4.11 to 4.15 shows the Young's modulus (YM) of the PALF/PP composites with reinforcing agent (PALF) modified with NaOH, ZnCl, $C_3H_6O_3$ and HNO_3 respectively; a similar trend is observed such that the YM increased from 0 % PALF content to 30 % PALF weight content, and a noticed decline is observed after the 30 % PALF weight content.

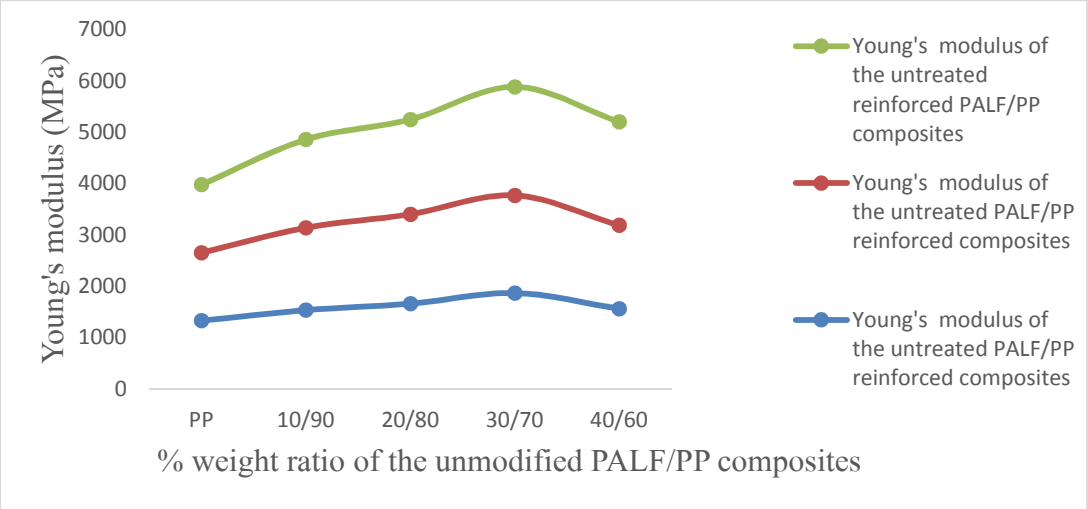


Figure 4.11 Young's modulus against % weight ratio of PALF/PP composites

From Figure 4.11, the untreated reinforced PALF/PP composites show the following behavior at the 30 % PALF weight ratio, the YM stood at 1864 MPa (48.67 %) to 2115 MPa (59.62 %) at the nano cellulose PALF dimension.

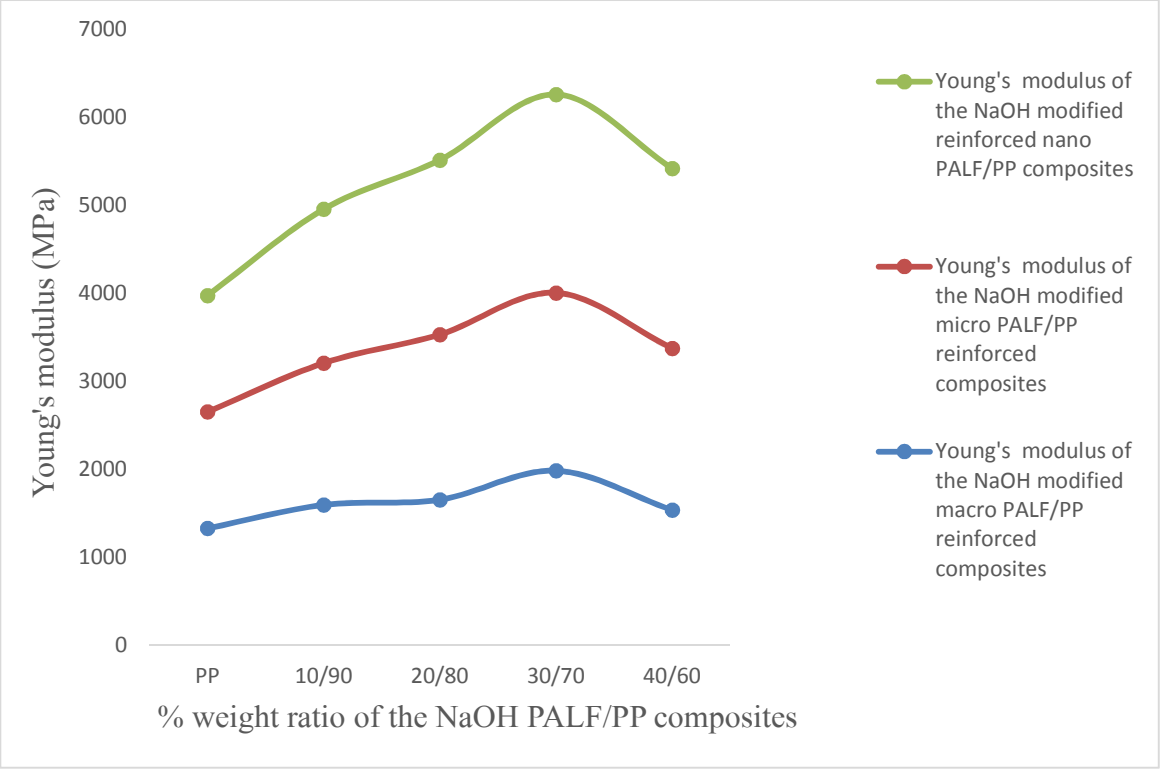


Figure 4.12 Young's modulus against % weight ratio of the NaOH modified PALF/PP composites

Figure 4.12 shows the behavior of the NaOH modified reinforced PALF/PP composite at the 30 % PALF weight ratio; there is an increase in the YM from 1980 MPa (49.93 %) at the macro PALF dimension to 2257 MPa (70.34 %) at the nano cellulose PALF dimension.

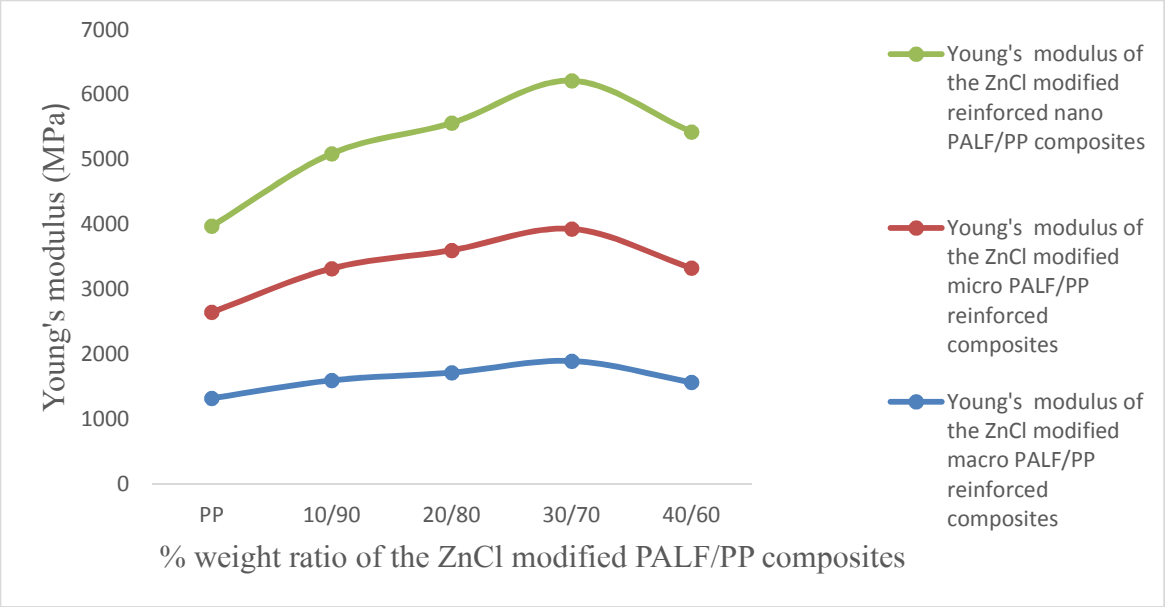


Figure 4.13 Young's modulus against % weight ratio of the ZnCl modified PALF/PP composites

Figure 4.13 shows the YM of the ZnCl modified reinforced PALF/PP composites; at the nano 30 % PALF weight ratio, the YM stood 1899 MPa (43.32 %) to 2281 MPa (72.34 %) at the nano cellulose PALF dimension.

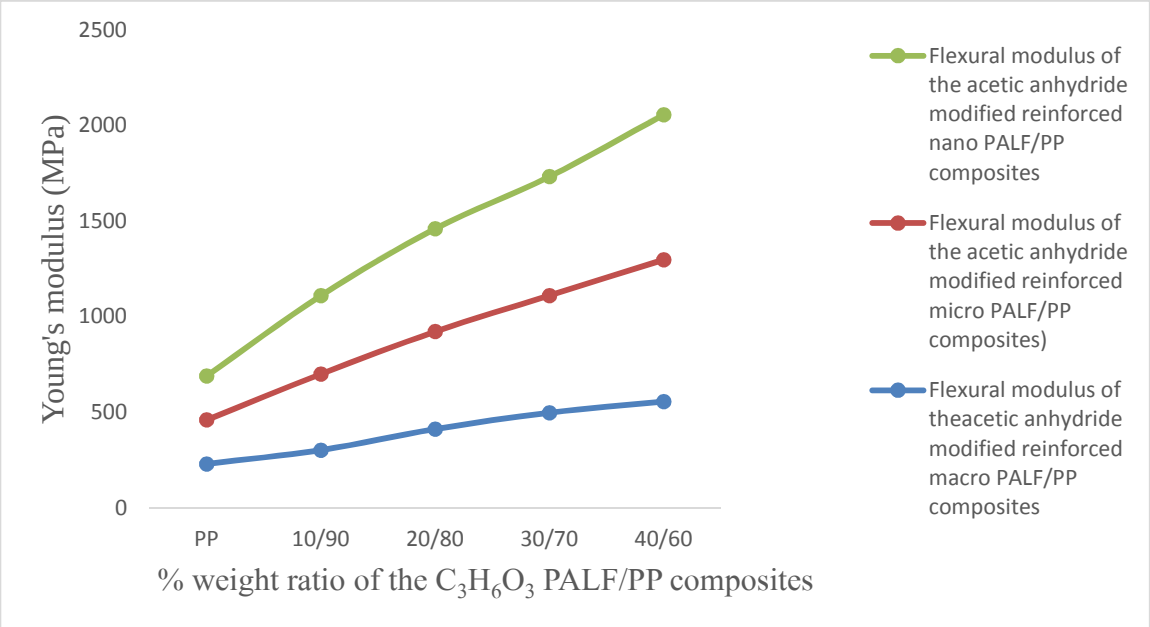


Figure 4.14 Young's modulus against % weight ratio of the $C_3H_6O_3$ modified PALF/PP composites

Figure 4.14 shows the YM of the $C_3H_6O_3$ modified PALF/PP composites; the YM at the 30 % PALF weight ration is 1861 MPa (40.45 %) at the macro PALF dimensions to 2346 MPa (70.06 %) at the nanocellulose dimension of the PALF.

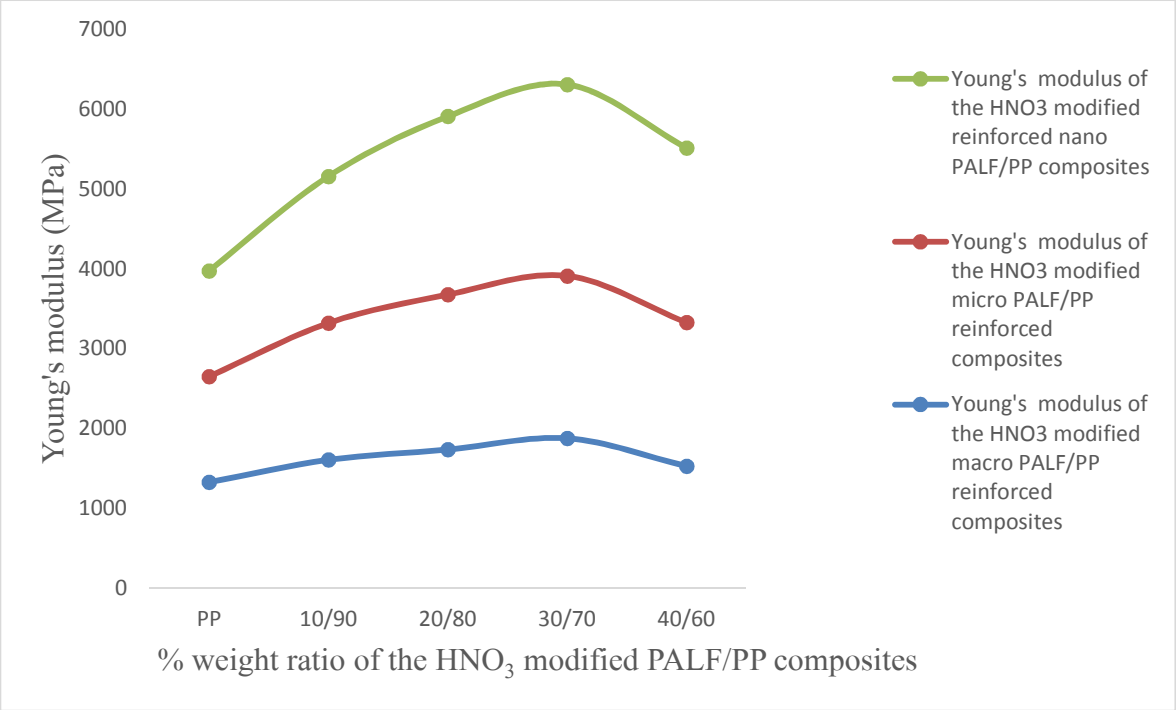


Figure 4.15 Young's modulus against % weight ratio of the HNO_3 modified PALF/PP composites

Figure 4.15 shows the plots of the YM of the reinforced PALF/PP composites, with the PALF modified with HNO_3, at the macro cellulose dimensions, the YM is 1874 MPa (41.43 %), at the micro cellulose dimensions, the YM is 2037 MPa (53.74 %) and at the nano cellulose PALF 2399 MPa (81.06 %).

4.12.3 Flexural Strength Data of the PALF/PP Composites

Figures 4.16 to Figure 4.20 show the plots of the flexural strength (FS) of the PALF/PP composites. The FS increased as the fibre content increased; at the macro PALF dimensions, the FS increased by 46.13 % (45.3 MPa) to 72.58 % (53.5 MPa) and 78.39 % (55.3 MPa).

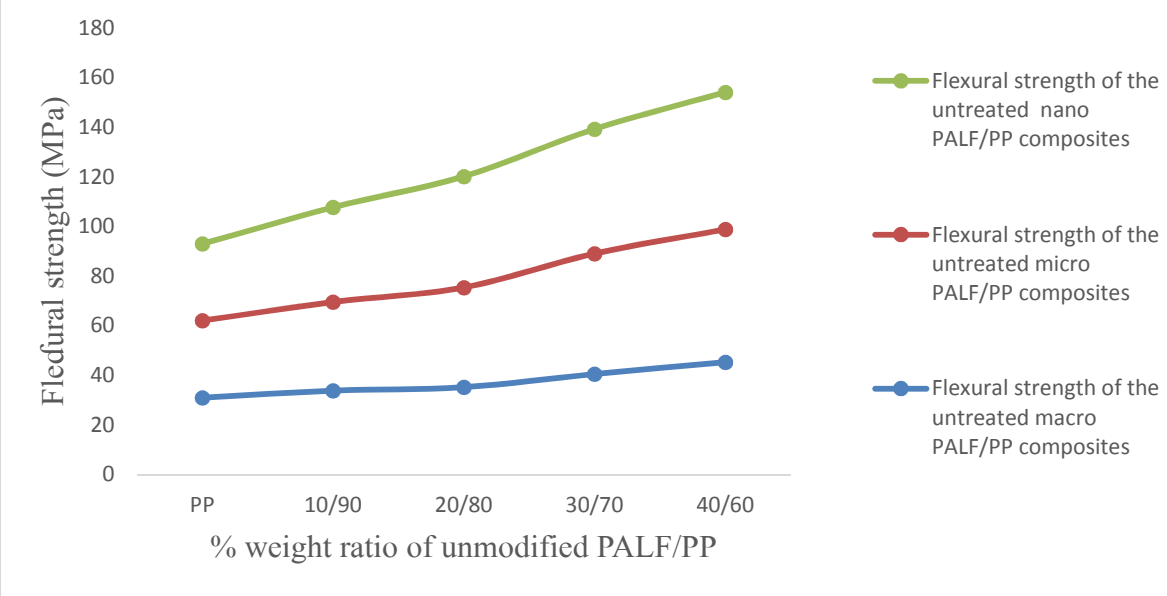


Figure 4.16 Flexural strength against % weight ratio of the unmodified reinforced PALF/PP composites

From Figure 4.16, the FS increased by 45 % at the macro PALF dimension to 75 % and 81 % at the micro and nano cellulose PALF respectively.

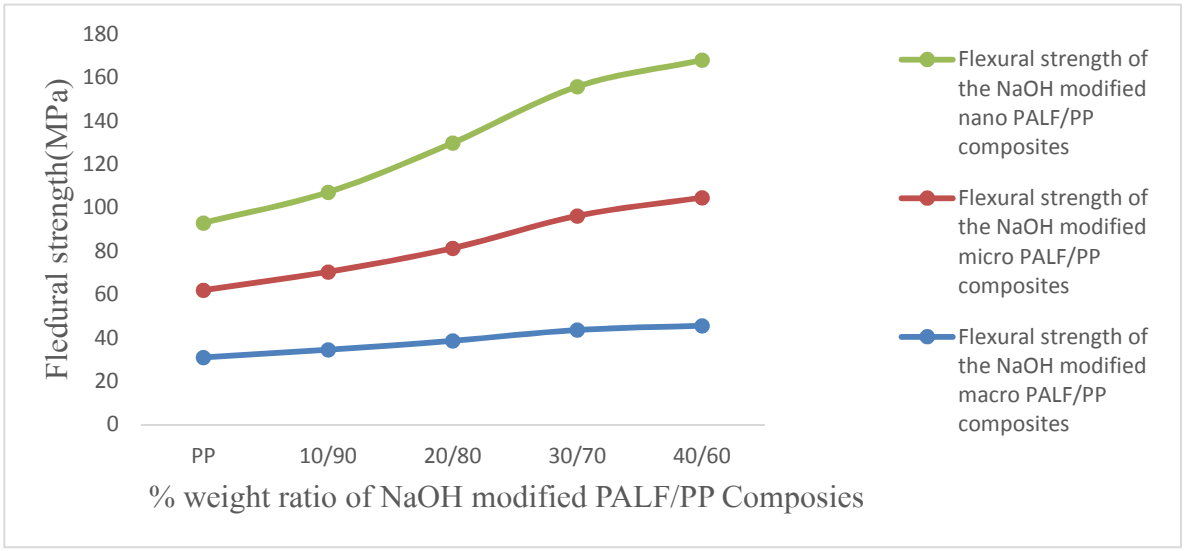


Figure 4.17 Flexural strength against % weight ratio of the NaOH modified reinforced PALF/PP composites

From Figure 4.17, the FS increased by 61 %, 77.13 % and 84.94 % at the macro, micro and nano PALF cellulose dimensions respectively.

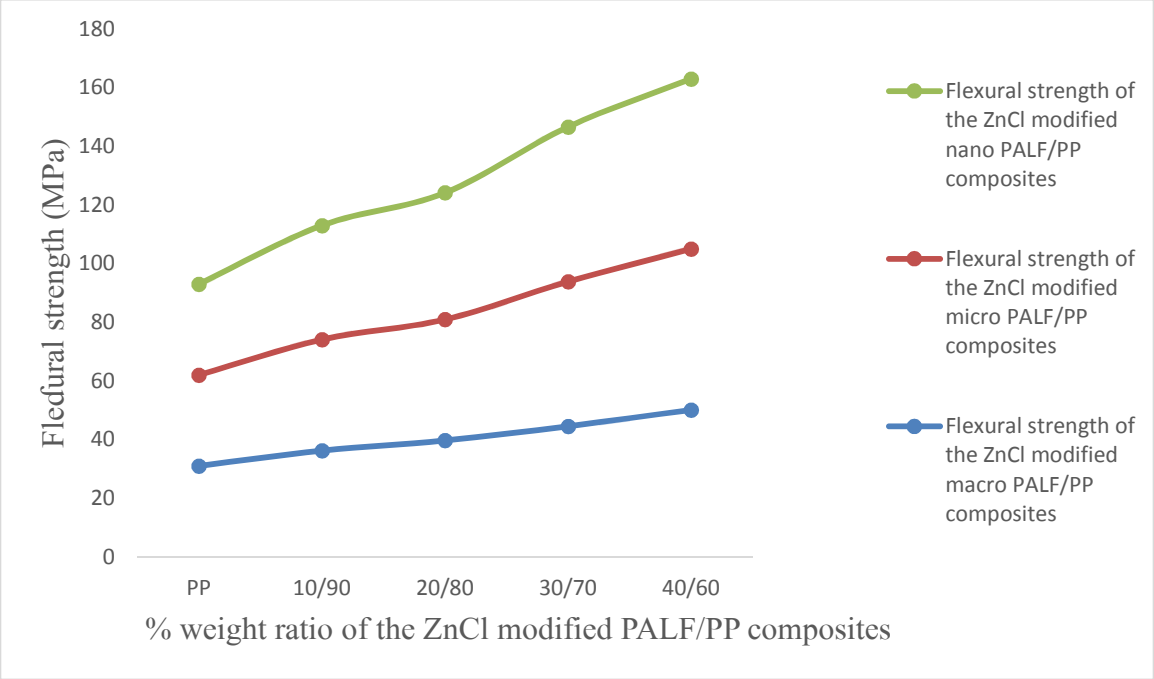


Figure 4.18 Flexural strength against % weight ratio of the ZnCl modified reinforced PALF/PP composites

Figure 4.18 shows an increase in FS by 41.97 %, 90.29 % and 96.80 % at the macro, micro and nano PALF cellulose dimensions respectively.

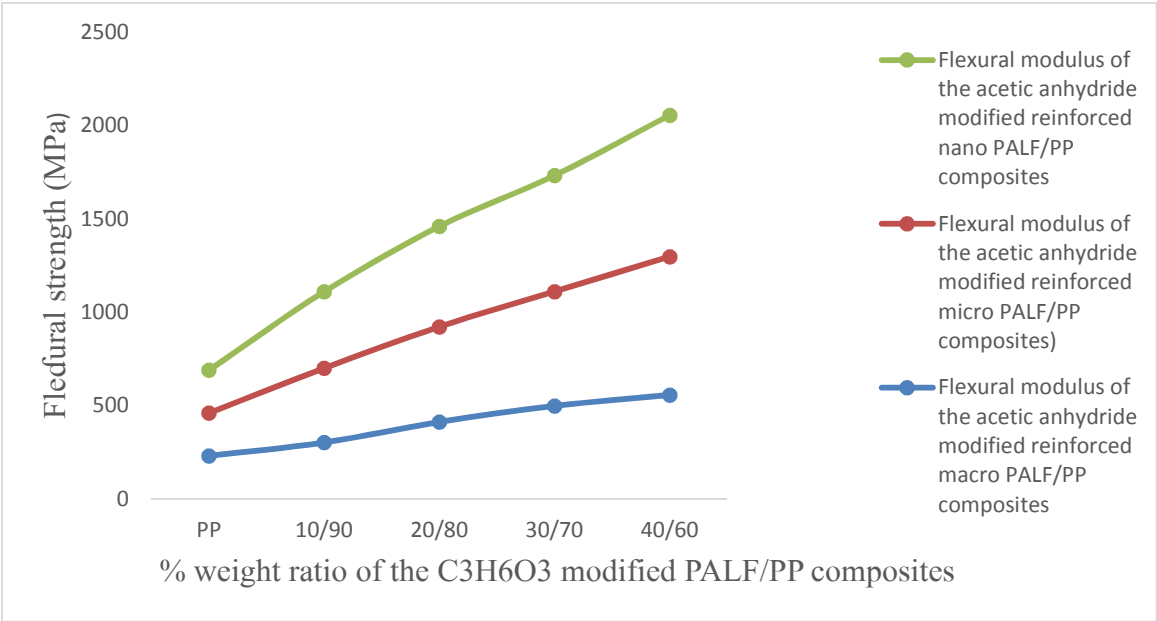


Figure 4.19 Flexural strength against % weight ratio of the $C_3H_6O_3$ modified reinforced PALF/PP composites

Figure 4.19 shows an increase of FS by 66.45 %, 102 % and 111.10 % for the PALF/PP composites reinforced with modified HNO_3 macro, micro and nano PALF respectively.

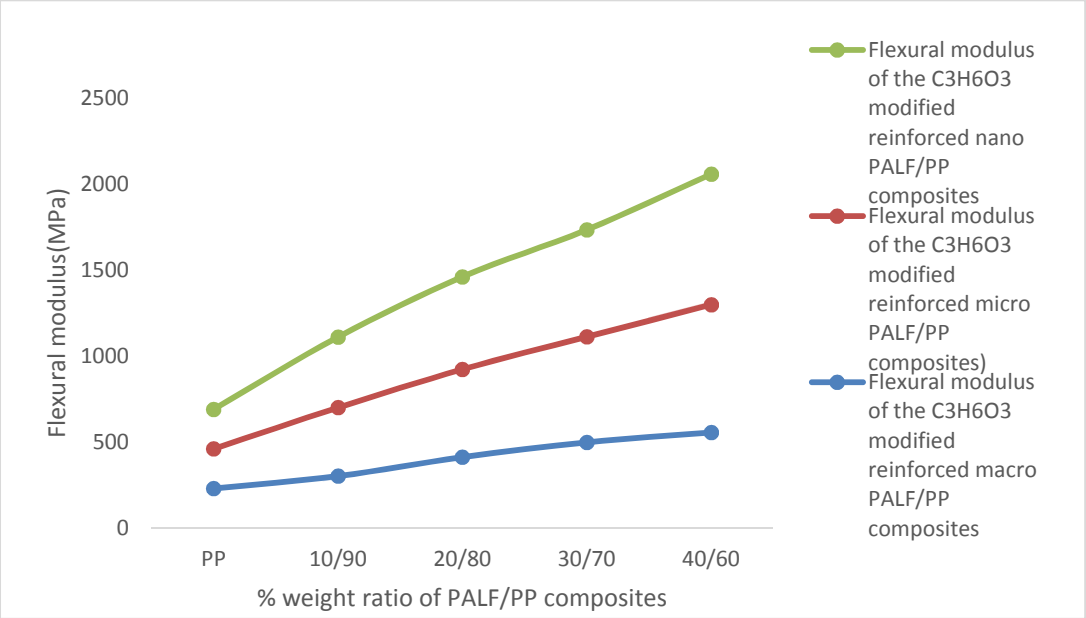


Figure 4.20 Flexural strength against % weight ratio of the HNO_3 modified reinforced PALF/PP composites

Flexural strength is the ability of the material to withstand the bending forces applied perpendicular to its longitudinal axis. Generally, in the case of composites, the resistance to interlaminar failure controls the flexural properties. Therefore, high flexural strengths of composite are due to better interfacial adhesion of at the fibre-matrix interface, which is a result of the chemical treatment of the PALF that enhanced the fibre-matrix interaction and thereby increased the interfacial bond strength and allowed strongest adhesion at the interface. The decrease in the flexural strength at higher fibre loading (40 weight % in this case) is as a result of non-uniform stress transfer due to PALFs touching each other within the matrix.

4.12.4 Flexural Modulus Data of the PALF/PP Composites

Figures 4.21 to 4.25 shows the FM of the reinforced PALF/PP composites. The FM increased as the fibre content increased in the composites.

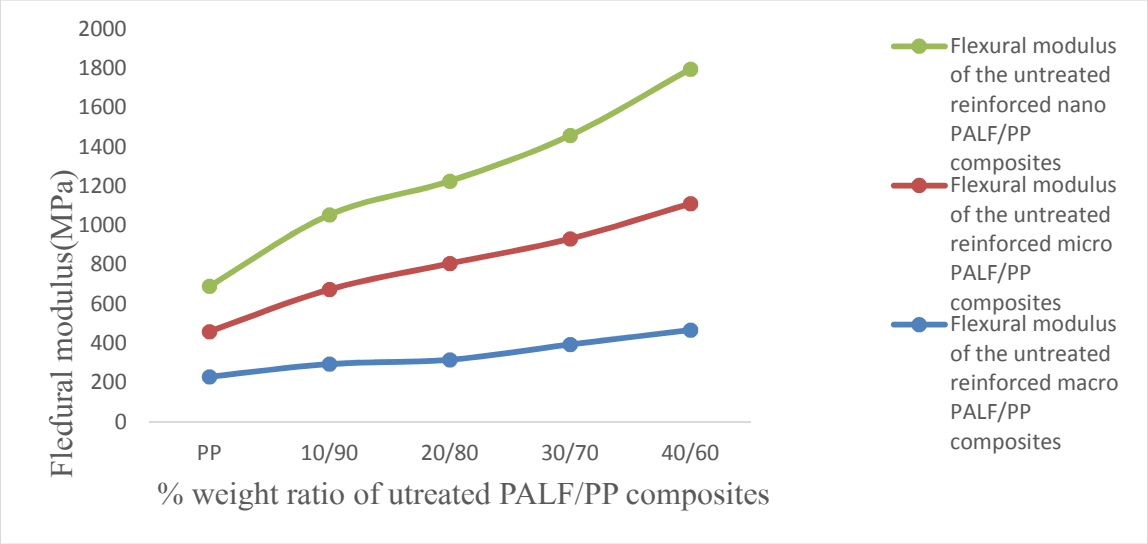


Figure 4.21 Flexural modulus against % weight ratio of PALF/PP composites

Figure 4.21 shows the FM which increased as the fibre content also increases in the composites, depicting an enhanced FM of 467 MPa (103 %), 644 MPa (180 %) and 685 MPa (197.83 %) with the macro, micro and nano cellulose PALF respectively as the reinforcing agents.

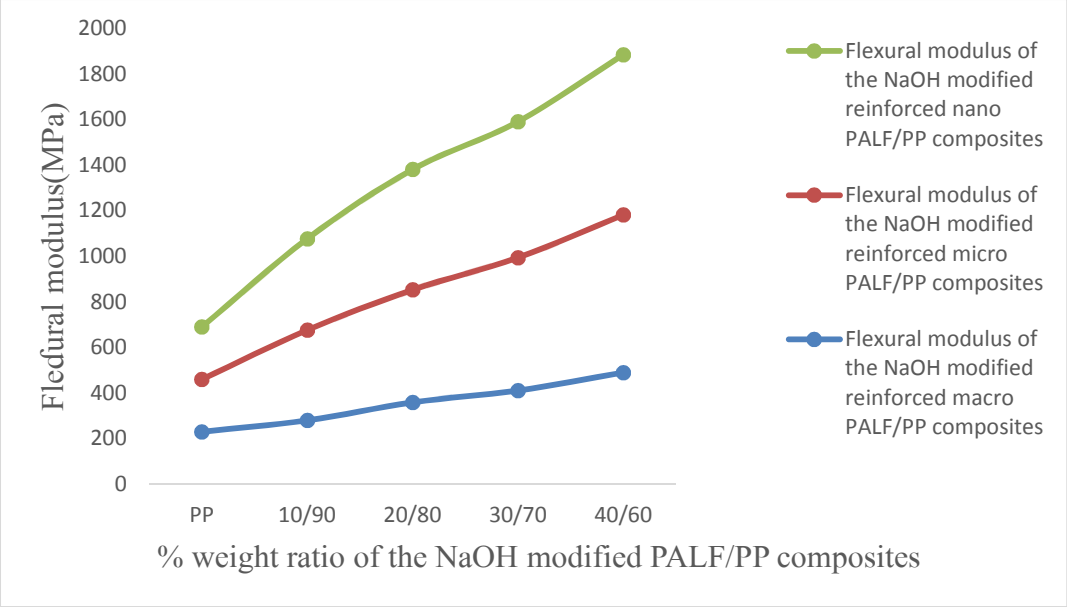


Figure 4.22. Flexural modulus of the NaOH modified PALF/PP composites against % weight ratio

Figure 4.22 shows the composites with modifies PALF using NaOH as the surface modification agent, there is an increase in FM by 113.04 %, 200.86 % and 205.65 % at the macro, micro and nano PALF dimensions.

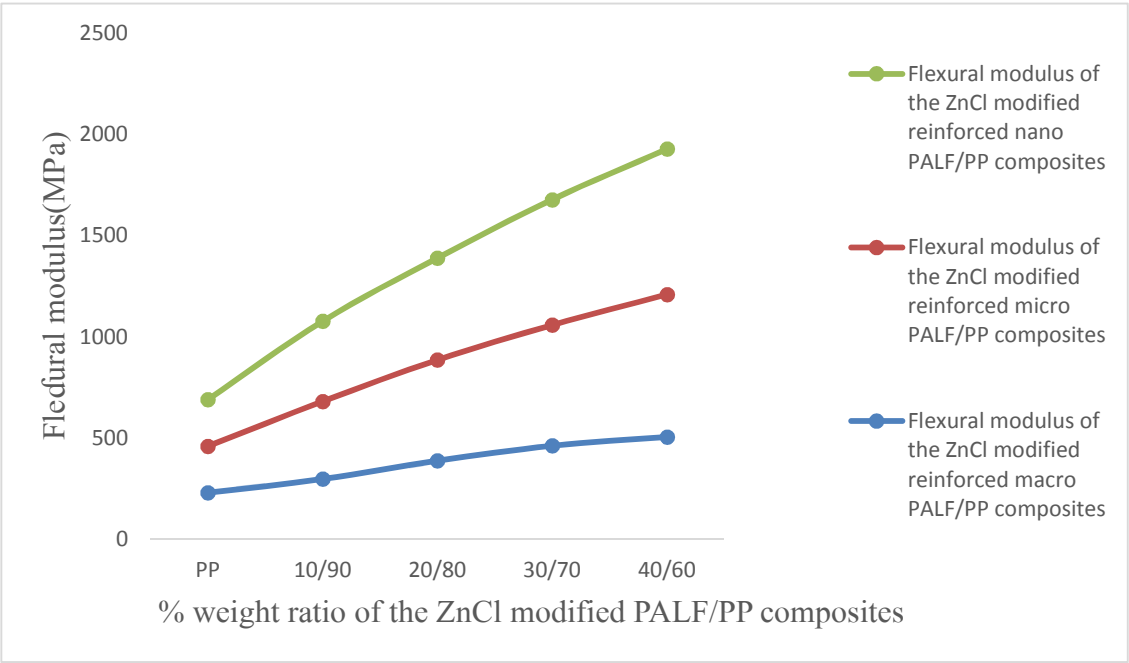


Figure 4.23 Flexural modulus of the ZnCl modified PALF/PP composites against % weight ratio

Figure 4.23 shows the FM of the reinforced PALF/PP composites modified with ZnCl. there is an observed increase in FM by 120 %, 205.65 % and 212.17 % with the reinforcements at the macro, micro and Nano dimensions.

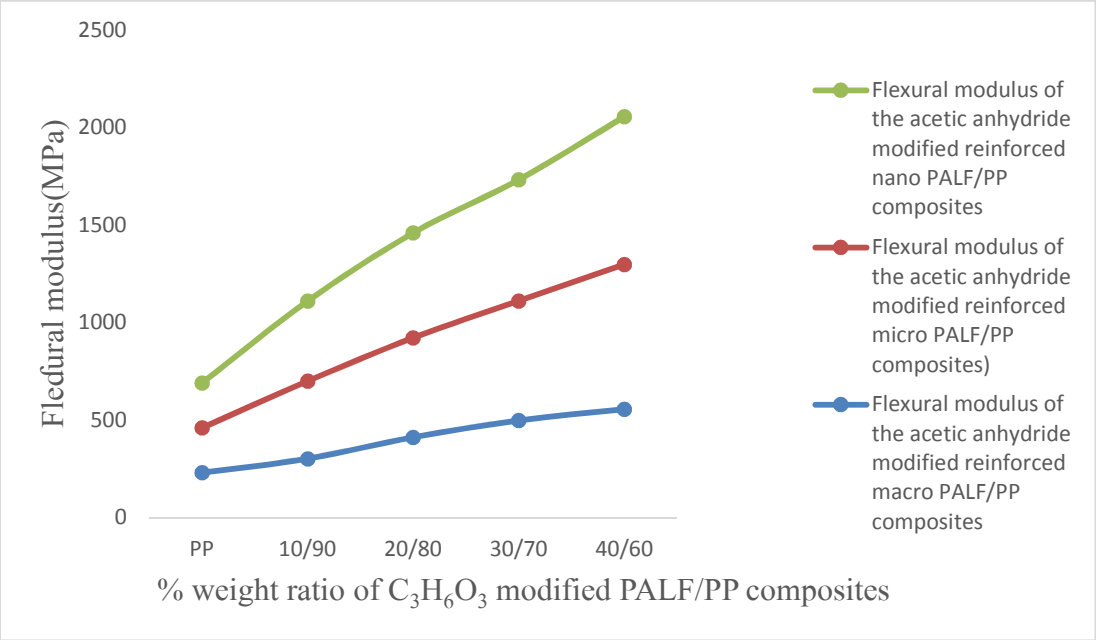


Figure 4.24 Flexural modulus of the $C_3H_6O_3$ modified PALF/PP composite against % weight ratio

Figure 4.24 shows the composites containing PALF that were modified with $C_3H_6O_3$, here, the FM increased by a 141.78 % (556 MPa), 222.61 % (742 MPa) and 229.57 % (758 MPa) with PALF at the macro, micro and nano cellulose dimensions.

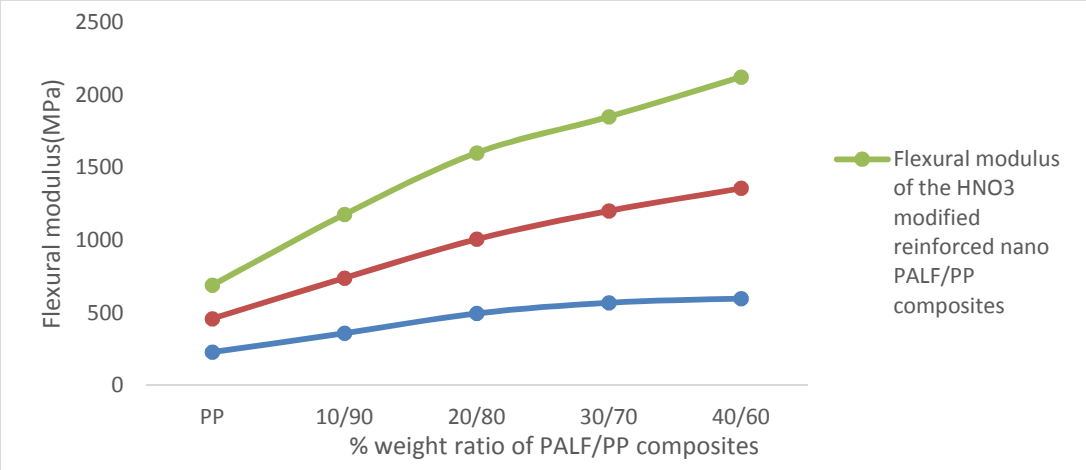


Figure 4.25 Flexural modulus of the HNO_3 modified PALF/PP composites against % weight ratio

Figure 4.25 shows the FM of the reinforced PALF/PP composites with maximum FM at the 40/60 PALF/PP ratio in the order 599 MPa (160.43 %), 758MPa (229.6 %) and 766 MPa (233.04 %) at the macro, micro and nano PALF cellulose dimensions.

Flexural modulus is used as an indication of a material's stiffness when flexed. It is well known that the improvement in the modulus depends on the morphology of composites. From the findings of earlier researchers, the flexural modulus of the neat polyester matrix is 500.55 MPa. The flexural modulus of the composites follows the same trend with the flexural strength, there was gradual increase in the modulus from 10 weight % - 20 weight % fibre loading and begin to decrease as from 30 weight % - 40 weight %. The optimum value for PALF / Polyester composite is 704.59 MPa which is about 40.76 % obtained at 20 weight % fibre loading. The reduction in the flexural modulus at higher fibre loading is a result the fibres touching each other which resulted into stress concentration at the tips of PALFs within the matrix.

4.12.4 Impact Strength Data of the PALF/PP Composites

Figures 4.26 to 4.30 show the impact strength (IS) in J/m of the reinforced PALF/PP composites. Here also, it has been observed that there is an increase in IS as the fibre content increases.

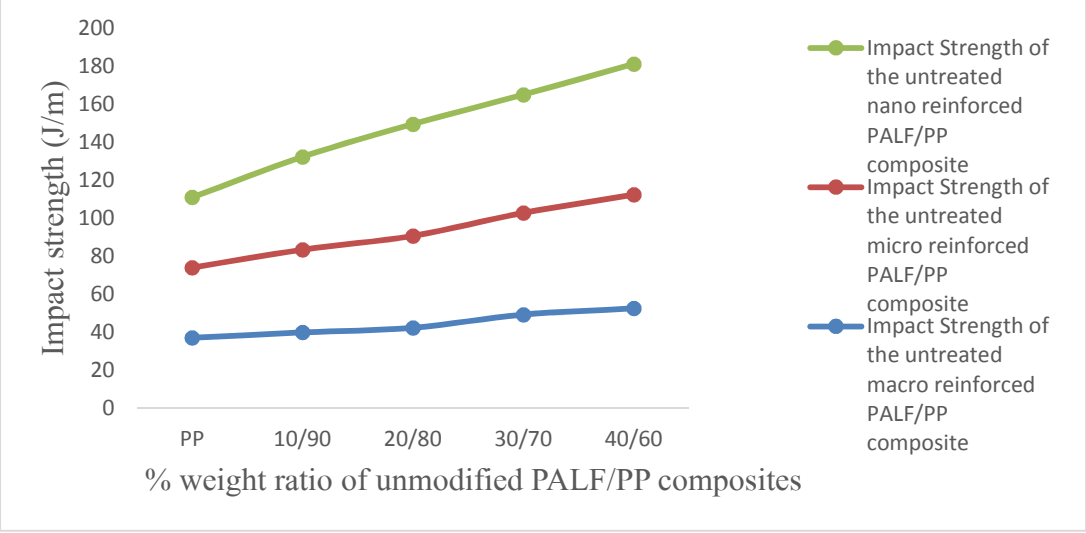


Figure 4.26 Impact strength against % weight ratio of unmodified /PP composites

Figure 4.26, there is a maximum increase in IS at the 40/60 PALF/PP weight ratio by 41.89 % (52.5 J/m), 61.89 % (59.9 J/m) and 86.22 % (68.9J/m) at the macro. Micro and nano PALF cellulose dimensions respectively.

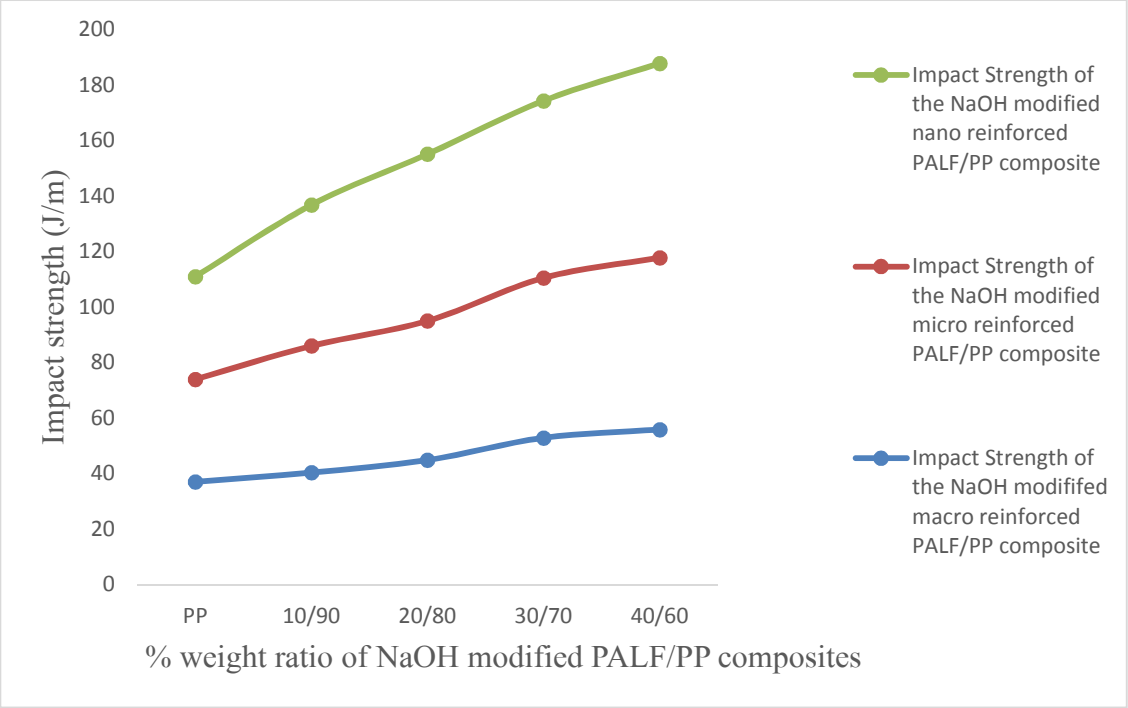


Figure 4.27 Impact strength against % weight ratio of NaOH modified PALF/PP composites

Figure 4.27 shows the IS of the NaOH modified PALF / PP composites with maximum IS observed at the 40/60 weight ratio, showing an increase by 51.08 % (55.9 J/m), 67.30 % (61.9 J/m) and 89.16 % (69.99 J/m) and 89.16 % (69.99 J/m) at the macro, micro and nano PALF cellulose dimensions.

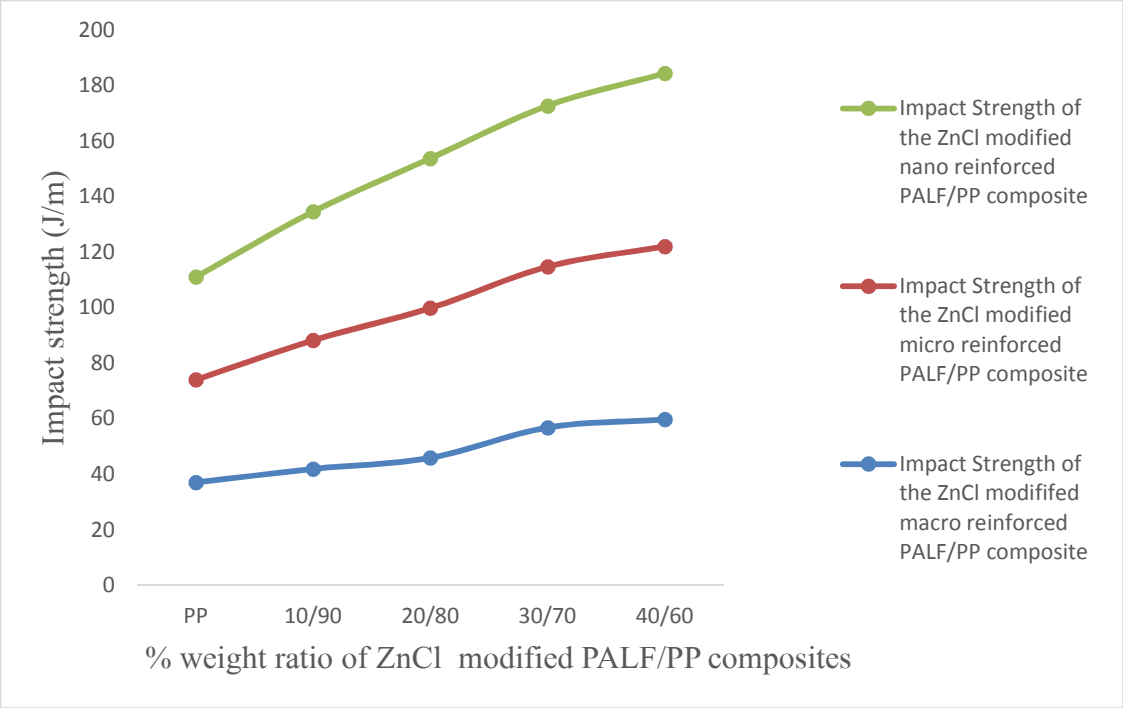


Figure 4.28 Impact strength against % weight ratio of ZnCl modified PALF/PP composites

Figure 4.28 shows a similar trend, with the following, information, at the 40/60 PALF/PP wright ratio, 68.38 % (62.3 J/m), 72.97 % (64 J/m) and 82.97 % (67.5 J/m) at the macro. Micro and nano PALF dimensions.

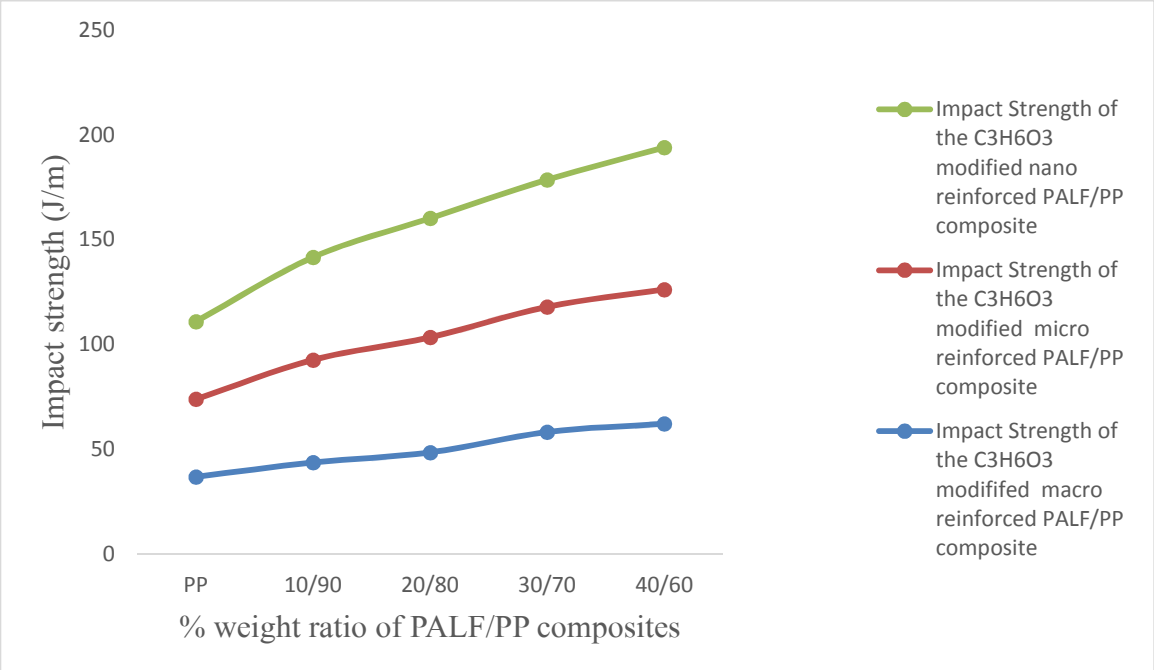


Figure 4.29 Impact strength against % weight ratio of $C_3H_6O_3$ modified PALF/PP composites

Figure 4.29 shows an increase by 68.37 % (62.3 J/m). 72.97 % (64 J/m) and 82.97 % (67.7 J/m) at the macro, micro and nano PALF for the PALF that was modified with $C_3H_6O_3$.

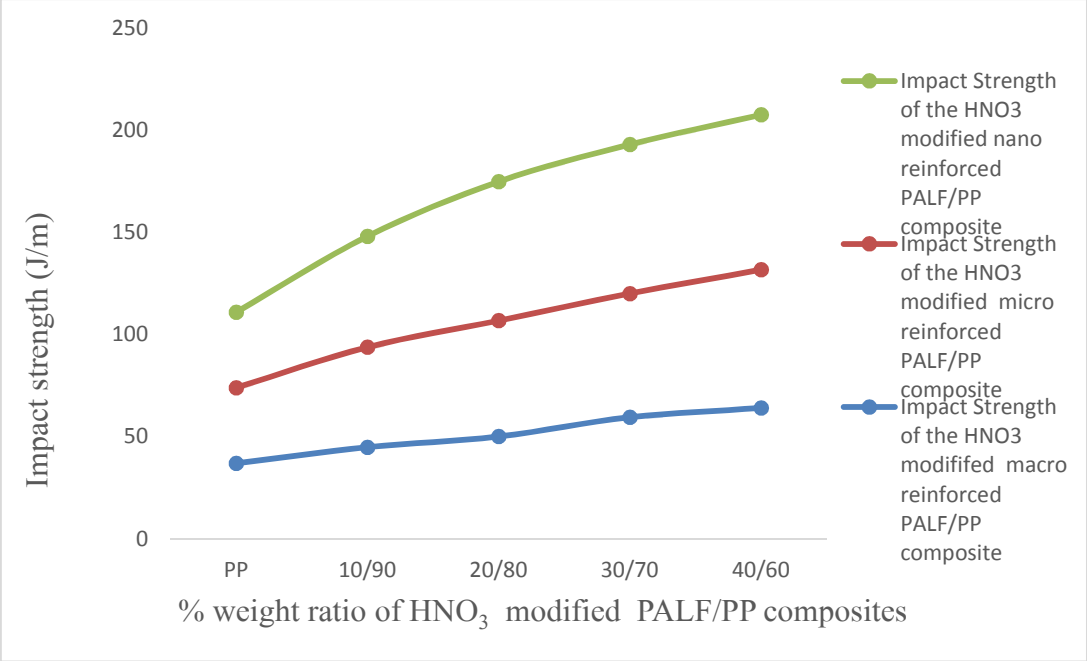


Figure 4.30 Impact strength against % weight ratio of HNO_3 modified PALF/PP Composites

Figure 4.30 shows the HNO_3 modified PALF/PP composites, with the following data; 73.24 % (64.1 J/m), 82.97 % (67.7 J/m) and 105.14 % (75.9 J/m) at the macro. Micro and nano PALF dimensions respectively.

Gomez *et al.*, (2016) reported that PALF significantly improve the Izod impact energy of epoxy matrix composites. The incorporation of continuous and aligned PALF fabrics results in a marked change with respect to pure epoxy matrix (0 % fibre) in which a totally transversal rupture occurs. The crack nucleated at the notch will initially propagate transversally through the epoxy matrix, as expected in a polymer. However, when the crack front reaches a fibre, the rupture will proceed through the low strength interface. As a consequence, after the Izod hammer hit the specimen, some fibres will be pulled out from the matrix but, owing to their flexural compliance, the PALF fabric will not break

The data above means that, with the increase of fibre content, all the mechanical properties increase. PALF composites gained huge mechanical properties over the matrix material and thus indicated good fibre matrix adhesion, more especially for the PALF with chemically enhanced surfaces

The superiority of mechanical properties of pineapple leaf fibre can be related to the high content of alpha-cellulose content with low microfibrillar angle (14°). As reinforcing agent PALF has both qualities, that is, high content of alpha-cellulose content with low microfibrillar angle (14°), the result of PALF based polymer composites show excellent stiffness and strength compared to other cellulose based composite materials.

The results obtained are in close agreement with those obtained by earlier researcher as reported by Santosh *et al.,* (2015). In their study of development of pineapple leaf fibre reinforced epoxy resin composites, they reported that different fibre volume ratios of 10 %, 20 % and 30 %. The composites are developed by using hand lay-up technique. From the results the tensile strength for volume ratio 10 %, 20 % and 30 % was obtained as 26.91 MPa, 35.8 MPa and 65.95 MPa. Hence it was concluded that the tensile strength increases as the volume ratio changes from 10 % to 30 % and maximum tensile strength was seen at 30 % volume ratio. Similarly, the specimens were subjected to flexural testing for volume ratio 10 %, 20 % and 30 %. The flexural strength obtained as 38.55 MPa, 58.37 MPa and 121.83 MPa. From their results it can be seen that there is a significant increase in flexural strength from 10 % to 20 % but drastic increase in flexural strength is seen at volume ratio 30 %. The hardness of the specimen was determined using Rockwell hardness tester. Hence it can be concluded that among 10 %, 20 % and 30 % volume ratio, the maximum tensile, flexural strength and hardness is seen in 30 % volume ratio.

Also, Daramola *et al.,* (2017) reported the variation of the ultimate tensile strength for neat Polyester and PALF / Polyester composites. The ultimate tensile strength of the neat polyester was 5.11 MPa. It was observed from the results that the strength of composites increases linearly from 10 weight% PALF/Polyester composite to 40 weight % PALF / Polyester composite where the optimum value of 29.19 MPa was observed. The incorporation of modified PALFs into polyester matrix at weight fraction of 40 weight % produced the increase in ultimate tensile strength by about 471 %, according to their results. The general improvement in the ultimate tensile strength of the modified PALF / Polyester composites are attributed to the enhancement of fibre-matrix interaction and more effective transfer of stress.

Kasim *et al.,* (2015) reported that an alkaline treatment was conducted to enhance the PALF properties. The fabrication was made by compression molding technique with random orientation of PALF. From the experimental study, the results revealed that the voids percentage and interfacial bonding between the PALF and PP affected the mechanical properties of the PALF/PP composite.

Nurrudin *et al.,* (2016) studied the Mechanical Properties of Natural Composite Containing Pineapple Leaf Fibre, Natural Rubber and Low-Density Polyethylene and reported that the composite containing PALF displayed the best mechanical properties with 1.32 MPa tensile strength, 11.56 MPa Young's Modulus.

Kaewpirom and Worrarat, (2014) studied pineapple leaf fibre-reinforced poly (lactic acid) green composites by blending of poly (lactic acid) polymer and short-length-chopped Pattawia pineapple leaf fibres (1 - 3 mm) using a twin-screw extruder. Effects of the fibre content and the addition of a coupling agent on mechanical properties and morphology of the composites were investigated.

Sri and Didit, (2018), in their study reported that study, the PALF is used as reinforced materials and epoxy is used as the matrix. Pineapple leaves are used from Cayyene varieties taken from Subang, Indonesia. Additionally, the effects of PALF loading and PALF fibre length on the mechanical properties of PALF/epoxy composites is also analyzed. Compositions volume fraction of PALF/epoxy composites is fixed at 10 / 90 %, 20 / 80 %, 30/70 % and 40 / 60 %. The lengths of the pineapple leaf fibre are fixed to 20 mm, 30 mm and 40 mm. Before the fabrication, PALF underwent alkaline treatment to increase the strength of fibre. All samples have undergone three different tests to determine the mechanical properties which are tensile test, impact and bending test. PALF loading of 30 / 70 % with 40 mm in length shows the higher values of tensile stress, impact and bending which are 22.17 MPa, 27.63 J/m^2 and 35.53 N/mm^2 respectively.

Among the various factors, the final performance of the composite materials depends to a large extent on the adhesion between the polymer matrix and the reinforcement and therefore, on the quality of the interface. To achieve optimum performance of the end product, sufficient interaction between the matrix resin and the cellulosic material is desired. This is often achieved by surface modification of the resin or the filler. Kasim *et al.,* (2015) investigated the mechanical properties of high impact polypropylene composite reinforced with pineapple leaf fibre from the Josapine cultivar as a function of fibre loading, the results they obtained are in tandem with the ones obtained in this report.

4.13 Thermal conductivity Analysis of the PALF/PP Composites

Figures 4.31 to 4.35 show the thermal conductivity (TC) in W/mK behavior of the reinforced PALF/PP composites. The plots show a gradual increase in TC with increase in the fibre content. A noticeable steadiness in TC was observed at the maximum fibre content of 40 % weight ratio.

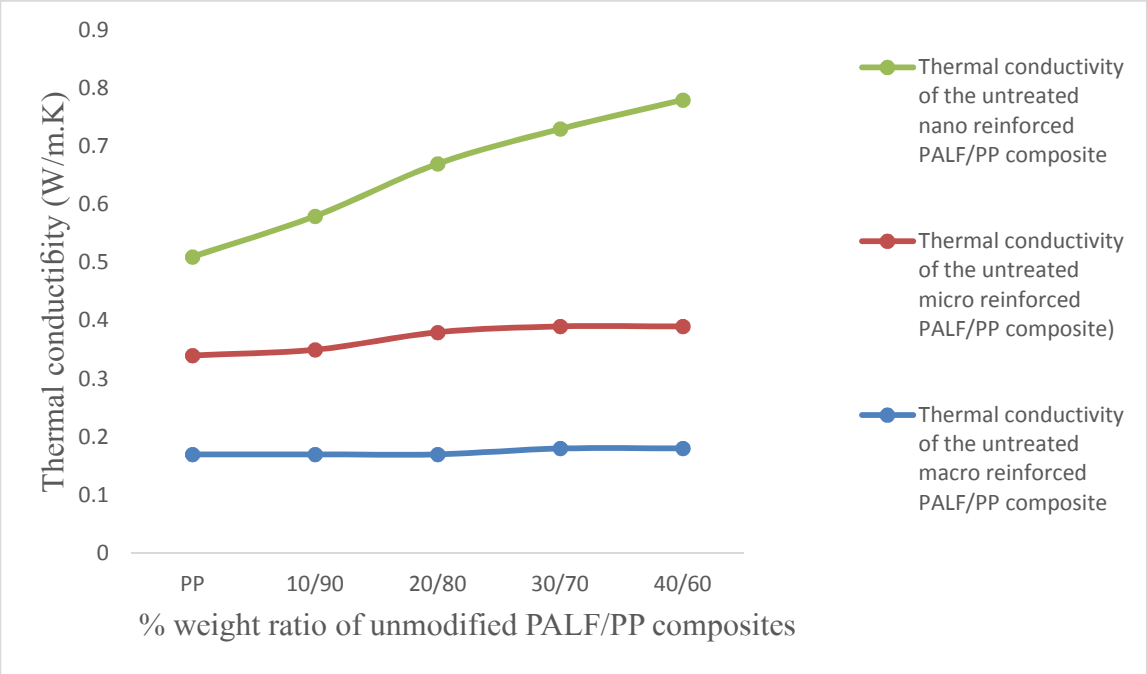


Figure 4.31 Thermal conductivity against % weight ratio of unmodified PALF/PP Composites

Figure 4.31 shows an increased TC by 6% (0.18 W/mK), 24 % (0.21 W/mK) and 129 % (0.39 W/mK), with PALF at the macro, micro and nano cellulose dimensions.

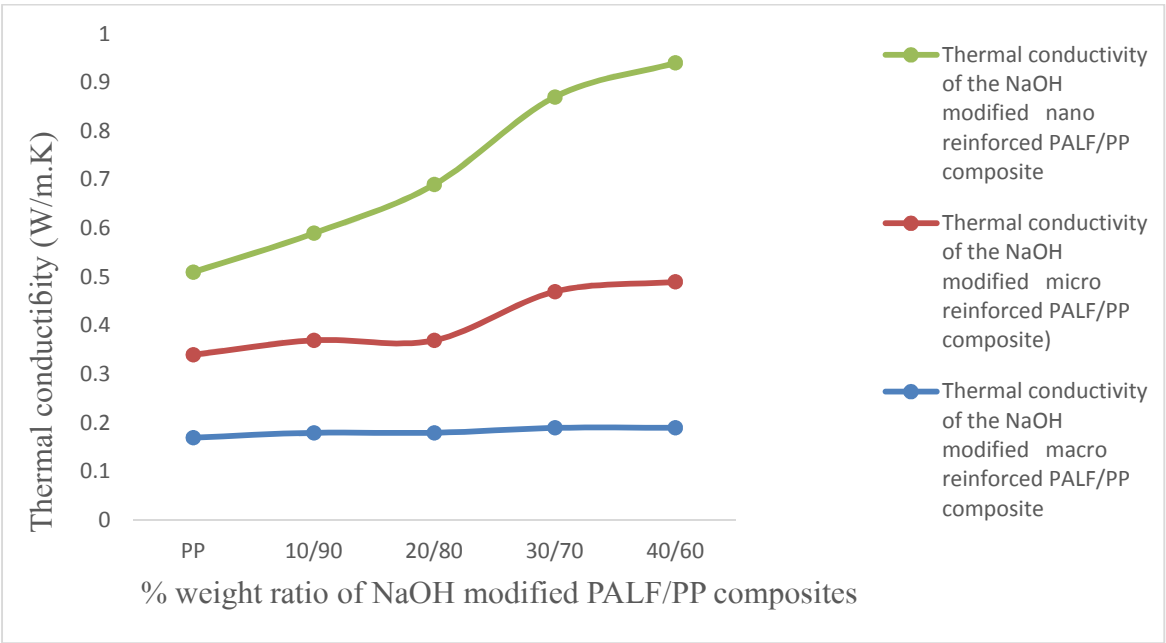


Figure 4.32 Thermal conductivity against % weight ratio of NaOH modified PALF/PP composites

From Figure 4.32, the TC increased by 12 %, 76 % and 165 %, that is by 0.19, 0.3 and 0.45 W/mK with PALF at the macro, micro and nano cellulose dimensions respectively.

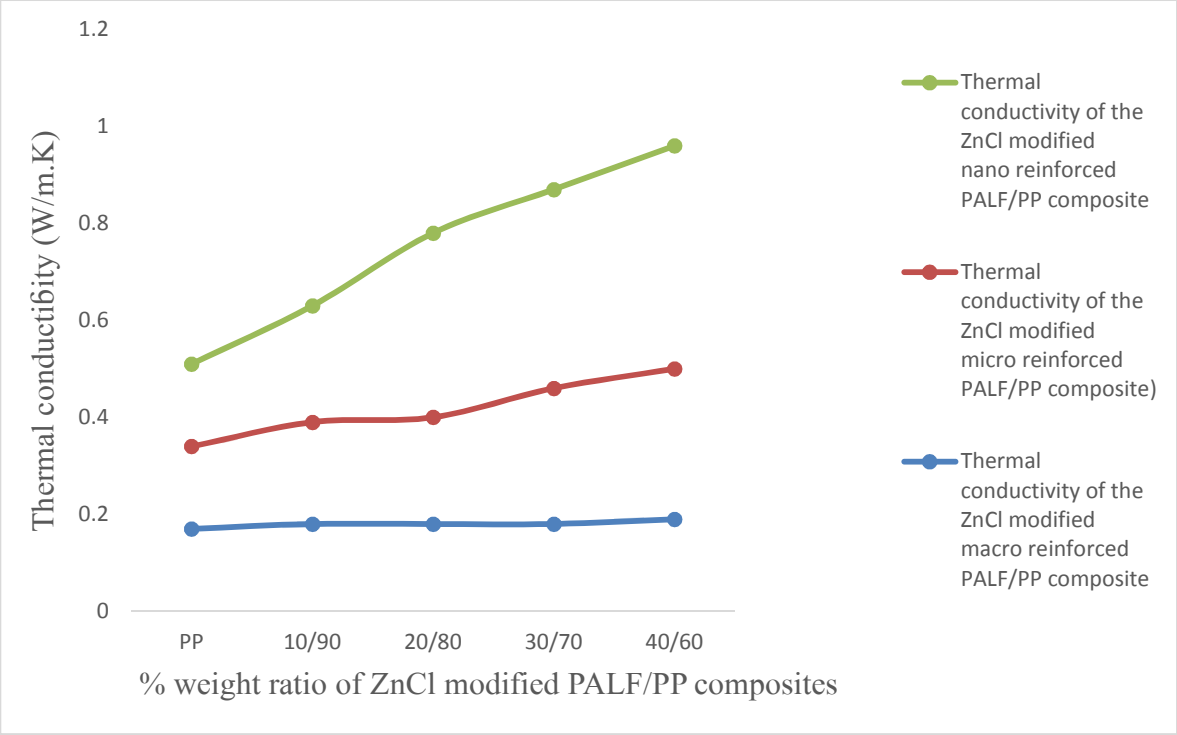


Figure 4.33 Thermal conductivity against % weight ratio of ZnCl modified PALF/PP composites

Figure 4.33 shows the TC plots of the ZnCl modified PALF/PP composites with the PALF in the macro, micro and nano dimensions, the observed TC was steady at 0.19 W/mK, 0.43 W/mK, and 0.52 W/mK respectively, this corresponds to a TC increase by 12 %, 82 % and 171 % in same order.

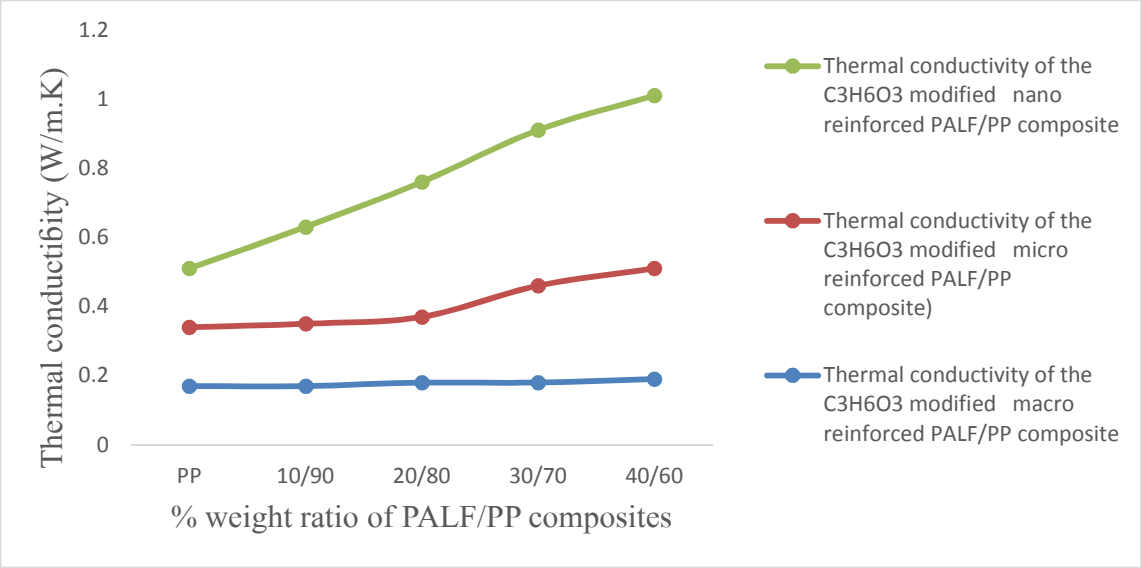


Figure 4.34 Thermal conductivity against % weight ratio of $C_3H_6O_3$ modified PALF/PP composites

Figure 4.34 shows a similar pattern, for the reinforced PALF/PP composites modified with $C_3H_6O_3$ as 12 % (0.19 W/mK), 88 % (0.32 W/mK) and 194 % for PALF at the macro. Micro and nano cellulose dimensions respectively.

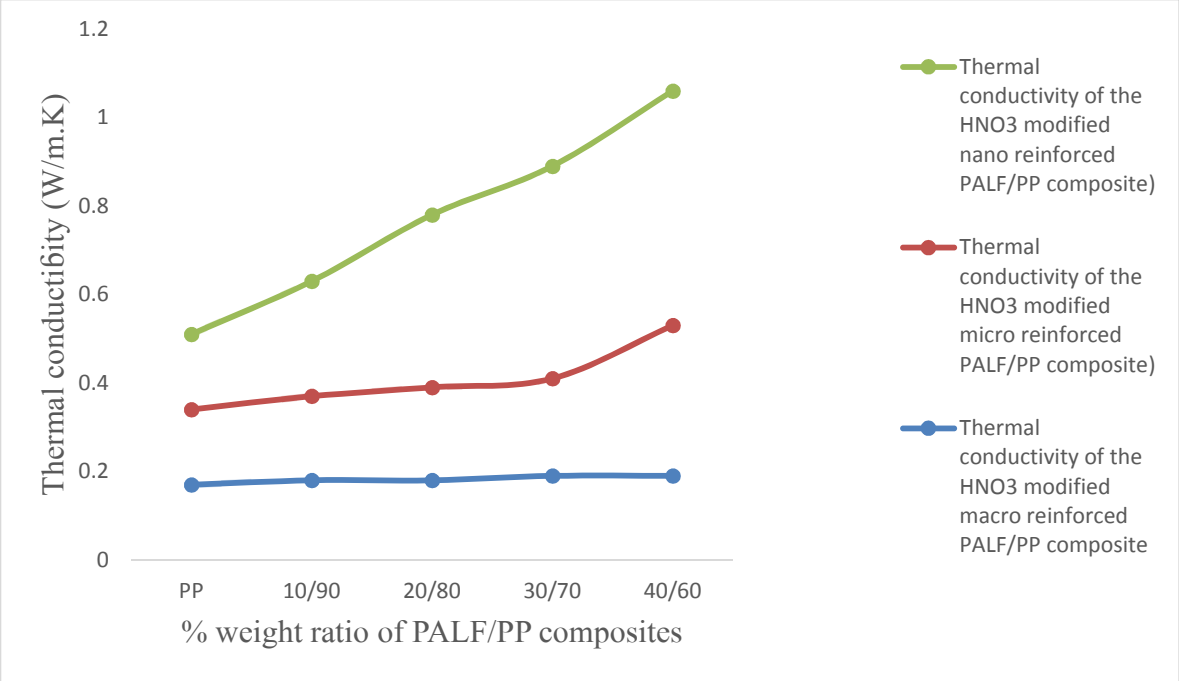


Figure 4.35 Thermal conductivity against % weight ratio of HNO_3 modified PALF/PP composites

Figure 4.35 shows the plots of HNO_3 modified PALF/PP composites with the PALF at the macro, micro and nano dimensions. A steady increased TC was observed at the 40 / 60 PALF /

PP weight ratio, depicting 0.19 W/mK (12 %), 0.34 W/mK (100 %) and 0.53 W/mK (212 %) at the macro, micro and nano PALF dimensions.

The results obtained in this research following a similar pattern obtained by other researcher and are with the acceptable values obtained by other researchers and are close agreement with those obtained by other researchers.

It has been reported by Termal *et al.*, (2014) that fillers with high aspect ratios, such as nano whiskers, flagella or platelets can form continuous thermally conductive network in polymer matrix, and thus, more effectively in enhancing thermal transfer. This factor explains why there is over 200 % increase in the TC property of the PALF nanocellulose / PP composite over and above the value obtained at the fibre micro nor macro particle levels.

The above mentioned factor combined with high intrinsic thermal conductivity of the PALF nanocellulose offered reasonable explanations form the larger increment in the TC of the PALF nanocellulose / PP composites with increasing filler content, partly, due to the Van de Waals attraction, a homogeneous network could be achieved under relatively high filler content.

This hypothesis could be collaborated by the TEM micrographs of the PALF nanocellulose, which could lead to interconnected network which leads to the decrease in the scattering of phonon transfer and promotes the diffusion of phonons in the overall PALF nanocellulose / PP composites

The TC of polymer composites are vital especially in injection or extrusion molding as reported by Patti and Acierno, (2018), that the greater would the TC of the processed materials, the lower would be the heating or cooling time, and the operating cost of the overall process is reduced, thereby maximizing profit and conserving energy. A similar work was done by

Cheewawuttipong *et al.*, (2013), they found out that TC increased by the increased in volume of nano fillers.

CHAPTER FIVE

SUMMARY, CONCLUSION AND RECOMMENDATION

5.1 Summary

In this study, composites of PALF/PP were produced, the PALF were extracted from pineapple leaves. This was achieved by adopting the mechanical scrapping method, on the course of this research, other fibre extraction methods such as retting were tried with low output and also, the retting method was time consuming, thus, it was abandoned and the mechanical scrapping method was utilized all through:

1. This method gave a yield between 32-37% which is more that the yield via the retting method which averaged around 12-14%.
2. The extracted PALF were modified with surface modification agents, knowing that natural fibres are hydrophilic in nature and they do not readily bond with synthetic fibres to form composites. It is an already established fact that surface modified composites exhibit enhanced properties. In this research, the extracted PALF were modified with 6% NaOH, 14% $C_3H_6O_3$, 6% HNO_3 and 3% ZnCl. The surface modified PALF as well as the control (untreated/unmodified) gave FTIR spectrum indicated that the modified PALF chemical structures were not significantly altered.
3. TAPPI methods were used to ascertain the composition of the PALF, specifically the percentage composition of lignin, hemicellulose and cellulose in the PALF. Elemental composition of the PALF were equally analyzed, the data were subsequently compared and analyzed with the data collected from analyzing same samples using a more accurate and state of the art equipment called the EDX-SEM, results obtained when compared with the data obtained from the conventional method, the results are in close agreement with results obtained by other researchers.
4. The obtained PALF micro fibrils were characterized using JEOL JSM 7500F SEM, the micrographs of the modified PALF showed morphologies of PALF that could easily

produce composites with enhanced properties. Similarly, the PALF nanofibrils were characterized using JEOL JEM 2100 High resolution (HR-TEM), the micrographs of the modified nanofibrils displayed a spider web-like structure with nano scale diameter cellulose fibrils or branches of similar fibril bundle hooked up to produced larger aggregates of nano cellulose as reported by other researchers.

5. The PALF went through particle size reduction stages, broadly classified into the macro (2-6 mm), micro (70-300 µm) and nano (20-500 nm); the macro cellulose PALF were obtained by cutting the long strands of fibre into smaller sizes of an average of 2-6 mm.
6. Attempts were made to achieved micro and nano fibrils of the pineapple leaf, attempts were made in suing acid hydrolysis, pulverization and ball milling, the former method did not yield meaningful output gave output that seem denatured in appearance, the ball milling method gave a charred PALF and completely denatured the PALF. The method adopted in the research that gave good results is actually novel and it is termed chemo-mechanical method. In this method, the PALF undergo alkalisation, followed by a bleaching process and the acid hydrolysis, the method's concluding part is the milling process with lead to micro/nano fibrils. For a 100 g of macro PALF, the yield is as summarized in this order; PALF modified with NaOH gave a yield of 44.0 % (44.0 g) of nano fibrils, PALF modified with $C_3H_6O_3$ yielded 54.9 % (54.9 g), the PALF modified with $HN0_3$ gave a yield of 59.9 % (59.5 g) and he PALF modified with Zncl gave a yield of 49 % (49.0 g).
7. Molds were fabricated using mild steel plates by adopted the modern methods of producing molds, with the aid of a computer numerically controlled machine (CNCm) called the vertical milling center (VMC). These molds were designed based on the standard ASTM dimensions for major mechanical and thermal properties tests, in producing the molds, the CNCm programming language G-code was used, the codes

were simulated to check errors in programming before the codes were then transferred to the VMC for the fabrication of the molds. This concept which is equally novel is informed by the fact that the conventional method of producing composites in laminates and cutting them into the required testing dimensions introduces shear strain on the grain arrangements of the composites, thus, altering the end results.

8. Microbial load analysis were carried out to ascertain and determine the shelf life for the PALF, aspergillus was identified as the microorganism that predominantly affected the PALF after a 12 months observation period.
9. The PALF/PP composites exhibits improved mechanical, thermal and chemical properties at the macro cellulose, micro and nano fibrils dimensions of PALF respectively. These enhanced behaviours are seen even in the unmodified PALF/PP composites, where the TS at the optimal performance with ratio of 30/70 of PALF/PP, there is an increase by 27.88 % of TS for the micro PALF/PP composite and an amazing 70.65 % increase at the nano fibrils PALF/PP composites level. However, the behaviour of the modified PALF are higher that the unmodified PALF/PP composites when compared. The results show that the reinforced HNO_3 modified PALF/PP composites have higher performance index than the reinforced $C_3H_6O_3$ modified PALF/PP composites which gives better performance index that the reinforced NaOH modified PALF/PP composites which performs higher than the reinforced ZnCl modified PALF/PP composites, which gave higher performance index that the unmodified reinforce PALF/PP composites.

5.2 Conclusion

This research has proved that PALF is a good reinforcing material in making a polypropylene composites. This study has introduced to the bank of knowledge a useful means of utilization

of the agricultural waste in discarded pineapple leave after the harvest of the pineapple fruit. The study considered the effect surface morphological changes PALF dimensions could have on major physical, mechanical and thermal properties of the PALF/PP composites. In the course of the study, a novel concept of isolation/ production of nano fibril cellulose was discovered. This approach led to acquiring a patent right since the idea is novel and has never been used to isolate PALF nano fibrils. The micro and nano fibrils yields were considered acceptable and the method environmentally safe and course effective.

In conclusion the objectives of this researched were achieved, PALF/PP composites were produced with enhanced properties. The research went further to fabricate articles that could be produced by interested entrepreneurs or investors. Products made from the PALF/PP composites from this search work include and not limited to:

1. Laboratory equipment such as hand lenses, test tubes, beakers

2. Everyday household products such as cups, plates, etc.

3. Teaching aids such as the human brain.

5.3 Recommendations

Further studies should be carried out on how to:

i. Where molds are available, further studies could be carried out on production of automobile parts such as radiator containers could be produced.
ii. Also, further studies could be carried ouit on the PALF nano fibrils produced in this research as it could find applicaations in drug delivery.
iii. Furtherstudies could be carried out since it has high cellulose content, the nano fibrils could be used in the paper industry in the production of paper.

iv. The nano fibrils could also be used in the production of filtration membrane in water purification applications.

v. Further studies could be carried out on the Local production of PALF extracting machine, extraction of the fibre from the PALF was a challenge on the course of this study.

5.4 Contribution to Knowledge

Contributions to knowledge as a result of this research work are as outlined below:

i. Outcome of this researcg prove that composites with fillers at the nano scale give spectacular physical, mechanical and thermal properties.

ii. This research has provided adequate data and information on the effects of PALF dimensional changes as the PALF particle dimensions change from macro to micro and to nano.

iii. The data if properly utilized can guide the entrepreneur on what better dimensions of PALF choices to make in production of polymeric products for the end user or as material for a particular industry.

iv. This research has established the fact that better performance can be obtained from reinforced composites when the fillers are at the nano particle level.

REFERENCES

Abasiwie Daniel-Luggard Akanzeriyomah, (2015). Mechanical Characterization of Bio-composites Fabricated from Natural Coconut Fibre and Linear Low Density Polyethylene - *A Thesis submitted to the Department of Chemistry,College of Science, Kwame Nkrumah University of Science and Technology*, Kumasi, Ghana

Abidi N, Hequet E, Cabrales L, Gannaway J, Wilkins T, Wells LW.(2018). Evaluating Cell Wall Structure and Composition of Developing Cotton Fibres using Fourier Transform Infrared Spectroscopy and Thermogravimetric Analysis. *Journal of Applied Polymer Science*. 107:476-486.

Ahola, S., Österberg, M. and Laine, J. (2008). Cellulose Nanofibrils—Adsorption with Poly(amideamine) Epichlorohydrin Studied by QCM-D and Application as a Paper Strength Additive. *Cellulose*, 15 (2): 303-314.

Åkerholm M, Hinterstoisser B, Salmén L. (2004).Characterization of the Crystalline Structure of Cellulose Using Static and Dynamic FTIR Spectroscopy. Carbohydrate Research. 339(3): pp. 569-578.

American Standard of Testing and Materials -ASTM International (2011). *Standard Test Method for Tensile Properties of Plastics*. United State, ASTM 638-11.

American Standard of Testing and Materials -ASTM International (2011). *Standard Test Methods for Flexural Properties of Unreinforced and Reinforced Plastics and Electrical Insulating Materials*. United State, ASTM D790-11.

American Standard of Testing and Materials -ASTM International (2017). *Standard Test Methods for Determining the Izod Pendulum Impact Resistance of Plastics*. United State, ASTM D256-17.

Ahmed K.S and Vijayarangan A (2006). Elastic Property Evaluation of Jute-Glass Fibre Hybrid Composite using Experimental and CLT Approach. *Indian Journal of Engineering and Materials Sciences*, vol. 13, no. 5, pp. 435 442

Andrady, Anthony L., and Mike A. Neal (2009), Applications and Societal Benefits of Plastics. Philosophical Transactions of the Royal Society B: Biological Sciences 364.1526, 1977-1984.

Andersons J, R. Joffe, , and L. Wallstrom (2003). Strength and Adhesion Characteristics of Elementary Flax Fibres with Different Surface Treatments," Composites Part A: Applied Science and Manufacturing, Vol. 34, No. 7, pp. 603–612, 2003.

Arib R. M.N., Sapuan S. M., Ahmad M. M. H. M., Paridah M. T. and. Zaman H. M. D. K (2006). Mechanical Properties of Pineapple Leaf Fibre Reinforced Polypropylene Composites," *Materials and Corrosion*, vol. 27, no. 5, pp. 391–396.

Araki, J., Wada, M. and Kuga, S. (2001). Steric Stabilization of a Cellulose Microcrystal Suspension by Poly(ethylene glycol) Grafting. *Langmuir*, 17 (1):21 - 27.

Asim, M., Abdan, K., Jawaid, M., Nasir, M., Dashtizadeh, Z., Ishak, M.R. & Hoque, M.E.(2015). A review on pineapple leaves fibre and its composites. *International Journal of Polymer Science.* 1-16.

Aulin, C., Gällstedt, M. and Lindström, T. (2010). Oxygen and oil Barrier Properties of Microfibrillated Cellulose Films and Coatings. *Cellulose*, 17 (3): 559-574.

Bledzki AK, Gassan J (1999). Composites Reinforced with Cellulose based Fibres. *Prog Polym Sci* 24:221–274. https:// doi.org/10.1016/S0079-6700(98)00018-5

Bledzki, A.K., Sperber, V.E. and Faruk, O. (1991). Natural and Wood Fibre Reinforcement in Polymers. *Rapra Review Reports*. 13(152).

Bledzki, A. K., Reinhmane, S. and Gassan, J. (1998). "Thermoplastics Reinforced with Wood Fillers". *Polym Plast. Technol. Eng.* 37:451-468.

Bledzki, A. K., Lucka, M., Mamun, A. A., and Michalski, J. (2009). "Biological and Electrical Resistance of Acetylated Flax Fibre Reinforced Polypropylene Composites". *BioResources* 4(1): 111-126

Bledzki A.K., A. A. Mamun, Lucka-Gabor M, Gutowski V.S. (2008). The Effects of Acetylation on Properties of Flax fibre and its Polypropylene Composites. *eXPRESS Polymer Letters* Vol.2, No.6 (2008) 413–422. Available online at www.expresspolymlett.com. DOI: 10.3144/expresspolymlett.2008.50

Beck-Candanedo, S.,M. R. and D. G. G. (2005). Effect of Reaction Conditions on the Properties and Behavior of Wood Cellulose Nanocrystal Suspensions. Biomacromolecules, 6 (2): 1048–1054.

Beg M.D.H and Pickering K.L. (2008). Accelerated Weathering of Unbleached and Bleached Kraft Wood Fibre Reinforced Polypropylene Composites.*Polymer Degradation and Stability.* 93:1939–1946

Bengtsson M, Gatenholm P, And Oksman K., (2005). The Effect of Crosslinking on the Properties of Polyethylene/Wood Flour Composites. *Composites Science and Technology*, Vol. 65, No. 10, Pp. 1468–1479, 2005.

Boluk Y, Lahiji R, Zhao L and McDermott M T (2012). Colloidal Surfaces *Physicochemical Engineering Aspects*. A 377 297

British Plastics Federation (2011). Polypropylene (PP). N.p., n.d. Web. Accessed on 13 September 2011.<http://www.bpf.co.uk/plastipedia/polymers/pp.aspx>.

Brydson, John Andrew (1999). Plastics Materials. *Butterworth-Heinemann*, USA. Pages 23-25.

Klein, Rolf (2011). Material Properties of Plastics. *Laser Welding of Plastics:Materials, Processes and Industrial Applications Pages 5*-35.

Cabiac, A., Guillon, E., Chambon, F., Pinel, C., Rataboul, F., and Essayem, N. (2011). Cellulose Reactivity and Gycosidic Bond Cleavage in Aqueous Phase by Catalytic and non Catalytic Tansformations. *Applied Catalysis A: General*, 402(1), 1-10.

Cao, Y., Jiang, Y., Song, Y., Cao, S., Miao, M., Feng, X., Shi, L. (2015). Combined Bleaching and Hydrolysis for Isolation of Cellulose Nanofibrils from Waste Sackcloth. *Carbohydrate Polymers*, 131, 152-158.

Chen, W., Yu, H., Liu, Y.; Hai, Y., Zhang, M and Chen, P. (2017). Isolation and Characterization of Cellulose Nanofibres from Four Plant Cellulose fibres using a Chemical-Ultrasonic Process. *Cellulose*, 18, 433–442.

Chand N, Tiwary R. K, and Rohatgi P.K. (1988). Bibliography Resource Structure Properties of Natural Cellulosic Fibres—an Annotated Bibliography. J*ournal of Materials Science*, Vol. 23, No.2, pp. 381–387.

Chen, D., Lawton, D., Thompson, M. and Liu, Q. (2012). Biocomposites Reinforced with Cellulose Nanocrystals Derived from Potato Peel Waste. *Carbohydrate Polymers*, 90: 709– 716.

Cherian, B.M., Leão, A.L, de Souza, S.F, Thomas, S and Pothan, L.A. (2010). Kottaisamy, M. Isolation of Nanocellulose from Pineapple Leaf Fibres by Steam Explosion. *Carbohydrate Polym*ers. 81, 720–725.

Cheewawuttipong Watthanaphon, Daisuke Fuoka, Shuichi Tanoue, Hideyuki Uematsu, and Yoshiyuki Iemoto. (2013). Thermal and Mechanical Properties of Polypropylene/ Boron Nitride. *Composites. Energy Procedia.* 34, 808-817

Chollakup, R., Tantatherdtam, R., Ujjin, S. & Sriroth, K. (2011) Pineapple Leaf Fibre Reinforced Thermoplastic Composites: Effects of fibre Length and Fibre Content on their Characteristics. *Journal of Applied Polymer Science* 119 (4), 1952-1960.

Cui, W.; Du, F.; Zhao, J. (2011). Improving Thermal Conductivity while Retaining High Electrical Resistivity of Epoxy Composites by Incorporating Silica-Coatedmulti-Walled Carbon Nanotubes. Carbon 2011, 49, 495–500. [CrossRef]

Danladi, A., & Shu'aib, J. (2014). Fabrication and Properties of Pineapple Fibre/High Density Polyethylene Composites. American Journal of Materials Science, 4(3), 139–143.

Daramola Oluyemi Ojo, Adediran Adeolu Adesoji, Adewuyi Benjamin Omotayo, and Adewole Olamigoke (2017). Mechanical Properties and Water Absorption

Behaviour of Treated Pineapple Leaf Fibre Reinforced Polyester Matrix Composites. *Leonardo Journal of Sciences.*ISSN 1583-0233. Issue 30, January-June 2017.p. 15-30

Deepak S.N, Vedha Hari B.N.(2013) Optimization, Development and Evaluation of Microemulsion for the Release of Combination of Guaifenesin and Phenylephrine, *Journal of Applied Pharmaceutical Science.*(09):048 -056.

Debasis N., and Sanjoy D. (2007). A Pineapple Leaf Fibre Decorticator Assembly,*India Patents* 2334/DEL/2007A.

Eriksen, Ø. Syverud, K. and Gregersen, Ø. (2008). The use of Microfibrillated Cellulose Produced from Kraft Pulp as Strength Enhancer in TMP Paper. *Nordic Pulp and Paper Research Journal*, 23 (3): 299–304.

Eichhorn S.J and Young R.J. (2001). The Young´s Modulus of a Microcrystalline Cellulose. *Cellulose* 2001, Vol., 8: 197.

FAOSTAT. (2016). *Statistical Database of the FAO.* http://faostat3.fao.org/home/E, accessed 25th September 2018

Gadzama S.W, O.K.Sunmonu ,U.S. Isiaku, and Abdullahi Danladi (2020).
Isolation and characterization of nanocellulose from pineapple leaf fibres via chemo-mechanical method. *Science World Journal. Vol. 15(No 2) 2020 www.scienceworldjournal.org ISSN 1597-6343. Published by Faculty of Science, Kaduna State University*

Galli, P., S. Danesi, and T. Simonazzi (1984). Polypropylene Based Polymer Blends: Fieldsof Application and new Trends. *Polymer Engineering and Science.* 24(8), 544-554.

George M, Mussone P.G, Abboud, Z and Bressler D(. 2014). Characterization of Chemically and Enzymatically Treated Hemp Fibres using Atomic ForceMicroscopy and Spectroscopy. *Applied Surface Science*, vol. 314, pp. 1019–1025, 2014.

George J, Bhagawan S, Prabhakaran N, Thomas S (1995). Short Pineapple-Leaf-Fibre Reinforced Low-Density Polyethylene Composites. *Journal of Applied Polymer Science*. 57:843-54.

George, J., Bhagawan, S.S. and Thomas, S. (2001). Thermogravimetric and Dynamic Mechanical Thermal Analysis of Pineapple Fibre Reinforced Polyethylene Composites. *Journal of Thermal Analysis*. 47: 1121-1140.

George, J., Bhagawan, S.S. and Thomas, S. (1998). Effects of Environment on the Properties of Low-Density Polyethylene Composites Reinforced with Pineapple Leaf Fibre. *Composites Science and Technology*. 58: 1471-1485.

George, J., Janardhan, R., Anand, J.S., Bhagawan, S.S. and Bhagawan, S.S. and Thomas, S. (1996). Melt Rheological Behaviour of Short Pineapple Fibre Reinforced Low Density Polyethylene Composites. *Polymer*. 37: 5421-5431

Goh, K.Y., Ching, Y.C, Chuah, C.H., Abdullah, C.L. and Liou, N.-S.(2016). Individualization of Microfibrillated Celluloses from oil Palm Empty Fruit Bunch: Comparative Studies Between Acid Hydrolysis and Ammonium Persulfate Oxidation. *Cellulose* 23, 379–390.

Gomez, S., Rendtorff, N.M. and Esteban, F. (2016) Surface Modification of MultiwallCarbon Nanotubes by Sulfonitric Treatment. Applied Surface Science, 379, 264-269. https://doi.org/10.1016/j.apsusc.2016.04.065

Hisham A. and Maddah (2016). Polypropylene as a Promising Plastic: A Review. *American Journal of Polymer Science.* 2016, 6(1): 1-11 DOI: 10.5923/j.ajps.20160601.01

Huda, M. S., Drzal, L. T., Mohanty, A. K., and Misra, M. (2008). Effect of Chemical Modifications of the Pineapple Leaf Fibre Surfaces on the Interfacial and Mechanical Properties of Laminated Biocomposites. Composite Interfaces, 15(2-3), 169–191.doi:10.1163/156855408783810920

HMC Polymers. Polypropylene. Accessed September 2019. http://www.hmcpolymers,com

Hubbe, M., Rojas, O., Lucia, L. and Sain, M. (2008). Cellulosic Nanocomposites: A Review. *Bioresources,* 3 (3): 929 980.

Idicula, M., Boudenne, A., Umadevi, L., Ibos, L., Candau, Y., and Thomas, S. (2006). Thermophysical Properties of Natural Fibre Reinforced Polyester Composites. Composites Science and Technology, 66(15), 2719 2725.doi:10.1016/j.compscitech.2006.03.007

Joffe R., Andersons J, and Wallstrom L (2003). Strength and Adhesion Characteristics of Elementary Flax Fibres with Different Surface Treatments," Composites Part A: *Applied Science and Manufacturing*, Vol. 34, no. 7, pp. 603–612, 2003.

John, M.J. and Anandjiwala, R.D. (2008) Recent Developments in Chemical Modification and Characterization of Natural Fibre-reinforced Composites. *Polymer Composites* 29 (2), 187-207.

Johnsy George, S.N Sabapathi (2015). Cellulose Nanocrystals: Synthesis, Functional Properties, and Applications. *Nanotechnology, Science and Applications*.2015:8 45–54

Jonoobi, M, Harun, J, Mishra, M and Oksman, K. (2015). Chemical Composition, Crystallinity and Thermal Degradation of Bleached and Unbleached Kenaf Bast (Hibiscus Cannabinus) Pulp and Nanofibre. *BioResources* , 4, 626–639.

Kalia, S., Kaith, B.S. (2011) *Cellulose Fibres: Bio- and Nano-Polymer Composites; Green Chemistry and Technology*. Berlin: Springer.

Kalia, S., Boufi, S., Celli, A., & Kango, S. (2014). Nanofibrillated Cellulose: Surface Modification and Potential Applications. *Colloid and Polymer Science*, 292(1), 5-31.

Khalilh H. P. S. A., Alwani S.M, and Omar, A.K.M (2006). Distribution and Cell Wall Structure of Malaysian pPant Waste fFbers. *BioResources*, Vol. 1, pp. 220–232,

Kasim A. N., Selamat M. Z., Aznan N., Sahadan S.N., Daud M. A. M., Jumaidin R., Salleh S. (2015). Effect of Pineapple Leaf Fibre Loading on the Mechanical Properties of Pineapple Leaf fFber – Polypropylene Composite. *Journal Teknologi*, 77, 117–123. https://doi.org/10.11113/jt.v77.6617

Kengkhetkit N, Amornsakchai T. (2014). A New Approach to ‘‘Greening’’ Plastic Composites Using Pineapple Leaf Waste for Performance and Cost Effectiveness. Materials and Design, 55:292-9.

Kaewpirom S., Worrarat C.: Preparation and Properties of Pineapple Leaf Fibre Reinforced Poly(lactic acid) green composites. Fibres and Polymers, 15, 1469–1477 (2014). https://doi.org/10.1007/s12221-014-1469-0

Kimura, F., Kimura, T., Tamura, M., Hirai, A., Ikuno, M. and Horii, F. (2005). Magnetic Alignment of Chiral Nematic Phase of Cellulose Microfibril Suspension *Langmuir*, 21 (5): 2034–2037.

Klemm D, Heublein B, Fink HP, Bohn A. (2005). Cellulose: Fscinating Biopolymer and Sustainable Raw Material. *Angew Chem Int Ed*. 2005;44:3358–3393.

Leao, A., Cherian, B., Narine, S., Souza, S., Sain, M., and Thomas, S. (2015). The use of Pineapple Leaf Fibres (PALFs) as Reinforcements in Composites. Biofibre Reinforcements. *Composite Materials*, 211-235.

Li Y., Mai Y.W. and Ye L. (2000). Sisal Fibre and its Composites: A Review of Recent Developments," *Composites Science and Technology*, vol. 60, no. 11, pp. 2037–2055, 2000.

Lopattananon N, Panawarangkul K, Sahakaro K, Ellis B. (2006). Performance of Pineapple Leaf fibre–Natural Rubber Composites: The Effect of Fibre surface Treatments. *Journal of Applied Polymer Science,* 102, 1974-84.

Lopattananon N, Payae Y, Seadan M. (2008). Influence of Fibre Modification on Interfacial Adhesion and Mechanical Properties of Pineapple Leaf Fibre-Epoxy Composites. *Journal of Applied Polymer Science,* 110, 433-43.

Lavoine, N., Desloges, I., Dufresne, A. and Bras, J. (2013). Microfibrillated Cellulose – Its Barrier Properties and Applications in Cellulosic Materials: A Review. *Carbohydrate Polymers*, 90 (2): 735– 764.

Liu, W., Misra, M., Askeland, P., Drzal, L. T., and Mohanty, A. K. (2005). Green' Composites from Soy Based Plastic and Pineapple Leaf Fibre: Fabrication and Properties Evaluation. *Polymer*, 46(8), 2710 2721.doi:10.1016/j.polymer.2005.01.027

Liu, D., Chen, X., Yue, Y., Chen, M. and Wu, Q. (2011). Structure and Rheology of Nanocrystalline Cellulose. Carbohydrate Polymers, 84: 316–322.

Mahardika Melbi , Hairul Abral, Anwar Kasim, Syukri Arief and Mochamad Asrofi. (2018). Production of Nanocellulose from Pineapple Leaf Fibres via High-Shear Homogenization and Ultrasonicatio. retrived from www.mdpi.com/journal/fibres on 6th July, 2019. *Fibres* 6, 28; doi:10.3390/fib6020028

Mahmood Zahed, Muhammad Yameen, Muhammad Jahangeer, Muhammad Riaz, Abdul Ghaffar and Irum Javid (2018). Lignin as Natural Antioxidant Capacity. http://www.intechopen.com/books/lignin-trends-and-applications

Mashego, Ditiro Victor (2016). Preparation, Isolation And Characterization of Nanocellulose from Sugarcane Bagasse. *Master of Applied Sciences In Chemistry Faculty of Applied Sciences at the Durban University of Technology, Chemistry Department*, Durban, South Africa

Mohammed Layth , M. N. M. Ansari, Grace Pua, Mohammad Jawaid and M. Saiful Islam (2015). A Review on Natural Fibre Reinforced Polymer Composite and Its Applications. Hindawi Publishing Corporation. *International Journal of Polymer Science*. Volume 2015, Article ID 243947, 15 pages http://dx.doi.org/10.1155/2015/243947

Mallick , P.K. (2008). Fibre-Reinforced Composites: Materials, Manufacturing, and Design, *CRC Press*, New York, NY, USA, 2008.

Munirah, M., Rahmat, A. R., and Hassan, A. (2007). Characterization and Treatments of Pineapple Leaf Fibre Thermoplastic Composite for Construction Application. Universiti Teknologi Malaysia.

Mwaikambo, L. Y., and Ansell, M. P. (2003). Hemp Fibre Reinforced Cashew Nut Shell Liquid Composites. Composites Science and Technology, 63(9), 1297–1305.doi:10.1016/S0266-3538(03)00101-5

Nurul Munirah Abdullah and Ishak Ahmad (2012).Effect of Chemical Treatment on Mechanical and Water Sorption Properties Coconut Fibre – Unsaturated Polyester from Recycled PET. *International Scholarly Research Network*. ISRN Material Science Volume 2012, Article ID 134683, 8 pages, 2001.

Patti Antonella and Domenico Acierno (2018).Thermal Conductivity of polypropylene-Based Materials. DOI:http://dx.doi.org/10.5772/intechopen.84477

Panthapulakkal S. and Sain M. (2007). Studies on the Water Absorption Properties of Short Hemp—Glass Fibre Hybrid Polypropylene Composites. *Journal of Composite Materials*, Vol. 41, no. 15, pp. 1871–1883, 2007.

Prukkaewkanjana, K., Thanawan, S., and Amornsakchai, T.(2015). High Performance Hybrid Reinforcement of Nitrile Rubber using Short Pineapple Leaf Fibre and Carbon Black. Polymer Testing, 45, 76–82. doi:10.1016/j.polymertesting.2015.05.004

Rahman M.R, Huque M.M, Islam M.N and Hasan M (2011). Improvement of Physico-Mechanical Properties of Jute Fibre *Composites Part A: Applied Science and Manufacturing*, vol. 39, no.11, pp. 1739–1747.

Reddy N. and Yang Y. (2005). Biofibres from Agricultural Byproducts for Industrial Applications," Trends in Biotechnology, Vol. 23, No. 1, pp. 22–27.

Rodriguez R. J. S., Monteiro S. N, Calado V, and Margem F. M. (2012).Thermogravimetric Stability Behavior of less Common Lignocellulosic Fibres-A Review. *Journal of Materials Research and Technology* **2012**, 1(3): 189-199.

Sofla M Rahimi Kord , R J Brown, T Tsuzuki And T J Rainey (2016). A Comparison of Cellulose Nanocrystals and Cellulose Nanofibres Extracted from Bagasse using Acid and Ball Milling Methods. Advances in Natural Sciences: Nanoscience and Nanotechnology. (2016) 035004 (pp) Doi:10.1088/2043-6262/7/3/035004

Santos, R. M. D., Neto, W. P., A.Silvério, H., Martins, D. F., Dantas, N. O. and Pasquinia, D. (2013). Cellulose Nanocrystals from Pineapple Leaf, a new Approach for there use of this Agro-Waste. *Industrial Crops and Products*, 50: 707– 714.

Santosh Kumar D S, Praveen B A, Kiran Aithal S, U N Kempaia (2015). Development of Pineapple Leaf Fibre Reinforced Epoxy Resin Composites. International Research Journal of Engineering and Technology (IRJET) e-ISSN: 2395-0056. Volume: 02 Issue: 03 | June-2015 www.irjet.net p-ISSN: 2395-0072

Sheltami, R., Abdullah, I., Ahmada, I., Dufresne, A. and Kargarzadeh, H. (2012). Extraction of Cellulose Nanocrystals from Mengkuang Leaves (Pandanus tectorius).*Carbohydrate Polymers*, 88: 772– 779.

Silvério, H., Neto, W., Dantas, N. and Pasquini, D. (2013). Extraction and Characterization of Cellulose Nanocrystals from Corncob for Application as Reinforcing Agent in Nanocomposites. *Industrial Crops and Products*, 44: 427– 436.

Sri Endah Susilowati, Didit Sumardiyanto (2018). Assessing Mechanical Properties of Pineapple Leaf Fibre (PLF) Reinforced Composites for Automotive Applications. *International Journal of Composite Materials* 2018, 8(3): 57-63. DOI: 10.5923/j.cmaterials.20180803.02

Stuart, B. (2005). *Infrared Spectroscopy: Fundamentals and Applications*. West Sussex, UK: John Wiley and Sons.

Syverud, K. and Stenius, P. (2009). Strength and Barrier Properties of MFC Films. *Cellulose*, 16 (1): 75-85.

Thakur, V. K. (2015). *Nanocellulose Polymer Nanocomposites - Fundamentals and Applications*. New Jersey, USA: Scrivener Publishing.

Mishra, S., Mohanty, A.K., Drzal, L.T., Misra, M., Parija, S., Nayak, S.K. and Tripathy, S.S. (2004). Studies on Mechanical Performance of Biofibre / Glass Reinforced Polyester Hybrid Composites. *Composites Science and Technology*.63: 1377-1385

Mohanty A.K, Mishra S, Misra M, Tripathy S.S, Nayak S.K, and A. K. (2001). Potentiality of Pineapple Leaf Fibre as Reinforcement in PALF-Polyester Composite: Surface Modification and Mechanical Performance," *Journal of Reinforced Plastics and Composites*, Vol. 20, No. 4, pp. 321–334.

Mohanty, A.K., Misra, M. & Drzal, L.T. (2005) *Natural Fibres, Biopolymers, and Biocomposites.* Boca Raton: Taylor & Francis.

Mwaikambo L. Y. (2006), Review of the History, Properties and Application of Plant Fibres. *African Journal of Science and Technology.* Vol. 7, no. 2, pp. 120–133.

Mwaikambo L.Y and Ansell M.P. (2003). Chemical Modification of Hemp, Sisal, Jute, and Kapok Fibres by Alkalization. *Journal of Applied Polymer Science.* Vol. 84, No. 12, pp. 2222–2234, 2002.

Natalia Jaramillo, David Hoyos and Juan F. Santa. (2016).Composites with Pineapple-Leaf Fibres Manufactured by Layered Compression Molding, *Ingeniería y Competitividad, Volume18, No. 2, p. 151 - 162*

Nadanthangam N, Karande K, Hadge G.B, Mheske S.T. and Bharimalla A.K.(2013).. Enzyme/ZnCl Pretreatment of Short Shape Cotton Fibres for Energy Reduction during Nano Fibrillation by Refining Process. *World Cotton Research Conference on Technologies for Property*.

Nayan Nadirul Hasraf Mat, Wan Aizan Wan Abdul Rahman and Rohah Abdul Majid (2013). The Effect of Mercerization Process on The Structural and Morphological Properties of Pineapple Leaf Fibre (PALF) Pulp. *Malaysian Journal of Fundamental and Applied Sciences* Vol.10, No.1 (2013), pp 12-16.

Nuruddin, M.D. Mahesh Hosur, M.D, Jamal Uddin, David Baah and Shaik Jeelan. (2016). A Novel Approach for Extracting Cellulose Nanofibres from Lignocellulosic Biomass by Ball Milling Combined with Chemical Treatment. *Journal of Applied Polymer Sciences*, DOI: 10.1002/APP.42990

Nwankwo CF (2014). Residential Water Demand and Supply in Awgu Local Government Area, Enugu State, Nigeria. Department of Geography, University of Nigeria: Unpublished B Sc Project.

Phanthong Patchiy A, Prasert Reubroycharoen C, Xiaogang Hao DD Guangwen Xue, EAbuliti Abudula A and Guoqing Guan. (2018). Nanocellulose: Extraction and Application. *Carbon Resources Conversion* Vol. 1, 32–43.

Prasanna SC, Ramesh C, Manivel R and Karthe M (2017). An Alternative Method for Synthetic Fibres and categorization of Natural Fibre Extracted from Sesbania rostrata, *Journal of Chemical and Pharmaceutical Sciences.* ISSN: 0974-2115. 2:203-207.

Rowell, R.M., Han, J.S. and Rowell, J.S. (2000). Characterization and Factors Effecting Fibre Properties. In: Frollini, E. Leão, A.L and Mattoso, L.H.C. ed. *Natural Polymers and Agrofibres Composites*. Sãn Carlos, Brazil. 115-129.

Rowell R. M., Sanadi A.R, Caulfield D.F, and Jacobson R.E.(1997). Utilization of Natural Fibres in Plastic Composites-Problems and Opportunities. in Lignocellulosic-*Plastics Composites*,

Sangeeta Sharma and Dinesh Kaushik. (2016). Microencapsulated Ciprofloxacin Hydrochloride Augmented Drug Delivery And Antibacterial Activity Against Pathogenic E. Coli Strain, ISSN 2349-8870. 3(6):370-376.

Siregar, J. P., Sapuan, S. M., Rahman, M. Z. A. & Zaman, H. M. D. K. 2012. Effects of Alkaline Treatments on the Tensile Properties of Pineapple Leaf Fibre Reinforced high Impact Polystyrene Composites.

Smitthipong, W., Tantatherdtam, R. and Chollakup, R. (2015) Effect of Pineapple leaf Fibre-Reinforced Thermoplastic Starch/Poly (lactic acid) Green Composite: Mechanical, Viscosity, and Water Resistance Properties. *Journal of Thermoplastic Composite Materials* 28 (5), 717-729.

Shubhra, Quazi TH, A. K. M. M. Alam, and M. A. Quaiyyum (2011). Mechanical Properties of Polypropylene Composites: A Review. *Journal of ThermoplasticComposite Materials,* 0892705711428659.

Sopie Edwige Salomé Yapo, Kouakou Laurent Kouakou, Jean Pierre Irénée Bognonkpe, Patrice Kouame and Tanoh Hilaire Kouakou (2011). Comparison of Pineapple Fruit Characteristics of Plants Propagated in Three Different Ways: By Suckers, Micropropagation and Somatic Embryogenesis. *Journal of Nutrition and Food Sciences.* 2011, 1:4. DOI: 10.4172/2155-9600.1000110

Tappi Method T204 cm-97. (1988). *Solvent Extractives of Wood and Pulp. Atlanta*, GA: TAPPI PRESS.

Tappi Method T222 cm-02. (1988). *Acid Insoluble Lignin in Wood and Pulp. Atlanta*, GA:TAPPI PRESS.

Taipale, T., Österberg, M., Nykänen, A., Ruokolainen, J. and Laine, J. (2010). Effect of Microfibrillated Cellulose and Fines on the Drainage of Kraft Pulp Suspension and Paper Strength. Cellulose, 17 (5): 1005-1020.

Thakur, V. K. (2015). Nanocellulose Polymer Nanocomposites - Fundamentals and Applications. New Jersey, USA: *Scrivener Publishing*. Pp 15-19.

Threepopnatkul, P., Kaerkitcha, N. & Athipongarporn, N. (2009). Effect of Surface Treatment on Performance of Pineapple Leaf Fibre-Polycarbonate Composites. Elsivier *Journal, composite part B: Engineering*. 40: 628-632.

Teixeira, E. M., Correa, A. C., Manzoli, A., Leite, F. L., Oliveira, C. R., & Mattoso, L. H. C. (2011). Cellulose Nanofibres from White and Naturally Colored Cotton Fibres. *Cellulose*, 17, 595–606.

Uddin N. (2013). Developments in Fibre-Reinforced Polymer (FRP) Composites for Civil Engineering, *Elsevier*,Pg 2-3..

University, P. 2014. https://www.purdue.edu/ehps/rem/rs/sem.htm#2. Available: https://engineering.purdue.edu/MSE/research/facilities/CharacterizationFacilities/AtomicForceMicroscopy (Accessed 06 June 2019).

Yuliasmi S, Nerdy, Husnita A. (2017). Characterization of Microcrystalline from Pineapple Leaf (Ananas comosus L. Merr). 1st Annual Applied Science and Engineering Conference IOP Publishing IOP Conference Series: Materials Science and Engineering 180 (2017) 012267 doi:10.1088/1757-899X/180/1/012267

Yamunadevi Mariswamy, Wesely Edward Gnanaraj, Johnson Marimuthu, Antonisamy.(2012). FTIR Spectroscopic Studies on Aerva Lanata (l.) Juss.ex Schult, ISSN 0974-2441, Asian *Journal of Pharmacuetical Clinical Research*. 52:82-86.

Yu T, Ren J, Li S, Yuan H, Li Y. (2012). Effect of Fibre Surface-Treatments on the Properties of Poly(lactic acid)/Ramie Composites. Composites Part A: *Applied Science and Manufacturing*, 41:499-505.

Yu, C. (2015). Natural Textile Fibres: Vegetable Fibres. In Textiles and Fashion (pp. 29–56). Woodhead Publishing.

Yaacob, Q. (2015). The effect of dispersion on the mechanical properties of PLA based polymer composites. (Unpublished undergraduate dissertation). Universiti Teknikal Malaysia Melaka.

Yusof, Y., Yahya, S. A., and Adam, A. (2015). Novel Technology for Sustainable Pineapple Leaf Fibres Productions. Procedia CIRP, 26, 756–760. doi:10.1016/j. procir.2014.07.160

Yusof Y. and Yahya S.A.B (2013). Comprehensive Review on the Utilization of PALF. *Advanced Materials Research*, Vol. 701, pp. 430–434, 2013.

Van de Weyenberg I, Chi Truong T, Vangrimde B, and Verpoest I. (2006) improving the Properties of UD Flax Fibre Reinforced Composites by Applying an Alkaline Fibre Treatment. Composites. Part A: *Applied Science and Manufacturing*, Vol. 37, No. 9, pp. 1368–1376.

Vautard F, Fioux P, Vidal L, Dentzer J, Chvctz J, Nardin M and Defonrt B (2013). Influence of an Oxidation of Carbon Fibre Surface by Boiling Nitric Acid on the Adhesion Strength in Carbon Fibre Acrylate Composite Covered by Electron Beam. *Surface and Interface Analysis.* Vol. 45, Issue 3, pg 722 – 741.

Wirawan R, Zainudin E.S, and Sapuan S.M. (2009). Mechanical Properties of Natural Fibre Reinforced PVC Composites: A Review, *Sains Malaysiana,* Vol. 38, No. 4, pp. 531–535.

Zawawi Daud, Mohd Zainuri Mohd Hatta, Angzzas Sari Mohd Kassim and Ashuvila Mohd Aripin (2014). Analysis of the Chemical Compositions and Fibre Morphology of Pineapple (Ananas comosus) Leaves in Malaysia. *Journal of Applied Sciences.* 14: 1355-1358. DOI: 10.3923/jas.2014.1355.1358 (http://dx.doi.org/10.3923/jas.2014.1355.1358)

Zhan J, Song L, Nie S, and Hu Y. (2009). Combustion Properties and Thermal Degradation Behavior of Polylactide with an Effective Intumescent Flame Retardant. P*olymer Degradation and Stability.* Vol. 94, no. 3, pp. 291–296,

Zheng, L., Tsuzuki, T., and Wang, X., (2015). Preparation of Cellulose Nanofibre from Softwood Pulp by Ball Milling,. *Cellulose* 22(3):1729-1741.

Zhou, S. F., Reekie, L., Chan, H. P., Chow, Y. T., Chung, P. S., and Man Luk, K. (2012). Characterization and modeling of Bragg Gratings Written in Polymer Fibre for use as Filters in the THz Region. Optics Express, 20(9), 9564–9571. doi:10.1364/OE.20.009564 PMID:22535048

APPENDICES
APPENDIX I

PICTURES OF ACTIVITIES CARRIED OUT ON THE RESEARCH



Appendix I.1 A sample of the polypropylene used



Appendix 1.2 The pineapple plantation (source of PALF used in this research) in Ihe, Awgu, Enugu state



Appendix 1.3 The mechanical extraction processes of the PALF



Appendix I.4 The extracted PALF before cleaning



Appendix I.5 Some of the equipment used in the surface modification experiments



Appendix I.6 The chemicals and reagents used in the surface modification experiment

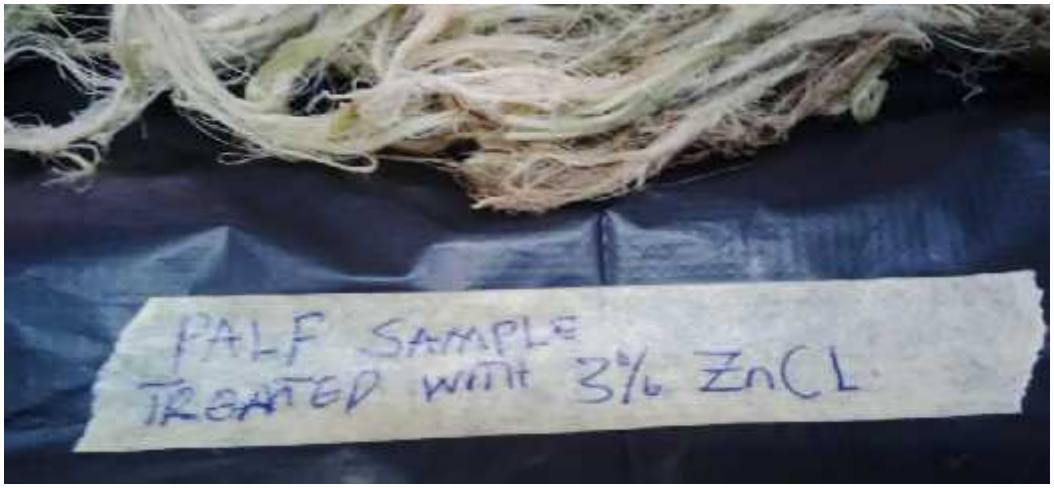


Appendix I.7 The surface modified PALF using NaOH used in this research


Appendix I.8 The surface modified PALF using Acetic anhydride used in this research



Appendix I.9 The fibre after being modified with nitric acid



Appendix 1.10 The PALF after being modified with zinc chloride


Appendix I.11 An array of the PALF used in this research work after been modified with the selected chemicals




Appendix I.12 The PALF before and after size reduction



Appendix I.14 The Soxhlet extractor set-up used in this research



Appendix I.15 The Muffle Furnace used in this Research



Appendix I.16 Fibre stock solution preparations



Appendix I.17 From left to right Samples under bacterial and fungal analysis



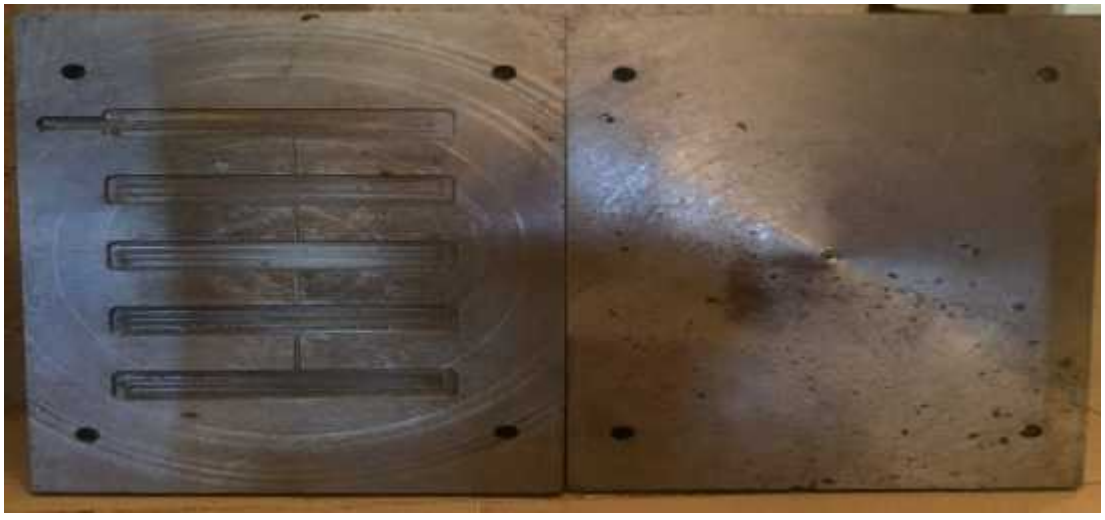
Appendix I.18 The Fourier Transform Infrared Equipment used for the analysis



Appendix I.19 The Computer Numerically Controlled (CNC) Machine used in the mold fabrication



Appendix I.12 Top view of the mold for tensile property test



Appendix I.13 Top view of the mold for flexural property test



Appendix I.14 Top view of the mold for thermal resistance property test



Appendix I.15 Top view of the mold for Impact property test



Appendix I.16 Top view of the mold for thermal conductivity test



Appendix I.20 Some of the heating and weighing equipment used in the research



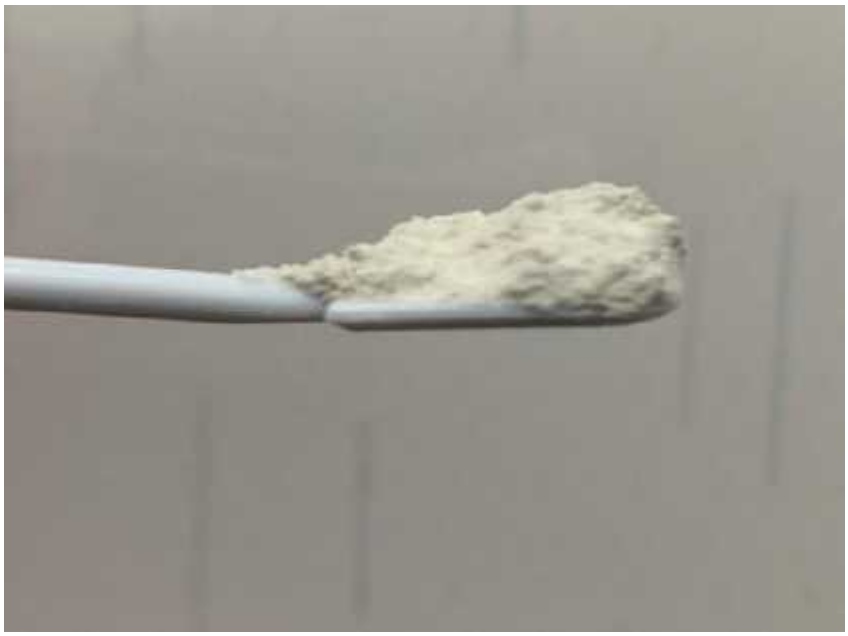
Appendix I.21 Thermoset oven and front view of the end-runner mill used in this research



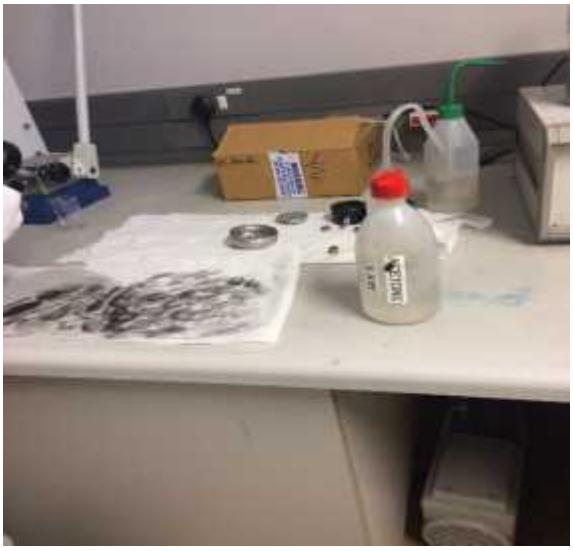
Appendix I.22 The End-Runner milling machine used in this research work



Appendix I.23 A sample of the micro cellulose produced



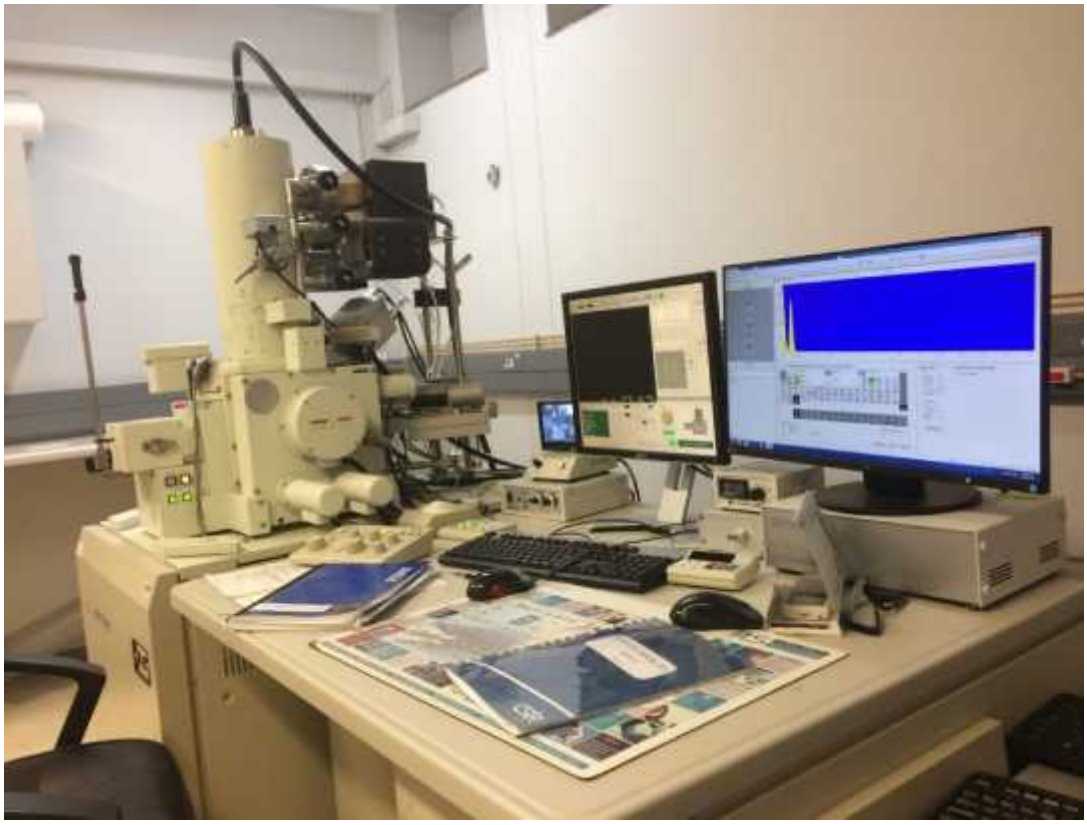
Appendix I.23 A Pinch of PALF Nanocellulose Fibrils

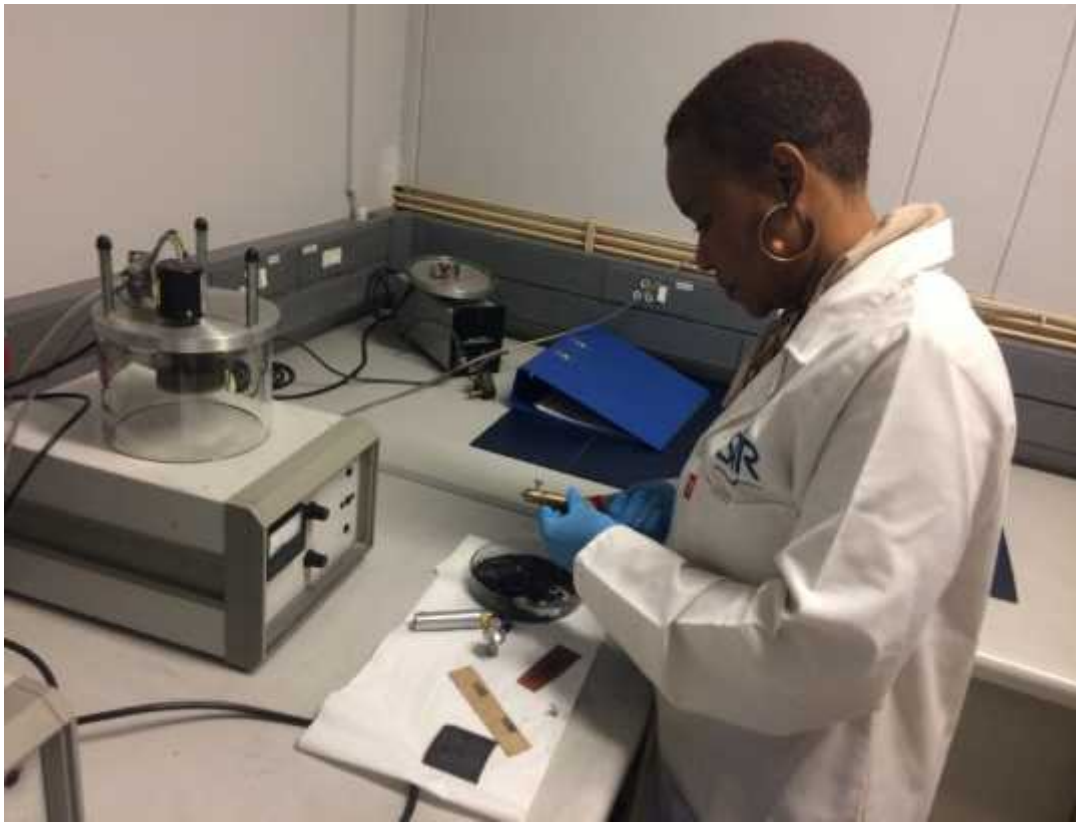
Appendix I.24 (a) The micro cellulose samples ready for SEM characterization
(b) equipment used




Appendix I.24 (a) The carbon coater used in the sample preparation (b) some components of the carbon coater



Appendix I.25 The JEOL JSM 7500F Scanning Electron Microscope (SEM) used in this research



Appendix I.26 The sample coating process



Appendix I.27 The PALF samples in the carbon coater



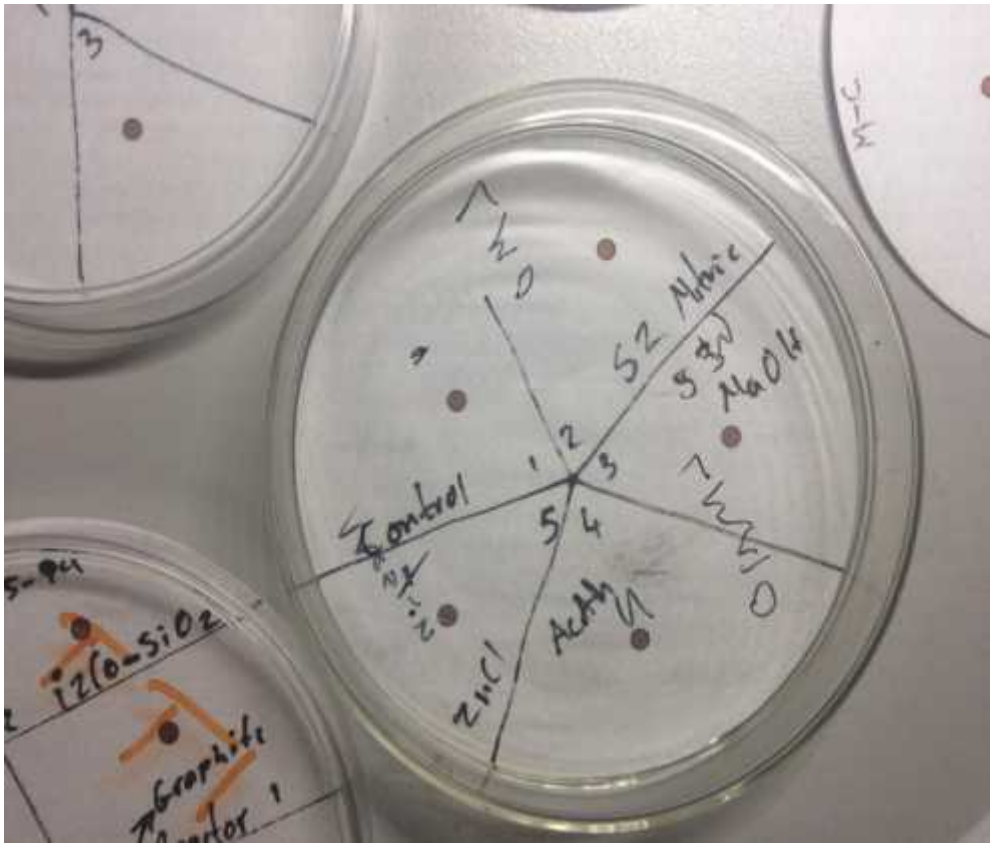
Appendix I.28 The ultrasonicator used in this research



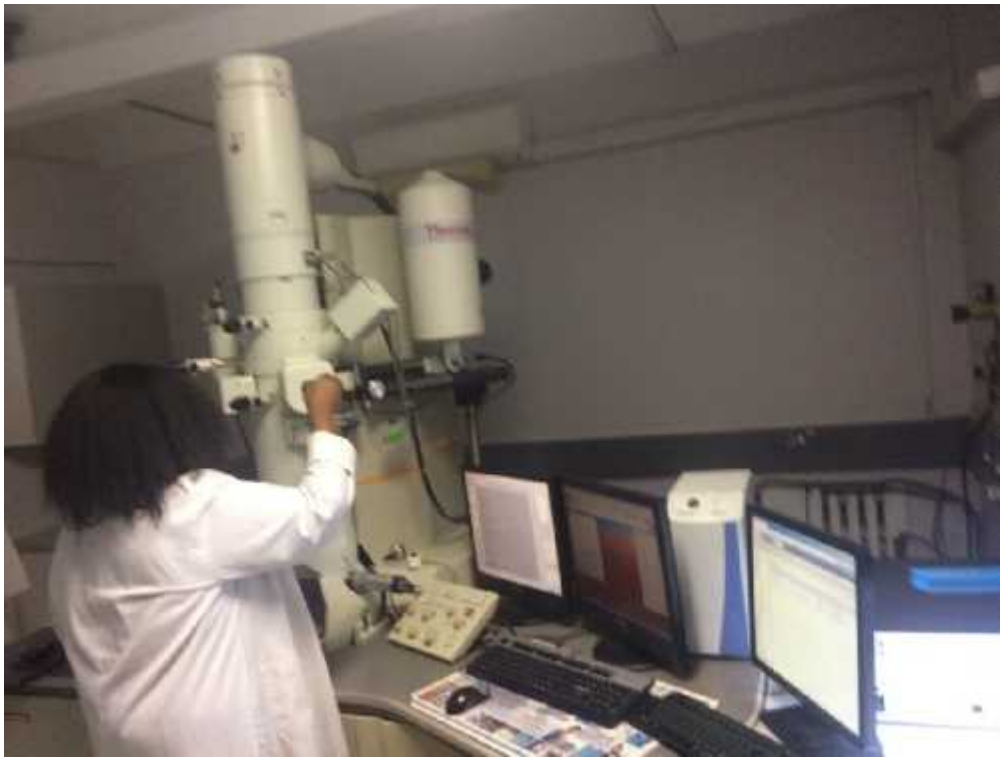
Appendix I.29 The JEOL JEM 2100 High Resolution Transmission Electron Microscope (HRTEM) used in this research



Appendix I.30 A top view of the PALF nano cellulose samples in the ultrasonicator



Appendix I.31 The dried samples ready for the TEM analysis


Appendix I.32 An operator loading the PALF samples into the TEM used in this research



Appendix I.33 The Carbon coating process



Appendix I.34 The Injection molding machine used in this research



Appendix I.35 The computerized universal testing machine used in this research



Appendix I.36 An operator using the computerized universal testing machine on one of the occasions on the course of this research



Appendix I.37 Danison Universal Pendulum Impact System for Izod-Charpy Tension and Puncture

APPENDIX II
TABLE OF VALUES FOR THE MECHANICAL PROPERTIES OF THE REINFORCED PALF/PP COMPOSITE PRODUCED

II.1 Tensile property of the untreated PALF/PP Composite at the macro level

S/N	Samples	Tensile (yield) strength (MPa)	Young (Elastic) modulus (MPa)
1	PP	33	1325
2	10/90	35.38	1531
3	20/80	38.78	1657
4	30/70	42.20	1864
5	40/60	34.07	1559

II.2 Tensile property of the PALF/PP Composite treated with NaOH at the macro level

S/N	Samples	Tensile (yield) strength (MPa)	Young (Elastic) modulus (MPa)
1	PP	33	1325
2	10/90	36.40	1592
3	20/80	41.70	1651
4	30/70	45.06	1890
5	40/60	40.50	1534

II.3 Tensile property of the PALF/PP Composite treated with ZnCl at the macro level

S/N	Samples	Tensile (yield) strength (MPa)	Young (Elastic) modulus (MPa)
1	PP	33	1325
2	10/90	40.20	1601
3	20/80	48.50	1720
4	30/70	55.90	1899
5	40/60	38.20	1570

II.4 Tensile property of the PALF/PP Composite treated with $C_3H_6O_3$ at the macro level

S/N	Samples	Tensile (yield) strength (MPa)	Young (Elastic) modulus (MPa)
1	PP	33	1325
2	10/90	34.90	1593
3	20/80	39.10	1781
4	30/70	44.90	1861
5	40/60	35.40	1550

II.5 Tensile property of the PALF/PP Composite treated with HNO_3 at the macro level

S/N	Samples	Tensile (yield) strength (MPa)	Young (Elastic) modulus (MPa)
1	PP	33	1325
2	10/90	41.20	1605
3	20/80	49.80	1733
4	30/70	61.50	1874
5	40/60	39.50	1528

II.6 Tensile property of the untreated PALF/PP Composite at the micro level

S/N	Samples	Tensile (yield) strength (MPa)	Young (Elastic) modulus (MPa)
1	PP	33	1325
2	10/90	39.40	1604
3	20/80	43.85	1743
4	30/70	49.60	1903
5	40/60	37.10	1505

II.7 Tensile property of the PALF/PP Composite treated with NaOH at the micro level

S/N	Samples	Tensile (yield) strength (MPa)	Young (Elastic) modulus (MPa)
1	PP	33	1325
2	10/90	38.23	1613
3	20/80	45.80	1879
4	30/70	51.38	1924
5	40/60	39.11	1840

II.8 Tensile property of the PALF/PP Composite treated with ZnCl at the micro level

S/N	Samples	Tensile (yield) strength (MPa)	Young (Elastic) modulus (MPa)
1	PP	33	1325
2	10/90	42.30	1723
3	20/80	52.40	1885
4	30/70	58.60	2035
5	40/60	38.90	1761

II.9 Tensile property of the PALF/PP Composite treated with $C_3H_6O_3$ at the micro level

S/N	Samples	Tensile (yield) strength (MPa)	Young (Elastic) modulus (MPa)
1	PP	33	1325
2	10/90	36.52	1738
3	20/80	41.02	1937
4	30/70	48.11	2069
5	40/60	34.90	1708

II.10 Tensile property of the PALF/PP Composite treated with HNO_3 at the micro level

S/N	Samples	Tensile (yield) strength (MPa)	Young (Elastic) modulus (MPa)
1	PP	33	1325
2	10/90	44.30	1715
3	20/80	51.53	1943
4	30/70	54.11	2037
5	40/60	36.53	1798

II.11 Tensile property of the untreated PALF/PP Composite at the nano level

S/N	Samples	Tensile (yield) strength (MPa)	Young (Elastic) modulus (MPa)
1	PP	33	1325
2	10/90	42.30	1719
3	20/80	48.60	1845
4	30/70	52.90	2105
5	40/60	40.60	2015

II.12 Tensile property of the PALF/PP Composite treated with NaOH at the nano level

S/N	Samples	Tensile (yield) strength (MPa)	Young (Elastic) modulus (MPa)
1	PP	33	1325
2	10/90	42.92	1750
3	20/80	48.94	1985
4	30/70	54.63	2257
5	40/60	38.50	2045

II.13 Tensile property of the PALF/PP Composite treated with ZnCl at the nano level

S/N	Samples	Tensile (yield) strength (MPa)	Young (Elastic) modulus (MPa)
1	PP	33	1325
2	10/90	44.60	1768
3	20/80	53.90	1959
4	30/70	60.30	2281
5	40/60	39.98	2097

II.14 Tensile property of the PALF/PP Composite treated with $C_3H_6O_3$ at the nano level

S/N	Samples	Tensile (yield) strength (MPa)	Young (Elastic) modulus (MPa)
1	PP	33	1325
2	10/90	38.10	1764
3	20/80	44.93	2124
4	30/70	50.10	2246
5	40/60	35.90	2100

II.15 Tensile property of the PALF/PP Composite treated with HNO_3 at the nano level

S/N	Samples	Tensile (yield) strength (MPa)	Young (Elastic) modulus (MPa)
1	PP	33	1325
2	10/90	46.13	539
3	20/80	53.58	667
4	30/70	60.59	799
5	40/60	39.11	721

II.16 Flexural property of the untreated PALF/PP Composite at the macro level

S/N	Samples	Flexural strength (MPa)	Flexural modulus (MPa)
1	PP	31	230
2	10/90	33.80	294
3	20/80	35.20	316
4	30/70	40.44	394
5	40/60	45.30	467

II.17 Flexural property of the PALF/PP Composite treated with NaOH at the macro level

S/N	Samples	Flexural strength (MPa)	Flexural modulus (MPa)
1	PP	31	230
2	10/90	34.50	328
3	20/80	38.63	459
4	30/70	43.60	521
5	40/60	45.60	624

II.18 Flexural property of the PALF/PP Composite treated with ZnCl at the macro level

S/N	Samples	Flexural strength (MPa)	Flexural modulus (MPa)
1	PP	31	230
2	10/90	36.21	334
3	20/80	39.65	488
4	30/70	44.53	592
5	40/60	50.10	643

II.19 Flexural property of the PALF/PP Composite treated with $C_3H_6O_3$ at the macro level

S/N	Samples	Flexural strength (MPa)	Flexural modulus (MPa)
1	PP	31	230
2	10/90	35.61	352
3	20/80	38.99	492
4	30/70	42.30	598
5	40/60	44-01	656

II.20 Flexural property of the PALF/PP Composite treated with HNO_3 at the macro level

S/N	Samples	Flexural strength (MPa)	Flexural modulus (MPa)
1	PP	31	230
2	10/90	38.01	360
3	20/80	44.40	496
4	30/70	48.30	590
5	40/60	51.60	660

II.21 Flexural property of the untreated PALF/PP Composite at the micro level

S/N	Samples	Flexural strength (MPa)	Flexural modulus (MPa)
1	PP	31	230
2	10/90	35.70	380
3	20/80	40.20	490
4	30/70	48.60	588
5	40/60	53.50	694

II.22 Flexural property of the PALF/PP Composite treated with NaOH at the micro level

S/N	Samples	Flexural strength (MPa)	Flexural modulus (MPa)
1	PP	31	230
2	10/90	35.90	356
3	20/80	39.66	494
4	30/70	47.60	583
5	40/60	49.04	692

II.23 Flexural property of the PALF/PP Composite treated with ZnCl at the micro level

S/N	Samples	Flexural strength (MPa)	Flexural modulus (MPa)
1	PP	31	230
2	10/90	37.88	383
3	20/80	40.29	498
4	30/70	46.30	596
5	40/60	51.91	703

II.24 Flexural property of the PALF/PP Composite treated with $C_3H_6O_3$ at the micro level

S/N	Samples	Flexural strength (MPa)	Flexural modulus (MPa)
1	PP	31	230
2	10/90	36.89	368
3	20/80	42.13	510
4	30/70	45.99	613
5	40/60	48.99	742

II.25 Flexural property of the PALF/PP Composite treated with HNO_3 at the micro level

S/N	Samples	Flexural strength (MPa)	Flexural modulus (MPa)
1	PP	31	230
2	10/90	39.10	380
3	20/80	44.96	511
4	30/70	49.60	632
5	40/60	52.80	758

II.26 Flexural property of the untreated PALF/PP Composite at the nano level

S/N	Samples	Flexural strength (MPa)	Flexural modulus (MPa)
1	PP	31	230
2	10/90	36.20	380
3	20/80	41.78	420
4	30/70	45.23	406
5	40/60	47.30	685

II.27 Flexural property of the PALF/PP Composite treated with NaOH at the nano level

S/N	Samples	Flexural strength (MPa)	Flexural modulus (GPA)
1	PP	31	230
2	10/90	36.69	401
3	20/80	41.53	528
4	30/70	49.60	597
5	40/60	53.33	703

II.28 Flexural property of the PALF/PP Composite treated with ZnCl at the nano level

S/N	Samples	Flexural strength (MPa)	Flexural modulus (MPa)
1	PP	31	230
2	10/90	38.91	396
3	20/80	43.20	503
4	30/70	51.78	619
5	40/60	53.99	718

II.29 Flexural property of the PALF/PP Composite treated with $C_3H_6O_3$ at the nano level

S/N	Samples	Flexural strength (MPa)	Flexural modulus (MPa)
1	PP	31	230
2	10/90	38.45	410
3	20/80	43.89	538
4	30/70	47.83	622
5	40/60	49.00	758

II.30 Flexural property of the PALF/PP Composite treated with HNO_3 at the nano level

S/N	Samples	Flexural strength (MPa)	Flexural modulus (MPa)
1	PP	31	230
2	10/90	39.99	438
3	20/80	46.04	594
4	30/70	50.83	648
5	40/60	53.44	766

II.31 Impact property of the reinforced untreated PALF/PP Composite at the macro level

S/N	Samples	Impact Strength (J/m)
1	PP	37
2	10/90	39.8
3	20/80	42.3
4	30/70	49.2
5	40/60	52.5

II.32 Impact property of the reinforced PALF/PP Composite treated with NaOH at the macro level

S/N	Samples	Impact Strength (J/m)
1	PP	37
2	10/90	40.4
3	20/80	44.9
4	30/70	52.9
5	40/60	55.9

II.33 Impact property of the reinforced PALF/PP Composite treated with ZnCl at the macro level

S/N	Samples	Impact Strength (J/m)
1	PP	37
2	10/90	41.9
3	20/80	45.89
4	30/70	56.78
5	40/60	59.69

II.34 Impact property of the reinforced PALF/PP Composite treated with $C_3H_6O_3$ at the macro level

S/N	Samples	Impact Strength (J/m)
1	PP	37
2	10/90	43.78
3	20/80	48.6
4	30/70	58.3
5	40/60	62.3

II.35 Impact property of the reinforced PALF/PP Composite treated with HNO_3 at the macro level

S/N	Samples	Impact Strength (J/m)
1	PP	37
2	10/90	44.89
3	20/80	50.10
4	30/70	59.55
5	40/60	64.10

II.36 Impact property of the reinforced untreated PALF/PP Composite at the micro level

S/N	Samples	Impact Strength (J/m)
1	PP	37
2	10/90	43.6
3	20/80	48.4
4	30/70	53.6
5	40/60	59.9

II.37 Impact property of the reinforced PALF/PP Composite treated with NaOH at the micro level

S/N	Samples	Impact Strength (J/m)
1	PP	37
2	10/90	45.6
3	20/80	50.1
4	30/70	57,6
5	40/60	61.9

II.38 Impact property of the reinforced PALF/PP Composite treated with ZnCl at the micro level

S/N	Samples	Impact Strength (J/m)
1	PP	37
2	10/90	46.3
3	20/80	53.9
4	30/70	57.91
5	40/60	62.3

II.39 Impact property of the reinforced PALF/PP Composite treated with $C_3H_6O_3$ at the micro level

S/N	Samples	Impact Strength (J/m)
1	PP	37
2	10/90	48.9
3	20/80	54.88
4	30/70	59.7
5	40/60	64.0

II.40 Impact property of the reinforced PALF/PP Composite treated with HNO_3 at the micro level

S/N	Samples	Impact Strength (J/m)
1	PP	37
2	10/90	48.96
3	20/80	56.77
4	30/70	60.6
5	40/60	67.7

II.41 Impact property of the reinforced untreated PALF/PP Composite at the nano level

S/N	Samples	Impact Strength (J/m)
1	PP	37
2	10/90	49.0
3	20/80	58.9
4	30/70	62.34
5	40/60	68.9

II.42 Impact property of the reinforced PALF/PP Composite treated with NaOH at the nano level

S/N	Samples	Impact Strength (J/m)
1	PP	37
2	10/90	50.8
3	20/80	60.1
4	30/70	63.8
5	40/60	69.99

II.43 Impact property of the reinforced PALF/PP Composite treated with ZnCl at the nano level

S/N	Samples	Impact Strength (J/m)
1	PP	37
2	10/90	50.92
3	20/80	63.0
4	30/70	68.3
5	40/60	70.4

II.44 Impact property of the reinforced PALF/PP Composite treated with $C_3H_6O_3$ at the nano level

S/N	Samples	Impact Strength (J/m)
1	PP	37
2	10/90	51.4
3	20/80	66.4
4	30/70	70.10
5	40/60	74.3

II.45 Impact property of the reinforced PALF/PP Composite treated with HNO_3 at the nano level

S/N	Samples	Impact Strength (J/m)
1	PP	37
2	10/90	54.3
3	20/80	68.08
4	30/70	72.99
5	40/60	75.90

APPENDIX III
TABLE OF VALUES FOR THE THERMAL PROPERTIES OF THE REINFORCED PALF COMPOSITES PRODUCED

III.1 Thermal conductivity property of the untreated PALF/PP Composite at the macro level

S/N	Samples	Thermal conductivity (W/mk)
1	PP	0.17
2	10/90	0.17
3	20/80	0.17
4	30/70	0.18
5	40/60	0.18

III.2 Thermal conductivity property of the PALF/PP Composite treated with NaOH at the macro level

S/N	Samples	Thermal conductivity (W/mk)
1	PP	0.17
2	10/90	0.18
3	20/80	0.18
4	30/70	0.19
5	40/60	0.19

III.3 Thermal conductivity property of the PALF/PP Composite treated with ZnCl at the macro level

S/N	Samples	Thermal conductivity (W/mk)
1	PP	0.17
2	10/90	0.18
3	20/80	0.18
4	30/70	0.18
5	40/60	0.19

III.4 Thermal conductivity property of the PALF/PP Composite treated with $C_3H_6O_3$ at the macro level

S/N	Samples	Thermal conductivity (W/mk)
1	PP	0.17
2	10/90	0.17
3	20/80	0.18
4	30/70	0.18
5	40/60	0.19

III.5 Thermal conductivity property of the PALF/PP Composite treated with HNO_3 at the macro level

S/N	Samples	Thermal conductivity (W/mk)
1	PP	0.17
2	10/90	0.18
3	20/80	0.18
4	30/70	0.19
5	40/60	0.19

III.6 Thermal conductivity property of the untreated PALF/PP Composite at the micro level

S/N	Samples	Thermal conductivity (W/mk)
1	PP	0.17
2	10/90	0.18
3	20/80	0.18
4	30/70	0.19
5	40/60	0.19

III.7 Thermal conductivity property of the PALF/PP Composite treated with NaOH at the micro level

S/N	Samples	Thermal conductivity (W/mk)
1	PP	0.17
2	10/90	0.19
3	20/80	0.19
4	30/70	0.20
5	40/60	0.21

III.8 Thermal conductivity property of the PALF/PP Composite treated with ZnCl at the micro level

S/N	Samples	Thermal conductivity (W/mk)
1	PP	0.17
2	10/90	0.21
3	20/80	0.22
4	30/70	0.23
5	40/60	0.24

III.9 Thermal conductivity property of the PALF/PP Composite treated with $C_3H_6O_3$ at the micro level

S/N	Samples	Thermal conductivity (W/mk)
1	PP	0.17
2	10/90	0.18
3	20/80	0.19
4	30/70	0.20
5	40/60	0.22

III.10 Thermal conductivity property of the PALF/PP Composite treated with HNO_3 at the micro level

S/N	Samples	Thermal conductivity (W/mK)
1	PP	0.17
2	10/90	0.19
3	20/80	0.21
4	30/70	0.22
5	40/60	0.24

III.11 Thermal property of the untreated PALF/PP Composite at the nano level

S/N	Samples	Thermal conductivity (W/mK)
1	PP	0.17
2	10/90	0.23
3	20/80	0.29
4	30/70	0.34
5	40/60	0.39

III.12 Thermal conductivity property of the PALF/PP Composite treated with NaOH at the nano level

S/N	Samples	Thermal conductivity (W/mk)
1	PP	0.17
2	10/90	0.22
3	20/80	0.32
4	30/70	0.40
5	40/60	0.45

III.13 Thermal conductivity property of the PALF/PP Composite treated with ZnCl at the nano level

S/N	Samples	Thermal conductivity (W/mk)
1	PP	0.17
2	10/90	0.24
3	20/80	0.38
4	30/70	0.41
5	40/60	0.46

III.14 Thermal conductivity property of the PALF/PP Composite treated with $C_3H_6O_3$ at the nano level

S/N	Samples	Thermal conductivity (W/mk)
1	PP	0.17
2	10/90	0.28
3	20/80	0.39
4	30/70	0.45
5	40/60	0.50

III.15 Thermal conductivity property of the PALF/PP Composite treated with HNO_3 at the nano level

S/N	Samples	Thermal conductivity (W/mk)
1	PP	0.17
2	10/90	0.26
3	20/80	0.39
4	30/70	0.48
5	40/60	0.52

APPENDIX IV
TABLE OF VALUES FOR THE PERCENTAGE WATER ABSORPTION PROPERTIES OF THE REINFORCED PALF COMPOSITE PRO DUCED

IV.1 Water absorption property of the reinforced untreated PALF/PP Composite at the macro level

S/N	Sample	24hrs	48hrs	72 hrs	96 hrs	120 hrs	144 hrs	168 hrs
1	PP	0	0	0	0	0	0	0
2	10/90	0.25	0.76	1.69	2.09	2.50	2.50	2.50
3	20/80	0.38	0.98	1.78	2.56	3.24	3.34	3.24
4	30/70	0.54	1.26	1.59	2.98	3.78	3.78	3.78
5	40/60	0.68	1.58	1.97	3.77	4.15	4.15	4.15

IV.2 Water absorption property of the reinforced PALF/PP Composite treated with NaOH at the macro level

S/N	Sample	24hrs	48hrs	72 hrs	96 hrs	120 hrs	144 hrs	168 hrs
1	PP	0	0	0	0	0	0	0
2	10/90	0.20	0.29	0.46	0.78	0.98	0.98	0.98
3	20/80	0.23	0.39	0.67	0.88	1.44	1.44	1.44
4	30/70	0.35	0.46	0.85	1.94	2.04	2.04.	2.04
5	40/60	0.48	1.54	1.98	2.43	2.33	2.33	2.33

IV.3 Water absorption property of the reinforced PALF/PP Composite treated with ZnCl at the macro level

S/N	Sample	24hrs	48hrs	72 hrs	96 hrs	120 hrs	144 hrs	168 hrs
1	PP	0	0	0	0	0	0	0
2	10/90	0.20	0.25	0.49	0.69	1.01	1.01	1.01
3	20/80	0.28	0.36	0.72	0.84	1.56	1.56	1.56
4	30/70	0.33	0.53	0.94	1.34	1.74	1.74	1.74
5	40/60	0.43	0.69	0.99	1.53	2.22	2.22	2.22

IV.4 Water absorption property of the reinforced PALF/PP Composite treated with $C_3H_6O_3$ at the macro level

S/N	Sample	24hrs	48hrs	72 hrs	96 hrs	120 hrs	144 hrs	168 hrs
1	PP	0	0	0	0	0	0	0
2	10/90	0.18	0.40	0.63	0.89	1.20	1.20	1.20
3	20/80	0.28	0.59	0.78	0.94	1.66	1.66	1.66
4	30/70	0.45	0.53	0.98	1.56	1.94	1.94	1.94
5	40/60	0.56	0.90	0.90	1.76	2.16	2.16	2.16

IV.5 Water absorption property of the reinforced PALF/PP Composite treated with HNO_3 at the macro level

S/N	Sample	24hrs	48hrs	72 hrs	96 hrs	120 hrs	144 hrs	168 hrs
1	PP	0	0	0	0	0	0	0
2	10/90	0.19	0.30	0.60	0.69	1.01	1.01	1.01
3	20/80	0.24	0.43	0.73	0.84	1.56	1.56	1.56
4	30/70	0.38	0.74	1.20	1.70	2.00	2.00	2.00
5	40/60	0.40	0.78	1.30	1.80	2.35	2.35	2.35

APPENDIX V
EDX -SEM OF THE MICRO/NANO CELLULOSE

V.1 Control (untreated)

Element	% composition
Carbon, C	71.04
Nitrogen, N	3.05
Oxygen, O	24.85
Sodium, Na	0.34
Aluminum, Al	0.09
Chlorine, Cl	0.43
Calcium	0.10

V.2 PALF treated with NaOH

Element	% composition
Carbon, C	70.71
Nitrogen, N	1.91
Oxygen, O	26.84
Sodium, Na	0.36
Aluminum, Al	0.10
Chlorine, Cl	-
Calcium	-

V.3 PALF treated with ZnCl

Element	% composition
Carbon, C	61.77
Nitrogen, N	-
Oxygen, O	37.97
Sodium, Na	0.31
Zinc, Zn	0.01
Chlorine, Cl	-
Calcium	-

V.4 PALF treated with $C_3H_60_3$

Element	% composition
Carbon, C	66.57
Nitrogen, N	0.72
Oxygen, O	32.12
Sodium, Na	0.31
Aluminum, Al	0.09
Chlorine, Cl	0.28
Calcium	-

V.5 PALF treated with HNO_3

Element	% composition
Carbon, C	68.45
Nitrogen, N	2.90
Oxygen, O	27.16
Sodium, Na	0.36
Aluminum, Al	0.23
Chlorine, Cl	0.76
Calcium	-

APPENDIX VI
CHARACTERIZATION DATA OF THE PALF

VI.1 Characterization of the PALF at the macro level

Cellulose	Lignin	Hemicellulose	Reagent used
58.15	5.06	13.16	NaOH
55.43	4.86	15.90	HNO_3
60.56	5.01	12.47	ZnCl
61.15	4.95	12.22	$C_4H_60_3$
70.87	5.34	13.92	Untreated PALF

APPENDIX VII: G-CODES FOR MOLDS FABRICATION

```
%
O0022 (WADZANI CIRCULAR MAIN PROGRAM)
G54
M3 S500 F60
M8
G80 G90 G0 X0 Y0 Z100
G99 G81 X-140 Y55 Z-18 R2 F60
X0
X-140
Y-55
X0
X-140
G90 G80 Z50
G99 G81 X-140 Y0 Z-4 R2 F60
G91 X90
X90
X90
X90
G90 G80 Z50
G90 G0 X140 Y0
#1=12
#2=[25-[#1/2]]
WHILE[#10LT5] DO 1
G0 Z-2 F60
G1 Z-5
#4=0
#5=1
WHILE[#4LT#2] DO 2
G91 G1 X1
G90 I#5 J0
#5=#5+1
#4=#4+1
END 2
G90 G0 Z10
G91 X-70
END 1
M30
%


%
O3360 (WADZANI FLEXURAL MAIN PROGRAM)
T1
M06
G54
M3 S450
M8
G94 G90 G0 X-100 Y0 Z100
```

```
G43 H1
G99 G83 X-189 Y0 Z-30 R3 Q5 F90
G83 X-107.8 Y76.5 Z-1 R3 Q5 F90
G91 X66.2
X66.2
X66.2
X66.2
G90 G83 X189 Y0 Z-30 R3 Q5 F90
#1=0

N10 G90 G99 G83 X149 Y107.5 Z-30 R3 Q5 F90
/X0
X-149
/Y0
Y-107.5
/X0
X-149
G90 G80 Z100
#1=#1+1

M0
/T2 (ø20 Drill bit)
M3 S210
IF [#1 LT 2] GOTO 10
M0

/T3
/M06
#3=0
G94 M3 S320 F60
G54
G90 G0 X-107.8 Y76.5 Z100
G90 Z2
WHILE [#3 LT 4] DO 1
G91 G1 Z-3.5
Y-165
X-6.5
Y165
X13
Y-165
X-6.5
G0 Z3.5
X40 Y165
END 1

G90 Z100
M30
%
```

```
%
O3360 (WADZANI FIRE MAIN PROGRAM)
T1
M06
G54
M3 S450
M8
G94 G90 G0 X-100 Y0 Z100
G43 H1
G99 G83 X-165 Y0 Z-37 R3 Q5 F90
G83 X-116 Y57.5 Z-1 R3 Q5 F90
G91 X52
X52
X52
X52
G90 G83 X165 Y0 Z-37 R3 Q5 F90
#1=0

N10 G90 G99 G83 X136 Y0 Z-37 R3 Q5 F90
Y79.75
/X0
X-136
Y0
Y-79.75
/X0
X-136
G90 G80 Z100
#1=#1+1

M0
/T2 (ø20 Drill bit)
M3 S210
IF [#1 LT 2] GOTO 10
M0

/T3
/M06
#3=0
G94 M3 S320 F60
G54
G90 G0 X-116 Y57.5 Z100
G90 Z2
WHILE [#3 LT 4] DO 1
G91 G1 Z-3.6
Y-115
Z3.6
X40 Y115
END 1
```

```
G90 Z100
M30
%



%
O3360 (WADZANI TENSILE MAIN PROGRAM)
T1
M06
G54
M3 S450
M8
G94 G90 G0 X-100 Y0 Z100
G43 H1
G83 X-175 Y0 Z-37 R3 Q5 F90
G83 X-100 Y0 Z-3.5 R3 Q5 F90
G91 X50
X50
X50
X50
G90 G83 X175 Y0 Z-37 R3 Q5 F90
#1=0

N10 G90 G83 X135 Y0 Z-37 R3 Q5 F90
Y116.5
X0
X-135
Y0
Y-116.5
X0
X-135
G90 G80 Z100
#1=#1+1

M0
/T2 (ø20 Drill bit)
M3 S210
IF [#1 LT 2] GOTO 10
M0

/T3
/M06
#3=0
G94 M3 S320 F60
G54
G90 G0 X-100 Y0 Z100
G43 H3

N25 G0 Z3
```

```
G90  G1  Z-3

#2=0

N30  G91  G1  Z-1
M98  P3363
G51.1  Y0
M98  P3363
G50.1  Y0
#1=#1+1
IF  [#2  LE  2]  GOTO  30
G90  G0  Z3

G90  G0  Z200
G91  G0  X50
#3=#3+1
IF  [#3  LT  5]  GOTO  25

G90  G0  Z200
M9
M30
%
```